

# NOTE TO USERS

Page(s) not included in the original manuscript and are unavailable from the author or university. The manuscript was scanned as received.

This reproduction is the best copy available.



**University of Alberta**

**The Weldability of TMCP Microalloyed Structural Steels**

by

**Shane Joseph Hoskins**



**A thesis submitted to the Faculty of Graduate Studies and Research in partial  
fulfillment of the requirements for the degree of Master of Science**

in

**Welding Engineering**

**Department of Chemical and Materials Engineering**

**Edmonton, Alberta**

**Fall 2002**



**National Library  
of Canada**

**Acquisitions and  
Bibliographic Services**

**395 Wellington Street  
Ottawa ON K1A 0N4  
Canada**

**Bibliothèque nationale  
du Canada**

**Acquisitions et  
services bibliographiques**

**395, rue Wellington  
Ottawa ON K1A 0N4  
Canada**

*Your file Votre référence*

*Our file Notre référence*

The author has granted a non-exclusive licence allowing the National Library of Canada to reproduce, loan, distribute or sell copies of this thesis in microform, paper or electronic formats.

The author retains ownership of the copyright in this thesis. Neither the thesis nor substantial extracts from it may be printed or otherwise reproduced without the author's permission.

L'auteur a accordé une licence non exclusive permettant à la Bibliothèque nationale du Canada de reproduire, prêter, distribuer ou vendre des copies de cette thèse sous la forme de microfiche/film, de reproduction sur papier ou sur format électronique.

L'auteur conserve la propriété du droit d'auteur qui protège cette thèse. Ni la thèse ni des extraits substantiels de celle-ci ne doivent être imprimés ou autrement reproduits sans son autorisation.

0-612-81410-6



**University of Alberta**

**Library Release Form**

**Name of Author:** Shane Joseph Hoskins

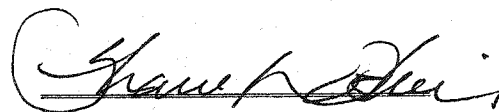
**Title of Thesis:** The Weldability of TMCP Microalloyed Structural Steels

**Degree:** Master of Science

**Year this Degree Granted:** 2002

Permission is hereby granted to the University of Alberta Library to reproduce single copies of this thesis and to lend or sell such copies for private, scholarly or scientific research purposes only.

The author reserves all other publication and other rights in association with the copyright in the thesis, and except as herein before provided, neither the thesis nor any substantial portion thereof may be printed or otherwise reproduced in any material form whatever without the author's prior written permission.



Shane Joseph Hoskins

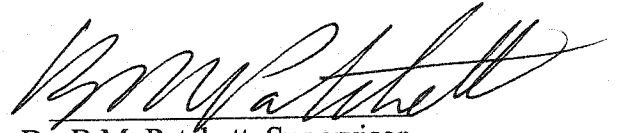
152 Tundra Drive  
Fort McMurray, AB  
T9H 4S7

  
Date

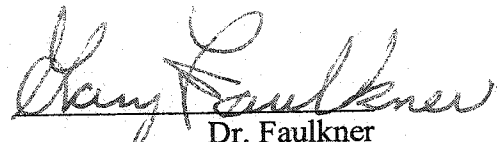
**University of Alberta**

**Faculty of Graduate Studies and Research**

The undersigned certify that they have read, and recommended to the Faculty of Graduate Studies and Research for acceptance, a thesis entitled The Weldability of TMCP Microalloyed Steels by Shane Joseph Hoskins in partial fulfillment of the requirements for the degree of Master of Science in Welding Engineering.

  
Dr. B.M. Patchett, Supervisor

  
Dr. D. Ivey

  
Dr. Faulkner

11/15/15-2002  
Date

## **Abstract**

The weldability of Grade 80 and Grade 100 structural steel was examined. Welding tests were conducted to examine the effects of Gas Tungsten Arc Welding, Shielded Metal Arc Welding, and Gas Metal Arc Welding on both of the materials. Weldability was assessed in terms of resulting microstructures, mechanical properties and susceptibility to cold cracking. The tests conducted in the study show that both materials exhibit good weldability. An increase in susceptibility to hydrogen assisted cold cracking was seen in the Grade 100 steel as compared with the Grade 80 material. Both steels demonstrated sensitivity to high heat input welding, with a decrease in yield strength observed. Both materials were successfully welded without the use of preheating while maintaining the required mechanical properties.

## **Acknowledgements**

I would like to thank Dr. Barry Patchett for his guidance and support over the past few years. I was drawn to his practical approach to engineering and have always been inspired by the depth of his knowledge and the diversity of his interests. He has been a great mentor and for this I am indebted. I would also like to thank Clark Bicknell for his help and input with the experimental work carried out in this study. He provided many insights that helped to direct the course of the study while teaching me a lot about welding.

Thanks also goes out to the other members of the IPSCO Research Group including Dr. Henein, Dr. Luo, Dr. Ivey, and Dr. Wiskel for their advice and comments during our many review sessions. I would also like to thank the members of the IPSCO Inc. Research Center, in particular Nathan Townley and Milos Kostic, for their input into the study.

## Table of Contents

<b>CHAPTER 1</b>	<b>INTRODUCTION .....</b>	<b>1</b>
<b>CHAPTER 2</b>	<b>LITERATURE REVIEW.....</b>	<b>3</b>
<b>2.1</b>	<b>TMCP Processing.....</b>	<b>4</b>
2.1.1	Controlled Rolling.....	5
2.1.2	On Line Accelerated Cooling (OLAC) .....	7
2.1.3	Effect of Processing on Weldability.....	8
<b>2.2</b>	<b>Chemical Composition and Mechanical Properties.....</b>	<b>9</b>
2.2.1	Chemical Composition .....	9
2.2.2	Mechanical Properties .....	12
2.2.3	Effect of Chemistry and Mechanical Properties on Weldability .....	13
<b>2.3</b>	<b>Microstructure .....</b>	<b>14</b>
2.3.1	Polygonal Ferrite.....	16
2.3.2	Acicular Ferrite .....	17
2.3.3	Bainite.....	18
2.3.4	M/A Constituent.....	19
<b>2.4</b>	<b>Welding Process .....</b>	<b>19</b>
2.4.1	Gas Tungsten Arc Welding.....	19
2.4.2	Shielded Metal Arc Welding .....	22
2.4.3	Gas Metal Arc Welding.....	25
2.4.4	Preheat Requirements.....	30
2.4.5	Heat Input .....	32
2.4.6	Consumables .....	32
<b>2.5</b>	<b>Weld Zone Properties .....</b>	<b>33</b>
2.5.1	Weld Metal .....	34
2.5.2	Weld Metal Properties.....	39
2.5.3	HAZ Properties .....	39
2.5.4	HAZ of Single Pass Welds .....	40
2.5.5	HAZ of Multi-Pass Welds .....	43
2.5.6	HAZ Hardenability.....	44
2.5.7	HAZ Toughness and Microstructure.....	45
2.5.8	HAZ Softening .....	46
<b>2.6</b>	<b>HAZ and Weld Metal Cracking .....</b>	<b>47</b>
2.6.1	Hot Cracking.....	47
2.6.2	Lamellar Tearing.....	48
2.6.3	Reheat Cracking.....	49

2.6.4	Cold Cracking .....	49
2.7	Post-Weld Heat Treatment .....	53
2.8	Weldability Testing .....	53
2.8.1	Mechanical Testing .....	54
2.8.2	Implant Testing .....	57
2.8.3	WIC Restraint Cracking Test.....	61
2.9	Literature Review Summary .....	63

## **CHAPTER 3 EXPERIMENTAL PROCEDURE..... 64**

3.1	Material .....	64
3.2	Welding Procedures .....	65
3.3	Welding Consumables.....	66
3.3.1	SMAW Consumables .....	66
3.3.2	GMAW Consumables .....	68
3.4	Tensile Test Welds .....	68
3.5	Tensile Tests .....	69
3.6	Cruciform Tests .....	70
3.7	Implant Tests.....	71
3.8	Diffusible Hydrogen Tests .....	73
3.9	WIC Rigid Restraint Cracking Tests .....	75
3.10	Metallurgical Samples.....	76
3.11	Microhardness Testing .....	77

## **CHAPTER 4 MICROSTRUCTURE ..... 78**

4.1	Grade 80 As Received .....	78
4.2	Grade 80 As Welded .....	79
4.2.1	Grade 80 Autoogenous Microstructures.....	79
4.2.2	Grade 80 Microhardness Measurements .....	83
4.2.3	Effect of Multipass Welding .....	84

<b>4.3</b>	<b>Grade 100 As Received .....</b>	<b>85</b>
<b>4.4</b>	<b>Grade 100 As Welded .....</b>	<b>86</b>
4.4.1	Grade 100 Autogenous .....	86
4.4.2	Grade 100 Microhardness Measurements .....	90
4.4.3	Effect of Multipass Welding .....	91

## **CHAPTER 5 MECHANICAL PROPERTIES ..... 92**

<b>5.1</b>	<b>Grade 80 .....</b>	<b>94</b>
5.1.1	Effect of Under and Over Strength Weld Metal .....	94
5.1.2	Effect of Heat Input on SMAW Process .....	97
5.1.3	Effect of Heat Input on GMAW Process .....	99
<b>5.2</b>	<b>Grade 100 .....</b>	<b>100</b>
5.2.1	Effect of Under and Over Strength Weld Metal .....	100
5.2.2	Effect of Heat Input on SMAW Process .....	101
5.2.3	Effect of Heat Input on GMAW .....	103
<b>5.3</b>	<b>Cruciform Tests .....</b>	<b>103</b>
5.3.1	Grade 80 .....	104
5.3.2	Grade 100 .....	104

## **CHAPTER 6 WELD AND BASE METAL CRACKING..... 106**

<b>6.1</b>	<b>Grade 80 Implant Tests .....</b>	<b>106</b>
<b>6.2</b>	<b>Hydrogen Analysis for Grade 80 Consumables .....</b>	<b>108</b>
<b>6.3</b>	<b>Grade 100 Implant Test .....</b>	<b>109</b>
<b>6.4</b>	<b>Hydrogen Analysis for Grade 100 Consumables .....</b>	<b>112</b>
<b>6.5</b>	<b>Comparison of Implant Results with Other Steels .....</b>	<b>113</b>
<b>6.6</b>	<b>Grade 80 WIC Rigid Restraint Cracking Tests .....</b>	<b>114</b>
<b>6.7</b>	<b>Grade 100 WIC Rigid Restraint Cracking Tests .....</b>	<b>118</b>
<b>6.8</b>	<b>Comparison of WIC Results with Other Steels.....</b>	<b>121</b>

## **CHAPTER 7 CONCLUSIONS AND RECOMMENDATIONS..... 123**

<b>7.1</b>	<b>Conclusions.....</b>	<b>123</b>
------------	-------------------------	------------

<b>7.2 Recommendations .....</b>	<b>125</b>
<b>REFERENCES .....</b>	<b>127</b>
<b>APPENDIX A.....</b>	<b>131</b>
<b>Consumable Information .....</b>	<b>131</b>
<b>APPENDIX B.....</b>	<b>133</b>
<b>Test Procedures.....</b>	<b>133</b>



## List of Tables

Table 2-1 Hydrogen Level in Various Electrodes [ASM, 1998 ] .....	52
Table 2-2 Experimental Procedures for Implant Tests [Bryhan, 1981] .....	59
Table 2-3 Restraint Intensities for Different Structural Applications [Datta, 1997] .....	62
Table 3-1 Chemical Composition of Grade 80 and Grade 100.....	64
Table 3-2 Mechanical Properties of Grade 80 and Grade 100.....	64
Table 3-3 Welding Procedures for SMAW for GMAW Process.....	65
Table 3-4 Specifications for Canadian Liquid Air 9018 .....	67
Table 3-5 Specifications for Canadian Liquid Air 11018.....	67
Table 3-6 As-Welded Properties of L-TEC HI-84 .....	68
Table 4-1 Grade 80 Microhardness Measurements of the Weld Zone.....	84
Table 4-2 CGHAZ Hardness Measurements of Varying Passes in Grade 80 Steel .....	85
Table 4-3 Grade 100 Microhardness Measurements of the Weld Zone.....	90
Table 4-4 CGHAZ Hardness Measurements of Varying Passes in Grade 100 Steel .....	91
Table 5-1: Grade 80 SMAW with Variable Consumables .....	94
Table 5-2: Grade 80 SMAW with Variable Heat Inputs .....	98
Table 5-3: Grade 80 GMAW with Variable Heat Inputs.....	99
Table 5-4: Grade 100 SMAW with Variable Consumables .....	100
Table 5-5: Grade 100 SMAW with Variable Heat Inputs .....	102
Table 5-6: Grade 100 GMAW with Variable Heat Inputs.....	103

Table 6-1: Effect of Hydrogen Level on Grade 80 Implant Specimens at 78% of SMYS.....	107
Table 6-2: Effect of Heat Input on Grade 80 Implant Specimens Welded with a 9018 Electrode.....	107
Table 6-3: Hydrogen Analysis of 9018 .....	108
Table 6-4: Effect of Hydrogen Level on Grade 100 Implant Specimens at 78% of SMYS.....	109
Table 6-5: Effect of Heat Input on Grade 100 Implant Specimens Welded with a 11018 Electrode.....	110
Table 6-6: Effect of Electrode Condition on Grade 100 Implant Specimens Welded with 11018 Electrodes.....	111
Table 6-7: Comparison of GMAW and SMAW Implant Tests for Varying Heat Inputs at a Constant Load for Gr. 100.....	112
Table 6-8: Diffusible Hydrogen Analysis for 11018 and HI 84 Electrodes .....	113
Table 6-9: WIC Test Results for Grade 80.....	115
Table 6-10: WIC Test Results for Grade 100 .....	119

## List of Figures

Figure 2-1 Schematic Illustration of the stages in TMCP Processing. [Tanaka, 1995 ] .....	5
Figure 2-2 Iron Carbon Phase Diagram [Smith, 1993] .....	14
Figure 2-3 CCT Diagram for Microalloyed Steel [Collins, 1983] .....	16
Figure 2-4 Optical Micrograph of Polygonal Ferrite(PF).....	17
Figure 2-5 Optical Micrograph of Acicular Ferrite (AF). .....	18
Figure 2-6 Typical GTAW Setup [AWS, 1991] .....	20
Figure 2-7 Typical GTAW Equipment [AWS, 1991]. .....	22
Figure 2-8 Typical Circuit for SMAW [AWS, 1991]. .....	23
Figure 2-9 SMAW Process [AWS, 1991].....	24
Figure 2-10 Typical GMAW Configuration [AWS, 1991]. .....	26
Figure 2-11 GMAW Gun [AWS, 1991]. .....	27
Figure 2-12 Schematic Illustration of the Various Zones in a Weld. [Patchett, 1998]. .....	34
Figure 2-13 The Effect of Heat Input and Welding Speed on the Shape of the Weld and Mode of Crystal Growth. (a) Low heat input and low welding speed, (b) High heat input and high welding speed, (c) High heat input and high welding speed, with heterogeneous nucleation at the weld pool centerline. [ASM, 1998].....	36
Figure 2-14 HAZ of a Single Pass Weld [Easterling, 1983].....	41
Figure 2-15 Schematic Illustration of the Effect of Multi-Pass Welding the Microstructure of the HAZ.....	44

Figure 2-16 Variations in the Hardness in the HAZ of a TMCP Steel [ASM, 1998] .....	47
Figure 2-17 Effect of Cooling Rates on the Yield Strength of AX-140 and E11018 Filler Metals. [ASM, 1993] .....	55
Figure 2-18 Moire Picture of the strain distribution in a Undermatched (top) and Overmatched (bottom) welded sample. [Denys, 1990] .....	56
Figure 2-19 The Effect of Weld Metal Overmatching (A) and Undermatching (B) on the stress strain distribution of a transversely loaded tensile sample. [Denys, 1989] .....	57
Figure 2-20 Typical Implant Test Setup .....	58
Figure 2-21 Effect of Test Variables on Implant Test Results [Bryhan, 1981] ....	60
Figure 2-22 WIC High Restrain Cracking Test .....	61
Figure 3-1 Picture of SMAW Tensile Test Set Up (a) Plan View (b) Side View.	69
Figure 3-2 Picture of GMAW Tensile Test Set Up (a) Plan View (b) Side View	69
Figure 3-3 Dimensions of Tensile Coupon .....	70
Figure 3-4 Schematic Diagram of Cruciform Joint Configurations .....	71
Figure 3-5 Detail of Helical Implant Sample .....	72
Figure 3-6 Diffusible Hydrogen Apparatus (a) Sample Jig & (b) Collection Apparatus [ISO 3690] .....	74
Figure 3-7 Modified WIC High Restraint Cracking Test .....	75
Figure 4-1 Microstructure of As Received Grade 80 .....	79
Figure 4-2 Effect of Heat Input (kJ/mm) on Weld Metal Microstructure of Gr. 80 Autogenous Welds: (a) 0.5 (b) 1.0 (c) 1.5 (d) 2.0 (e) 2.5 .....	80

Figure 4-3 Effect of Heat Input (kJ/mm) on CGHAZ Microstructure of Gr. 80	
Autogenous Welds: (a) 0.5 (b) 1.0 (c) 1.5 (d) 2.0 (e) 2.5.....	81
Figure 4-4 Effect of Heat Input (kJ/mm) on FGHAZ Microstructure of Gr. 80	
Autogenous Welds: (a) 0.5 (b) 1.0 (c) 1.5 (d) 2.0 (e) 2.5.....	83
Figure 4-5 Microstructure of As Received Grade 100 .....	85
Figure 4-6 Effect of Heat Input (kJ/mm) on Weld Metal Microstructure of Gr. 100	
Autogenous Welds: (a) 0.5 (b) 1.0 (c) 1.5 (d) 2.0 (e) 2.5.....	87
Figure 4-7 Effect of Heat Input (kJ/mm) on CGHAZ Microstructure of Gr. 100	
Autogenous Welds: (a) 0.5 (b) 1.0 (c) 1.5 (d) 2.0 (e) 2.5.....	88
Figure 4-8 Effect of Heat Input (kJ/mm) on FGHAZ Microstructure of Gr. 100	
Autogenous Welds: (a) 0.5 (b) 1.0 (c) 1.5 (d) 2.0 (e) 2.0.....	89
Figure 5-1 Sample Stress-Strain Curve showing the Variations in yield Stress...	93
Figure 5-2 Schematic Drawing of Failure in 12018B Weld Sample.....	97
Figure 6-1 SMAW Grade 80 45 Bevel vs. Straight Edge.....	115
Figure 6-2 SMAW Grade 80 45° Bevel vs. Straight Edge at 100°C.....	116
Figure 6-3: SMAW Grade 80 45° Bevel vs. 45° Bevel.....	117
Figure 6-4 : GMAW Grade 80 45° Bevel vs. Straight Edge .....	117
Figure 6-5: Transverse Section of GMAW WIC Test.....	118
Figure 6-6 SMAW Grade 100 45° Bevel vs. Straight Edge .....	119
Figure 6-7 SMAW Grade 100 45° Bevel vs. Straight Edge at 100°C.....	120
Figure 6-8 SMAW Grade 100 45° Bevel vs. 45° Bevel.....	120
Figure 6-9 GMAW Grade 100 45° Bevel vs. Straight Edge.....	121

## List of Symbols

<u>Symbol</u>	<u>Meaning</u>
ASTM	American Society for Testing and Materials
CGHAZ	coarse grain heat affected zone
El	elongation
FGHAZ	fine grain heat affected zone
GMAW	gas metal arc welding
GTAW	gas tungsten arc welding
HAZ	heat affected zone
HACC	hydrogen assisted cold cracking
Hv	hardness Vickers
HSLA	high strength low alloy
PMZ	partially mixed zone
SAW	submerged arc welding
SMAW	shielded metal arc welding
SMYS	specified minimum yield strength
TMCP	thermo mechanical controlled process
UMZ	unmixed zone
UTS	ultimate tensile strength
$\sigma$	stress
$\sigma_{ys}$	yield stress

## Chapter 1 Introduction

With increasing threats from alternative materials for structural applications, steels producers are constantly seeking opportunities for more cost effective utilization of steel. Production of steels with increasing yield strength without having to resort to costly heat treatments is one means of competing with new materials. The use of higher strength steels provides for new design options for engineers, due to the down gauging that results from increased yield strengths. To make these new grades of steels cost effective there must not be any increase in the fabrication costs above that of conventional steels. This requires that the plate steel be capable of being welded without preheat or restrictive welding conditions. [Langley, 1998]

A better understanding of physical metallurgy with regard to optimizing solution precipitation and dislocation hardening as well as reduction in carbon and impurities has created a wide range of new weldable structural steels with improved properties. Steels produced via Thermomechanical Controlled Processing (TMCP) are currently being produced with yield strength values greater than 100 ksi (690 MPa). While considerable research has gone into the making of these steels, little work has been done on the weldability of these steels. Steels with yield strength levels greater than 100 ksi (690 MPa) currently fall outside of the limitations of the AWS Structural Welding Code (AWS D1.1:2000) and the CSA W59 Standard for steel.

The objective of this project is to assess the weldability of Grade 80 and Grade 100 structural steel by examining the effect of welding on the metallurgical and mechanical properties of both materials.

A literature review of the factors affecting the weldability of TMCP structural steels is covered in Chapter 2. It examines the effect of processing, chemistry and welding on the properties of TMCP steel. The experimental procedures used in the study are outlined in Chapter 3. Chapters 4 through 6 present the results of study in terms of the microstructures, mechanical properties and cracking susceptibility that result from the welding of both materials. Conclusions found in regards to the weldability of both materials are given in Chapter 7 along with recommendations for future work.



## Chapter 2 Literature Review

Weldability is a term used to describe how a material responds to welding. While no precise definition exists for the term, materials are usually classified as having good or poor weldability. In the case of microalloyed steels, the weldability can be assessed in terms of fabrication and service. Fabrication weldability deals with the materials ability to be welded without the introduction of detrimental flaws. It deals with flaws such as hydrogen-assisted cold cracks (HACC), hot cracks, reheat cracks, lamellar tearing, and porosity. Service weldability addresses the issue of whether or not the resulting weld has the required properties. Obtaining a balance among the properties of the weld metal (WM), heat affected zone (HAZ) and the unaffected base metal is an important aspect of service weldability. It involves the effect of the welding thermal cycle on the material and determines how the material may be welded. Whether or not the fabrication and service weldability of a material is good or bad depends on the particular application, as it is the application of the weld that determines what the weldability requirements are. [Somers, 1998]

Thermal Mechanical Controlled Processed (TMCP) steels are a relatively new family of steels that exhibit improved weldability over carbon steels of equal strength levels. They are produced by controlled rolling, followed by controlled or accelerated cooling or online quenching. The use of these variables allows for an increase in strength without the addition of carbon, making the steel much

more weldable. This chapter will examine the factors that determine the weldability of TMCP steels in terms of processing, chemistry and the welding process.

## ***2.1 TMCP Processing***

Thermo-Mechanical Control Processing (TMCP) involves both the controlled rolling and accelerated/controlled cooling of steel during primary processing. The goal of thermo-mechanical processing is to achieve microstructural refinement in the as-rolled austenite prior to transformation. Grain refinement is based on controlling the kinetics of recrystallization and subsequent grain growth, which occurs during the interpass time between deformations in a multi-pass schedule. [DeArdo, 1995] Accelerated cooling is carried out to enhance the ferrite nucleation rates to result in finer microstructures. The details of each of the stages involved in TMCP processing shown in Figure 2-1 and are outlined below.

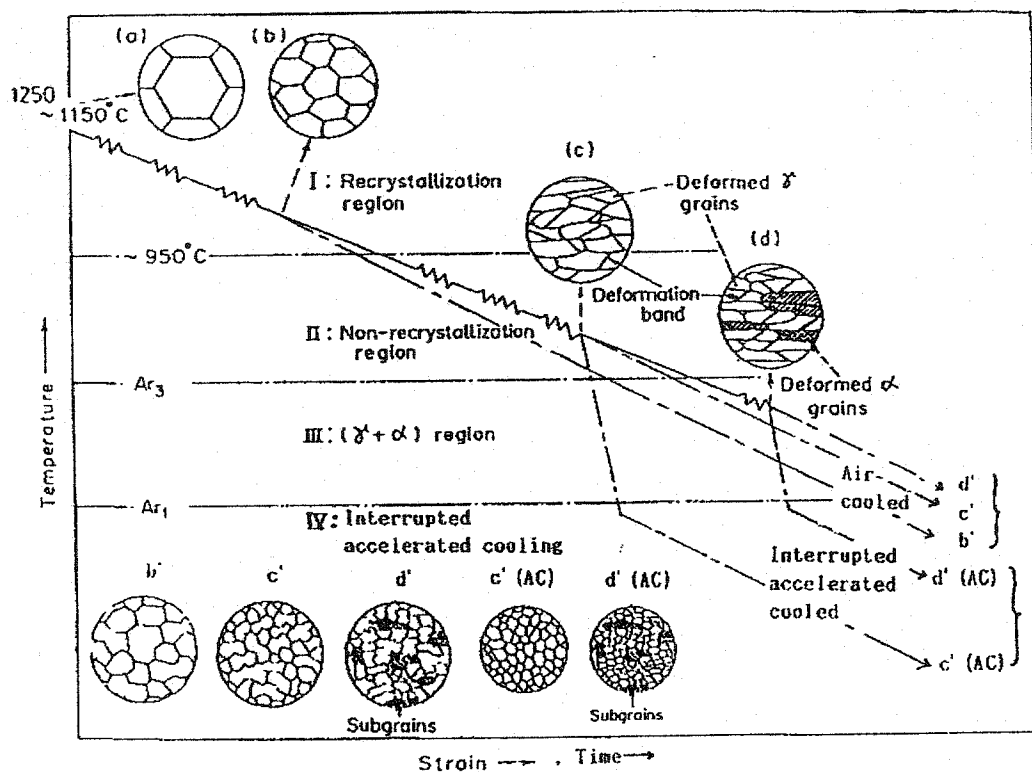


Figure 2-1 Schematic Illustration of the stages in TMCP Processing.[Tanaka, 1995 ]

### 2.1.1 Controlled Rolling

The TMCP process starts with the reheating of slabs to produce a relatively uniform microstructure and even distribution of alloying elements in the material. This is shown as points (a) and (b) in Figure 2-1. In this stage, the coarse grains resulting from reheating undergo repeated deformation and recrystallization. The second stage in the process is deformation in the non-recrystallization region below 950°C and above the  $A_{r3}$  temperature. Deformation in this region causes the austenite grains to become elongated with deformation bands within the grain (c). Ferrite nucleates on the austenite grain boundaries as well as on the deformation bands resulting in a very fine microstructure (c'). [Tanaka, 1995]

Controlled rolling involves careful manipulation of the rolling schedule at various temperatures in order to produce the optimum microstructure for a given chemistry. At high temperatures, elements like niobium are soluble in austenite. As the temperature is decreased in the austenite region, Nb will precipitate out in the form of niobium carbonitrides. These carbonitrides help to stabilize the deformed austenite and retards their recrystallization. The addition of other elements such as vanadium and titanium has a similar effect. In order to maximize the benefits of these elements the final rolling temperature should be below the  $Ar_3$  line to prevent grain growth of the recrystallized austenite grains. Upon cooling, ferrite will start to nucleate in small grains of austenite to produce a very fine ferrite grain size. While the primary function of these alloying elements is to act as grain refiners, they also help to increase the overall strength level of the steel due to precipitation hardening via the formation of carbonitride and carbides. Upon cooling after rolling, the carbonitrides and carbides will precipitate out of solution. If the cooling rate is slow, the precipitates will form and grow as incoherent inclusions in the ferrite matrix. This will result in a decrease in the toughness. With a fast cooling rate, the strength increase will also be limited as the elements have a higher probability of undergoing substitutional or interstitial hardening rather than precipitation hardening. In order to maximize the benefits of these alloying elements, the effects of grain refinement and precipitation hardening must be combined. This requires a great deal of control over not only the actual rolling but also the finishing temperature and the cooling rates after rolling. [de Meester, 1997][Honeycombe, R, 1995]

As a result of the control that is exhibited over the rolling practice, decreases in toughness associated with any increase in strength level can be minimized. This makes it possible to reduce the carbon content of the material without any loss of strength. It is important to note, however, that because these steels rely on the rolling practice to obtain their strength and toughness levels. Any reheating above 580°C will likely result in an alteration in strength and/or toughness.

#### 2.1.2 On Line Accelerated Cooling (OLAC)

The most recent development in rolling that has lead to the production of TMCP steels is the use of online accelerated cooling. Immediately following rolling, the steels are subjected to varying cooling rates to obtain the desired microstructures and mechanical properties. [Collins, 1985] OLAC involves the application of water or an air-water mixture after finish rolling to refine the as-rolled microstructure. [Lin, 1999] Through the use of accelerated cooling, manufacturers have another process that allows for more control over the thermal history of the material. Grain refinement and dislocation hardening are enhanced and the lower transformation temperatures that result from accelerated cooling lead to a finer microstructure when compared with controlled rolling alone. Steel producers can now manipulate chemistries to take advantage of not only the grain refinement and precipitation hardening, but also control the amount and composition of transformation products such as bainite and martensite. The addition of other alloying elements such as nickel and chromium also aid in achieving the desired hardenability of the steel. Accelerated cooling may also be

applied to very low carbon steels to promote the formation of acicular rather than polygonal ferrite. [de Meester, 1997][Honeycombe, R, 1995]

If the cooling rates imposed by accelerated cooling are high enough, precipitation hardening can be suppressed. However, if the cooling is stopped at a high enough temperature, it can allow for a self-tempering to occur during the final cooling in air. The use of a high cooling rate will likely result in the formation of bainitic or martensitic microstructures, which will be tempered during slow cooling in air. Because of this, the thickness to which a uniform microstructure can be obtained is limited. [de Meester, 1997][Honeycombe, R, 1995]

### 2.1.3 Effect of Processing on Weldability

The high levels of strength found in TMCP microalloyed steel are mainly a result of three strengthening mechanisms; austenite and ferrite grain refinement, dispersion strengthening by carbonitrides and carbides, and increased dislocation densities. These three mechanisms have allowed steel makers to reduce the carbon content of steel to improve the weldability. [Gladman, 1997] During the welding process, the steel undergoes a rapid thermal cycle with temperatures above the melting point. As a result of the thermal cycle, the three strengthening mechanisms used to produce the steel are adversely affected. Of particular importance is the region of the base material closest to the fusion zone. It is important to note that steels produced by controlled rolling, followed by accelerated cooling, have properties that cannot be duplicated with any thermal

heat treatment, making it impossible to restore the properties found prior to welding. [de Meester, 1997] The effects of welding will be further discussed in a later section.

## ***2.2 Chemical Composition and Mechanical Properties***

The chemical compositions of most TMCP steels are proprietary. This results in a number of variations from one manufacturer to another in terms of composition, microstructure, and mechanical properties. Along with chemistry, manufacturers can also manipulate the rolling schedule, reduction, and temperature any number of times in conjunction with or without accelerated cooling to obtain varying properties.

### **2.2.1 Chemical Composition**

The chemical composition of TMCP microalloyed steels, is designed with two main purposes in mind. The first is to decrease the overall hardenability of the steel, and the second is to add the appropriate amounts of alloying elements and reduce the residual elements to achieve the desired mechanical properties. The role of each of the alloying elements used in both grades of steels being examined is outlined below.

#### **2.2.1.a.1 Carbon**

Carbon is the principal hardening agent in steel. A decrease in carbon content improves the weldability of the steel by decreasing its hardenability of the weld zone. [Losz, 1990]

#### 2.2.1.a.2 Manganese

Manganese is an austenite stabilizer that helps to decrease the transformation temperature and slow the rate of transformation. This aids in the formation of finer grains of ferrite leading to increased strength and toughness in the steel. [Collins, 1983]

#### 2.2.1.a.3 Copper

Copper is added to steel due to its precipitation hardening ability, which increases the strength. [Loza, 1990]

#### 2.2.1.a.4 Nickel

The addition of nickel increases both the strength and toughness of steel. It is also helpful in improving the low temperature fracture toughness. [Collins, 1983]

#### 2.2.1.a.5 Chromium

Chromium is used to stabilize austenite promoting the formation of low temperature transformation products. [Collins, 1983]

#### 2.2.1.a.6 Niobium

Niobium is predominantly effective as a strengthening mechanism via grain refinement. It is the most important element in retarding austenite recrystallization [Hulka, 1988]



#### 2.2.1.a.7 Vanadium

Vanadium is particularly effective in precipitation hardening which has a detrimental effect on toughness. [Hulka, 1988] It causes an increase in the ferrite start temperature and therefore promotes the formation of ferrite.

#### 2.2.1.a.8 Molybdenum

Molybdenum additions to steel affect the decomposition kinetics in the 600-700<sup>0</sup>C range. It causes a shift in the CCT diagram promoting the formation of acicular ferrite and bainite rather than ferrite and pearlite. [Collins, 1983]

#### 2.2.1.a.9 Aluminum

Aluminum is an austenite stabilizer, which leads to fine austenite grains and subsequent fine ferrite grains increasing both the strength and toughness. [Sage, 1983]

#### 2.2.1.a.10 Nitrogen

The benefit of nitrogen comes from its interaction with other alloying elements to form nitrides. Ti, Nb, and V all form nitride particles that are effective in increasing the austenite grain growth temperature. This prevents grain growth during the high temperatures experienced during welding. [Zajac, 1995]

#### 2.2.1.a.11 Titanium

When combined with nitrogen, TiN particles, which are stable at the high peak temperatures associated with welding, limit grain growth in the HAZ, which helps to ensure adequate toughness and strength. [Hulka, 1988]

#### 2.2.1.a.12 Sulphur and Phosphorus

Both sulphur and phosphorus exist as impurity elements. Modern microalloyed steels typically have combined levels less than 0.025%.

### 2.2.2 Mechanical Properties

#### 2.2.2.a.1 Tensile Properties

In order to obtain adequate strength levels in thicker sections of steel, manufacturers often add additional carbon to the chemistry. While this does improve the tensile strength of the material it has little effect on the yield strength. Yield strength is the standard by which many new designs are based upon, requiring that a steel meet a Specified Minimum Yield Stress (SMYS) and not a set tensile strength. The chemical composition of TMCP steels does not provide a good indication of strength level as the rolling and cooling schedule have a major effect. As steels increase to higher and higher tensile strength levels, the ratio of the yield stress to the tensile stress decreases. Normalized steels typically have ratios in the 0.70 range whereas TMCP steels are often in the 0.90 range. This increase is a concern because it reduces the strain hardening capacity of the steel making its ability to redistribute strains around defects much more difficult. The

concern is somewhat reduced due to the steel's higher toughness values, which decreases its notch sensitivity. [de Meester, 1997][Somers, B, 1993]

#### 2.2.2.a.2 Toughness

There are many different ways of defining a materials toughness. Most methods assess the toughness in relation to the application of the material. The two common assessments used in the evaluation of steels are the charpy and drop weight tear test ductile energy shelf and impact transition temperature. It is well known that decreasing the carbon content of steel reduces the impact transition temperature and extends the ductile energy shelf. [Gladman, 1997] Because of the low carbon contents of TMCP steels, they can be customized in terms of composition, microstructure, and processing to achieve the varying toughness requirements necessary for different applications. [de Meester, 1997]

#### 2.2.3 Effect of Chemistry and Mechanical Properties on Weldability

The main effect of chemistry on the weldability of TMCP microalloyed steel is the reduction in hardenability through reduction in carbon content. Lowering the carbon content of steel for welded constructions allows for crack free welding at reduced or even eliminated preheat. As a result, modern structural steels are based on less than 0.10%C, guaranteeing also that significant deterioration of the heat affected zone toughness by local brittle zones (LBZ) is avoided. [Hulka, 1999] The addition of alloying elements such as Ti, Nb, and V has led to improved properties in the HAZ by promoting the formation of low temperature transformation products. While mechanical properties do not have a direct effect

on welding, the main strengthening mechanisms use in microalloyed TMCP steels are adversely affected by welding. With higher levels of strength, it is increasingly difficult to produce welds with satisfactory properties.

### 2.3 Microstructure

A basic understanding of the microstructure of steel starts with the examination of the iron carbon phase diagram show in Figure 2-2.

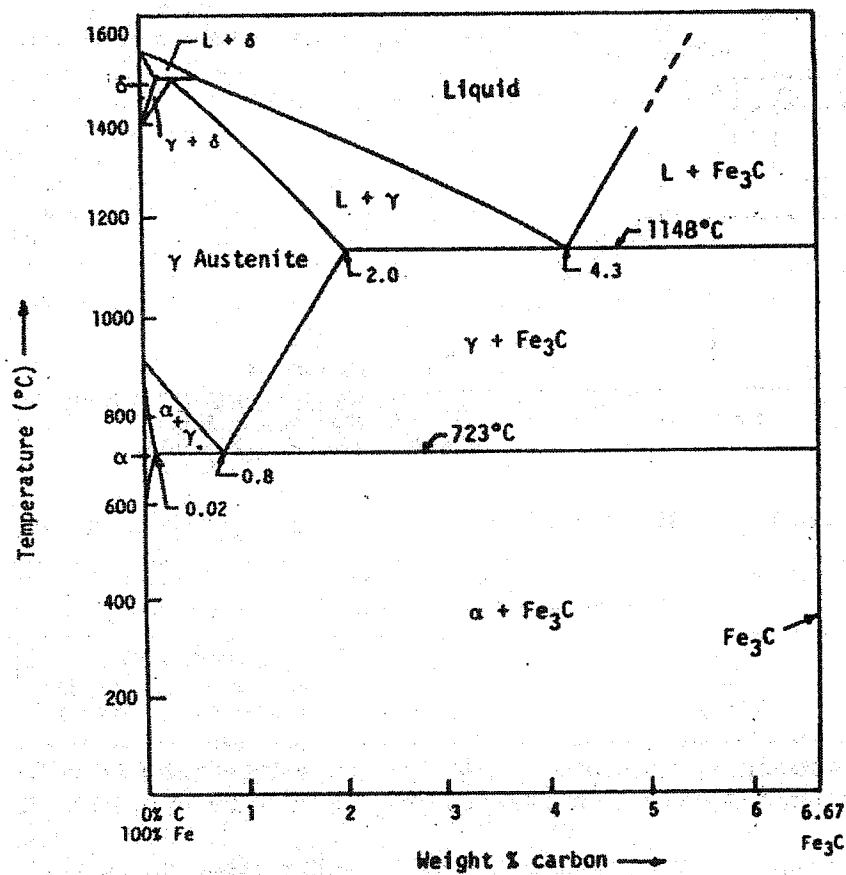


Figure 2-2 Iron Carbon Phase Diagram [Smith, 1993]

The diagram shows the various phase transformations that occur in steel during heating or cooling under equilibrium conditions. For the purpose of understanding the structure of modern TMCP steel, the regions of interest on the

diagram are the austenite ( $\gamma$ ) to ferrite ( $\alpha$ ) region at carbon contents below 0.8%.

In this region austenite with transform to a two-phase structure of ferrite and cementite. The amount of the ferrite & cementite depends on the carbon content of the steel and the other alloying elements. [Smith, 1993] In the steel making process, steel is not formed under equilibrium conditions. The microstructure that results, is dependent upon both the chemistry of the steel and processing that it undergoes.

In order to understand the effects of welding on the microstructure of TMCP microalloyed steels, the microstructure of the as rolled steel along with the various transformation products that can form in these steels must be examined. The microstructure of steel is governed by the kinetics of transformation making the structure dependant on the time and temperatures experienced during processing. The effects of time and temperature on the structure of steel is best represented in a continuous cooling transformation (CCT) diagram as shown in Figure 2-3.

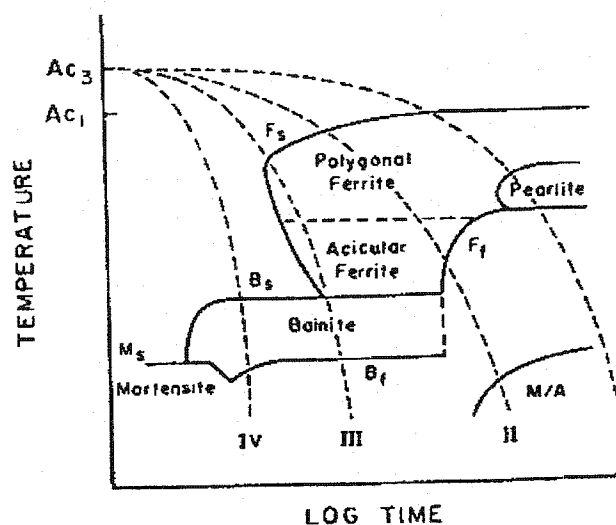


Figure 2-3 CCT Diagram for Microalloyed Steel [Collins, 1983].

While this CCT diagram is representative of microalloyed steels, the features of a specific steel will depend on the exact chemistry and processing history. In general, the common microstructures found in microalloyed steels are polygonal ferrite, acicular ferrite, bainite and martensite. [Collins, 1983] A description of the features associated with each of the microstructures is given in the following sections.

### 2.3.1 Polygonal Ferrite

Polygonal ferrite forms when cooling from the austenite region is slow enough to allow the transformation to approach equilibrium conditions. When the temperature of the steel is between  $900^{\circ}\text{C}$  and  $700^{\circ}\text{C}$  ferrite starts to nucleate and grow on grain boundaries. The carbon in the solution is able to diffuse to the remaining austenite causing the carbon concentration in the austenite to increase. As more and more grains of ferrite form, the remaining austenite approaches the eutectoid composition causing the remaining austenite to turn into pearlite. The

addition of carbide forming elements such as Nb, Ti, and V and the reduction in carbon content found in modern TMCP microalloyed steels can result in a structure that is free of pearlite. A typical micrograph of polygonal ferrite is shown in Figure 2-4.

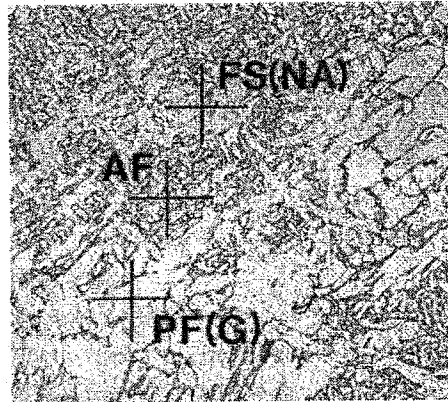


**Figure 2-4 Optical Micrograph of Polygonal Ferrite(PF).**

### 2.3.2 Acicular Ferrite

As the rate of cooling is increased austenite will transform at a lower temperature into a fine irregular structure called acicular ferrite. Acicular ferrite is a highly substructured, non-equiaxed ferrite. It forms by a mix of diffusion and shear processes at temperatures above the bainite start temperature and tends to form intragranularly. An example of acicular ferrite is shown in Figure 2-5.

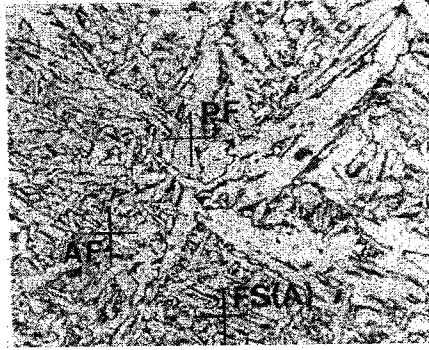


**Figure 2-5 Optical Micrograph of Acicular Ferrite (AF).**

As shown in the figure, the microstructure consists of irregularly shaped ferrite grains with indistinct planar boundaries. The parallel and planar segments seen on individual grains suggest a preferred orientation relationship with prior austenite grains. Prior austenite grain boundaries are not visible in this structure as the ferrite nucleating at the boundary grows into adjoining grains. [Collins, 1983] Alternatively, the ferrite may nucleate within austenite grains, which also tends to mask prior austenite grain boundaries.

### 2.3.3 Bainite

Bainite forms in steel when austenite transforms below the acicular ferrite temperature and above the martensite start temperature. Bainite when present in steel, usually exists as only a minor component. [Collins, 1983] Its structure when examined optically is very similar to acicular ferrite with the main difference being a more elongated structure. Upper bainite forms by a shear transformation when carbon diffusing into the austenite ahead of the  $\gamma/\alpha$  interface is trapped between laths. Lower bainite traps some of the carbides within the laths. The trapped austenite may remain between the laths or transform into martensite or cementite. Unlike acicular ferrite, prior austenite grain boundaries



are visible in bainite as the laths cannot extend across grain boundaries. [Collins, 1983]

#### 2.3.4 M/A Constituent

Small areas of martensite mixed with retained austenite (M/A) can form in steel if the carbon content in the final amounts of austenite to transform is high enough. Steels with high alloy content favor the formation of martensite while a low alloy steel favors the formation of bainite. [Collins, 1983]

### 2.4 *Welding Process*

Microalloyed TMCP steels can be welded using any of the common arc welding processes. [Gladman, 1997] The most common processes employed by fabricators are shielded metal arc welding (SMAW), gas metal arc welding (GMAW), flux cored arc welding (FCAW), and submerged arc welding (SAW). The three processes that will be used in this study are SMAW, GMAW and gas tungsten arc welding (GTAW) with the latter being used to form weld metal without changing chemistry. The following section taken directly from the AWS Welding Handbook Vol 2: Welding Process, outlines the essential elements of each of the processes used in this study.

#### 2.4.1 Gas Tungsten Arc Welding

Gas Tungsten Arc Welding (GTAW) is a welding process that uses a nonconsumable tungsten electrode to create an arc between a torch and the base

material. In the process, inert or reducing shielding gas is passed through the torch to provide shielding against atmospheric contamination for the electrode and weld metal. An arc, which is produced when current is passed through the conductive shielding gas, melts the base metal without melting the electrode. When a weld pool of sufficient size is generated, the arc is moved along the joint. A typical GTAW operation is shown in Figure 2-6.

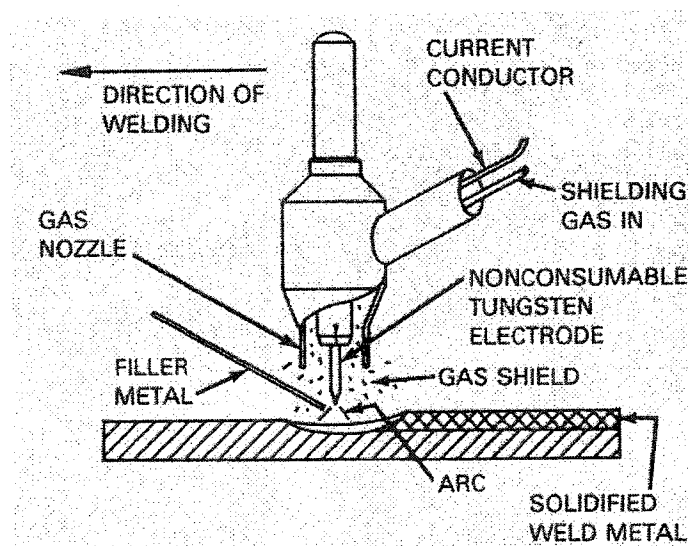


Figure 2-6 Typical GTAW Setup [AWS, 1991]

The advantages of the GTAW process are it produces superior quality welds without spatter, which are generally free of flaws due to a lack of gas metal reactions. It can be used with or without filler metal allowing for the production of autogenous welds. There is precise control over the welding variables and there is independent control over the heat source and filler metal additions. Even with the high quality of welds produced there are limitations. Deposition rates are

low in comparison to other processes that use a consumable electrode and the gas shielding can be displaced by drafts.

The primary variables in the GTAW process are the current, voltage, speed, and shielding gas, all of which are somewhat interdependent. Current controls the penetration of the weld with higher values causing deeper penetration. It also affects the voltage, as the voltage of a fixed arc length increases in proportion to the current. Current can be either direct or alternating depending on the material to be welded. Direct current (DC) with the electrode negative is the most common setting as it allows for deep penetration and fast welding speeds. Using an electrode positive setting is rare as it causes overheating of the electrode. The use of alternating current (AC) is generally restricted to aluminum and magnesium as it provides a cathode cleaning effect that removes oxides from the surface. Arc voltage is the measure of the potential drop between the electrode and the work piece. It depends on the current, shape of the electrode, distance, and the type of shielding gas. Voltage controls the length of the arc, which in turn controls the width of the weld pool. Travel speed affects both the width and penetration of the weld with slower speeds producing wider and deeper welds. The main significance of welding speed is that it governs productivity. As a result, the other variables are usually set around speed to make the process economical.

The set up used in this study consists of a water cooled torch with a 2% thorium oxide tungsten electrode on a constant current power source set on DCEN. Pure Argon gas is used as the shielding gas. A water-cooled torch is used to allow for higher currents on a continuous duty cycle. The addition of thorium oxide to tungsten improves the thermionic emission of the electrode enabling the use of higher currents. In the DCEN setting, electrons flow from the electrode to the workpiece with positive ions flowing in the reverse. With this setting, approximately 70% of the heat is generated at the anode (work piece), which helps to give deep welds. Argon is used as a shielding gas for the GTAW process because of its low cost, availability and its lower ionization potential. Figure 2-7 shows the equipment used in the GTAW process.

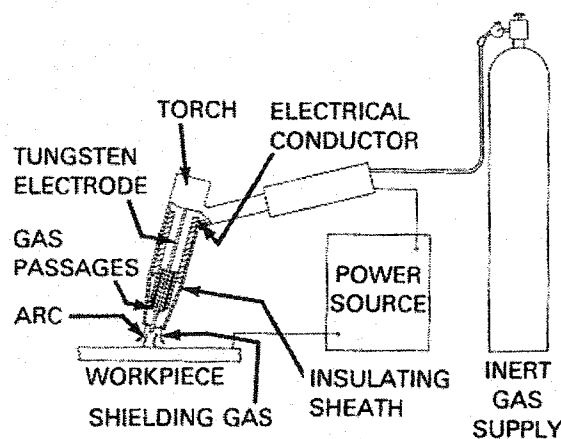
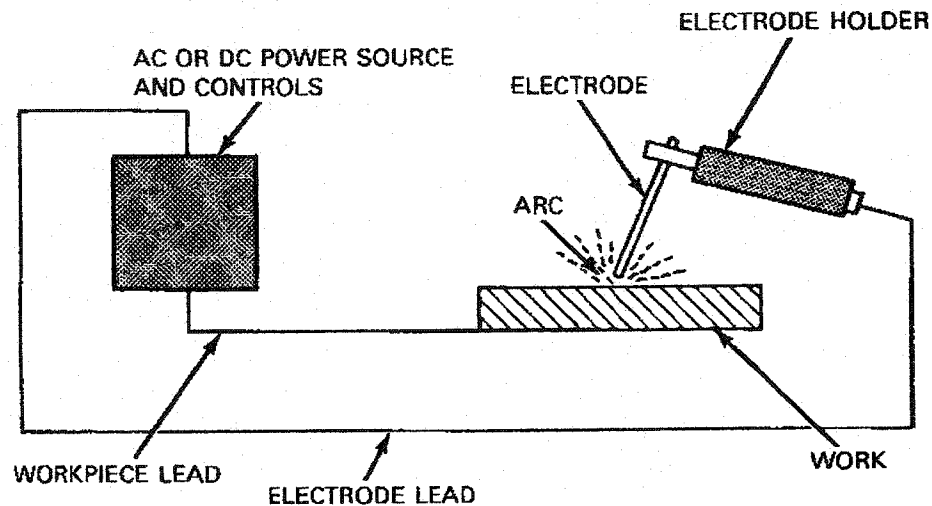


Figure 2-7 Typical GTAW Equipment [AWS, 1991].

#### 2.4.2 Shielded Metal Arc Welding

Shielded Metal Arc Welding (SMAW) is the most commonly used welding process. In this process, the heat of the arc is used to simultaneously melt both the base material and the tip of the electrode. The process consists of simple

electrical circuit consisting of a power source, welding cables, electrode holder, ground connection, work piece, and an electrode. A typical circuit is shown in Figure 2-8.



**Figure 2-8 Typical Circuit for SMAW [AWS, 1991].**

Welding starts when an arc is struck between the electrode and the work piece by bringing the electrode in close enough proximity to overcome the potential threshold. This usually requires the electrode to be scraped against the work piece. The heat produced from the arc melts the base metal and the tip of the consumable electrode simultaneously. Small droplets of metal are transferred from the electrode, through the arc and to the base material by various arc forces. The filler metal is continuously added as electrode is consumed. The arc is moved over the length of the work piece at an appropriate arc length and travel speed to control the heat input. Figure 2-9 illustrates the SMAW process.

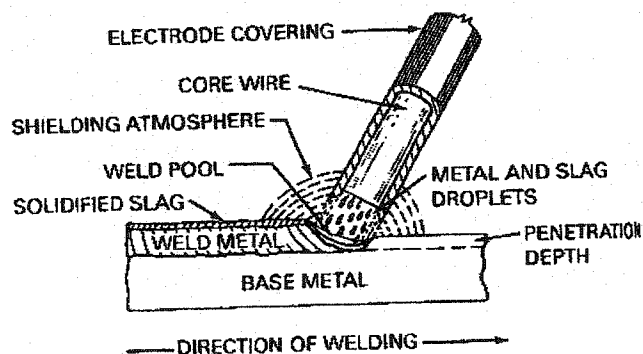


Figure 2-9 SMAW Process [AWS, 1991].

As with other welding processes, the primary variables in SMAW are current, voltage, travel speed and the electrode type. Welding is typically carried out using a constant current power source in either the DC or AC mode. The process requires that enough current is available to melt the electrode and an appropriate amount of base material. Typical values range from 20 to 550 amps. The gap between the electrode and the work piece, which is controlled manually by the welder, determines the circuit voltage. Considerable skill is required to maintain a constant arc length during welding. The voltage typically ranges from 16 to 40 volts. The travel speed, which is also controlled manually by the welder or through the use of a guide, must be slow enough to provide complete fusion with the base material and fast enough to prevent excessive metal build-up and to be productive. While there are a number of different electrodes available, all consist of a metal core and a flux covering. The covering on the electrode serves a number of functions. It provides a shielding gas for the arc to prevent atmospheric contamination and provides the fluxing agents required to produce a clean weld. It forms a protective slag on top of the weld bead to shield the hot

metal from the air. It also establishes the electrical characteristics of the arc and provides a mean to add alloying elements to the deposited metal.

The wide spread use of SMAW can be attributed to a number of factors that make it more viable than other welding processes. The equipment required for the process is relatively inexpensive and is portable making it viable for field and repair work. The large number of commercially available electrodes makes SMAW viable for most of the commonly used steels. There are, however, a number of drawbacks associated with SMAW. When compared with other welding methods SMAW is far less productive in terms of metal deposited per hour due to the limited electrode length and the time required for slag removal.

#### 2.4.3 Gas Metal Arc Welding

Gas Metal Arc Welding (GMAW) is a welding process in which an arc is produced between a continuous consumed metal electrode and the work piece. The arc is shielded from the atmosphere by an inert or slightly oxidizing gas. When a current is passed through the shielding gas, an arc is initiated causing the simultaneous melting of the electrode and base metal. A typical GMAW set up is shown in Figure 2-10.





is used to guide the electrode and deliver the electric current and shielding gas to the work piece.

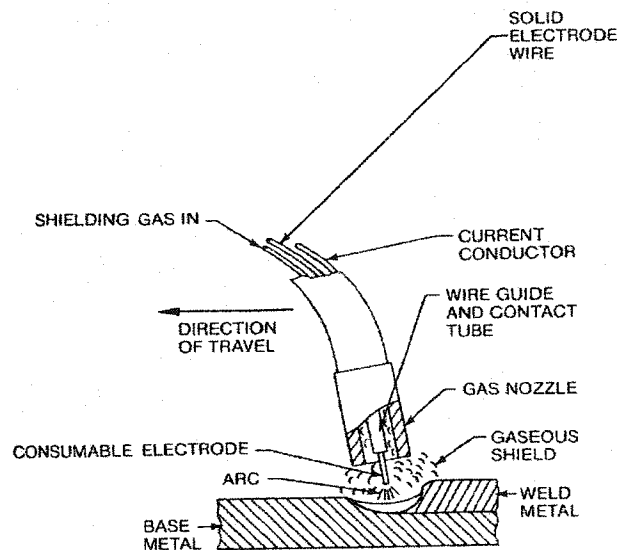


**Figure 2-11 GMAW Gun [AWS, 1991].**

Power sources for the process can be either a constant voltage with a constant speed electrode feeder or a constant current with an arc voltage controlled electrode feed unit. The constant voltage supply is the most common power source. With this source, changes in the position of the torch or length from the electrode tip to the work piece will cause an immediate change in the current to maintain the desired heat input level.

The process utilizes one of three modes of metal transfer to move molten metal from the electrode to the work piece. The first mode of transfer, which occurs at low current levels, is short-circuiting. Short-circuiting transfer is typically used for welding thin materials, out-of-position welding and for large root openings.

Molten metal is transferred from the electrode to the work piece when the pool at the end of the electrode is large enough to contact the base material and cause a short circuit. When the molten metal contacts the work piece, the current increases and pinches off the metal, thus reestablishing the arc. No metal is transferred across the arc. Short-circuiting typically occurs at a rate of 20 to 200 times per second. The second mode of metal transfer is globular. In globular transfer, molten metal is melted at the electrode tip until the volume of metal is large enough to be acted upon by gravity. Globular transfer occurs in the direct current electrode positive setting (DCEP) at low current settings or at any current settings if carbon dioxide and helium are used as a shielding gas. In order to prevent the molten drop from short-circuiting with the base metal, the arc length must be long enough to allow for metal detachment. The third form of metal transfer is spray or small droplet. When welding is carried out in the DCEP setting at a current level above a critical transition level in the presence of argon shielding gas, an axial spray of metal can be established. Below the transition current level globular transfer (dominated by gravity) will occur, but when the current is increased above this value, transfer will occur in the form of many droplets per second. At the higher current levels, the low thermal conductivity of the argon shielding gas causes the arc area to move up from the bottom of the electrode to surround the electrode tip. This results in an increase in the arc forces present, causing the tiny droplets of molten metal to be continuously stripped of the electrode. [Patchett, 2001] A fourth form of metal transfer also exists between

the globular and spray transfer settings. Pulsed transfer occurs by alternating current levels between the globular and spray settings.

Due to the complexity of the GMAW process, there are a number of process variables to consider. All the variables are somewhat interdependent upon each other, as a change in one variable usually requires a change in another variable. The welding current is dependent upon the feed rate of the electrode. As the feed rate of the electrode is increased the current must also be increased. Increasing the current will result in an increase to the size of the weld zone and an increase in deposition rates. Welding is usually done in the DCEP setting due to the stable arc and smooth metal transfer that results. The arc length is the distance between the tip of the electrode and the work piece. The arc voltage is dependent on the arc length and other variables such as the electrode, shielding gas and length of the welding cables. Changes in the arc length can result in porosity and spatter if the voltage is too high, while a low arc length results in a deep narrow bead with high penetration. The rate of travel during welding affects the degree of penetration. At low travel speeds the arc can impinge on the molten weld pool rather than the base metal, reducing the penetration. At high rates of travel there is a tendency for some undercutting to occur, as there is insufficient heat available to melt the necessary amount of base metal. Obtaining the correct travel speed requires trial and error to produce the appropriate degree of penetration and the correct weld profile. The distance between the electrode tip and the bottom of the contact tube is referred to as the electrode extension. The electrode extension determines the electrical resistance in the electrode. As the extension is increased,

there is an increase in the electrical resistance of the electrode, which causes the temperature of the electrode to increase, thereby increasing the melting rate. Unless corrected by the welding machine controls, the metal will be deposited with a high crown on the weld bead. Other variables that can affect the properties of GMAW are the electrode orientation and weld joint position. All of the welds carried out in this study were done in the flat position with the electrode in the vertical position to minimize the effects of both of these variables.

Regardless of the process used, low hydrogen procedures are required to avoid cracking in most carbon and low alloy steels. Development of a qualified welding procedure requires consideration of the preheat, heat input, and consumables necessary to produce quality welds. [AWS, 1998]

#### 2.4.4 Preheat Requirements

From a manufacturing perspective, one of the main advantages of TMCP steels is that they generally do not require a preheat. If a preheat is required, it will depend upon the thickness of the material, filler metal, and welding process (hydrogen level) being used. [AWS, 1998] With the development of lower hydrogen potential consumables, the possibility of welding thicker sections of steel without a preheat is becoming more feasible. [Kinsey, 2000] In order to develop a qualified welding procedure, attention must be given to the preheat along with the levels of hydrogen in the process. The use of a preheat is beneficial because it reduces the cooling rate in the weld zone, which can prevent the formation of martensite, resulting in a softer HAZ. It also enables more hydrogen to diffuse

out of the weld zone thereby reducing the possibility of cold cracking. [Kotecki, 1994] Preheating also helps to reduce the high stress levels that develop in welds during solidification. [de Meester, 1997]

The level to which a material should be preheated should be based on the chemistry of the base and filler metals. This can be done using a carbon equivalent and composition parameter formula such as the,

$$CE_{I\dot{W}} = C + \frac{Mn}{6} + \frac{Cr + Mo + V}{5} + \frac{Ni + Cu}{15}, \text{ I\dot{W} formula.}$$

$$P_{cm} = C + \frac{Si}{30} + \frac{Mn}{20} + \frac{Cu}{20} + \frac{Ni}{60} + \frac{Cr}{20} + \frac{Mo}{15} + \frac{V}{10} + 5B, \text{ Ito-Bessyo for pipeline steels.}$$

$$CE = C + \frac{Mn}{6} + \frac{Si}{24} + \frac{Cr}{5} + \frac{Mo}{4} + \frac{V}{14} + \frac{Ni}{40}, \text{ for low carbon steel.}$$

Using these values, recommended preheats and interpass temperatures can be looked up in tables depending on the level of restraint that will be present. [AWS, 1998]

The preheat temperature used must be high enough to prevent cracking in combination with the heat input and level of diffusible hydrogen. In order for the preheating to be effective, it must be done in a region at least equal to the thickness of the joint or 75 mm (3 inches), with the larger of the two governing. [AWS, 1998] Past experience has shown that it is not necessary to preheat TMCP steels with  $CE_{I\dot{W}}$  values of 0.30-0.35 and thicknesses below 40mm if low hydrogen filler metals are used. [de Meester, 1997]

### 2.4.5 Heat Input

It is necessary to control the level of heat input during welding to ensure that it is neither too high or too low. The heat input is a function of the welding current, arc voltage, and welding speed. It is calculated according to the equation

$$HI(kJ/mm) = \frac{I \times V \times n}{u \times 1000}, \text{ where } I \text{ is the current in amps, } V \text{ is the voltage in volts, } n$$

is the process efficiency (assumed to be 1.0 for industrial purposes) and  $u$  is the welding speed in mm/sec. The heat input and thickness of the material being welded determine the thermal cycle. If the heat input is too high, significant grain growth can occur in the HAZ of the base material along with the dissolving of precipitates. This will result in a decrease in the strength and toughness of the weld zone. Decreasing the heat input will minimize grain growth and dissolution but if it is too low, the cooling rate will be high, producing a bainitic or martensitic type microstructure. Toughness will be decreased although strength is high. Because it is often not possible to restore the mechanical properties of the welded regions with a heat treatment, control of the heat input is very critical. [AWS, 1998] [de Meester, 1997]

### 2.4.6 Consumables

The primary considerations when selecting a filler metal to be used in the welding of TMCP microalloyed steels is whether or not the weld metal is chemically compatible with the base metal and can it provide satisfactory mechanical properties. These characteristics are determined by the:

- Chemistry of the electrodes

- Dilution of the base metal (amount of base metal that is melted and mixed into the weld pool)
- Flux system or shielding gas
- Weld-pool solidification and subsequent cooling and transformation

Selection of a filler metal is not done based on the chemistry of base material but on the service properties required of the weld. The use of a filler metal with a similar chemistry to that of the base metal can result in large discrepancy in properties due to the change in microstructure resulting from the rapid cooling rates imposed by the welding process.[ AWS, 1998] [de Meester, 1997]

The melting of the base metal and filler metal during the welding process results in a deposit that has a overall composition somewhere between the two materials. Depending on the heat input of the process and the joint configuration, the dilution of the weld metal can be between 5% and 25%. In creating a welding procedure, the amount of dilution that will occur must be taken into consideration in order to obtain the desired properties in the resulting weld. [AWS, 1998] [de Meester, 1997]

## ***2.5 Weld Zone Properties***

As a result of welding a unique area of varying properties and microstructures is created in the area surrounding a weld. The weld zone consists of the weld metal, the heat affected zone (HAZ) and the unaffected base metal as seen in Figure 2-12.

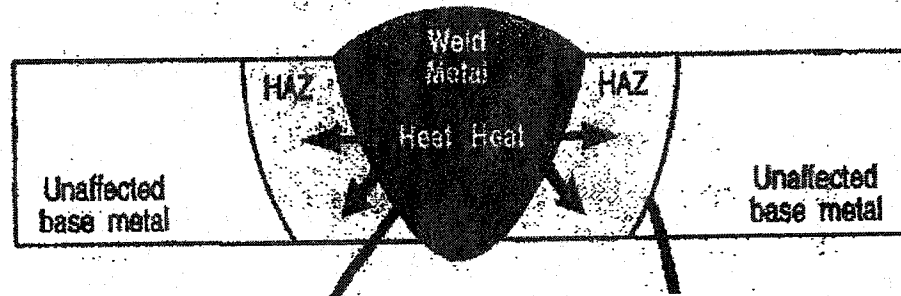


**Figure 2-12 Schematic Illustration of the Various Zones in a Weld. [Patchett, 1998].**

The variations in properties that exist in the weld zone are a result of the different thermal cycle each area experiences. This section will examine the effect of welding on the areas in the weld zone.

### 2.5.1 Weld Metal

The weld metal is essentially a cast structure that solidifies under very different conditions than typical castings. The main differences between typical cast structures and weld metal are:

1. The weld metal must create a metallurgical bond with the base material, where as cast material must release from its mold.
2. There is constant source of heat addition in a weld compared to no heat addition to the as cast material.
3. Solidification at the fusion line occurs as epitaxial growth, whereas casting involves heterogeneous nucleation at the mold wall.
4. The stirring action of the arc results in thorough mixing of the molten weld pool, compared to restricted mixing in the casting.

As a result of these differences the structure of weld metal is quite different from that of cast metal. [ASM, 1998]



The resulting microstructure and properties of the weld metal are affected by variables such as the weld metal chemistry, welding speed, thermal cycle, and base metal chemistry. While a number of these variables have been addressed in previous sections a few variables still need to be covered. The welding speed has two important effects. For a set current and voltage, increasing the welding speed results in a decrease in the heat input (see Section 2.4.5) and a decrease in the size of the weld pool. Changes in the speed of welding affect the mode of crystal growth in the weld pool. Slow rates of welding allow crystal growth to keep up with the heat source in an orderly and symmetrical way, while increased rates cause the crystals to make sudden changes in direction at the centerline to maintain the continuity of the weld. [Easterling, 1983] The effect of welding speed is shown in Figure 2-13. Even though Figure 2-13 c shows the presence of heterogeneous nucleation of grains in between the adjacent columnar grains, it is the authors' belief that this is a result of sectioning the sample in the alternate direction. The perceived heterogeneously nucleated grains are usually the ends of columnar grains.

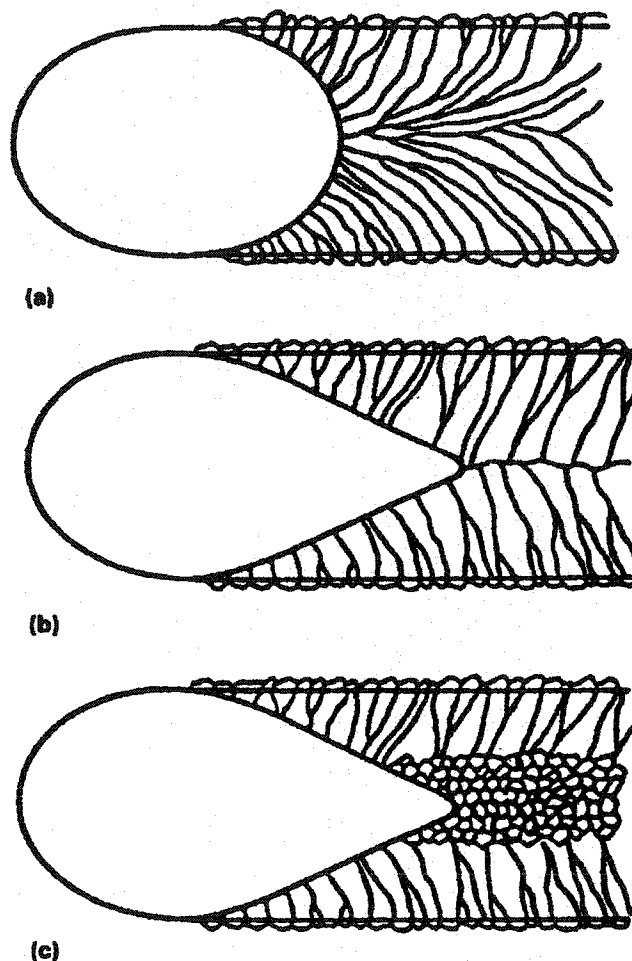


**Figure 2-13 The Effect of Heat Input and Welding Speed on the Shape of the Weld and Mode of Crystal Growth. (a) Low heat input and low welding speed, (b) High heat input and high welding speed, (c) High heat input and high welding speed, with heterogeneous nucleation at the weld pool centerline. [ASM, 1998]**

The composition of the weld pool is controlled by the amount of base material that is melted into the pool and the composition of the filler metal. The composition of the weld pool along with the thermal cycle determines what the resulting microstructure will be. The microstructure resulting from consumables used in the welding of TMCP microalloyed steel is usually a ferritic weld metal. Characterization of the various microstructures that can form in the weld pool is complicated by the large amount of terminology used to describe various

microstructures. As a result, characterization of the weld metal microstructures will be done in accordance with the IIW "Guide to Light Microscope Examination of Ferritic Steel Weld Metals". The basis of the guide is to provide a systematic approach to classification of microstructures. A description of the various constituents as taken from the guide is given below.

**Primary Ferrite: (PF)** can occur in two forms.

**Grain boundary ferrite: PF(G)**

Ferrite (veins or polygonal grains) associated with prior austenite grain boundaries.

**Intragranular polygonal ferrite: PF(I)**

PF(I), Ferrite grains, usually polygonal, found within prior austenite grains, and which are larger than about three times the average width of surrounding AF or FS laths (defined below).

**Acicular Ferrite: AF**

Small non-aligned ferrite grains found within prior austenite grains. A region of AF often includes isolated laths of high aspect ratio (ratio of major to minor axes).

**Ferrite with Second Phase: FS**

This may occur in two forms, which may be counted as separate constituents if the operator is confident that the distinction is clear:

**Ferrite with Aligned Second Phase: FS(A)**

Two or more parallel laths of ferrite. Where there are only two laths, these should be classified as FS if their aspect ratio is greater than 4:1.

Otherwise class as AF or PF.

If the operator is confident that this constituent can be identified as side plates, bainite, upper or lower bainite, then it should be abbreviated as FS(SP), FS(B), FS(UB), or FS(LB). However, these distinctions will not normally be possible when using the light microscope alone.

**Ferrite with Non-Aligned Second Phase: FS(NA)**

Ferrite completely surrounding either (i) microphases which are approximately equiaxed and randomly distributed or (ii) isolated laths of acicular ferrite.

**Ferrite carbide aggregate: FC**

Fine ferrite/carbide structures, including ferrite with interphase carbides and pearlite. If the aggregate can be clearly identified as pearlite, it should be termed FC(P). If the colony is smaller than adjacent laths within prior austenite grains, it should be treated as a microphase.

**Martensite: M**

Colonies of martensite, which are larger than adjacent ferrite laths within prior austenite grains. Smaller colonies should be treated as microphases. If the operator is confident that this constituent can be identified as either lath or twinned martensite, then it should be abbreviated as M(L) or M(T).

However, this distinction will not normally be possible when using the light microscope alone.

### 2.5.2 Weld Metal Properties

As with most materials, it is desirable that the yield and tensile strength of the weld metal be equal to or slightly higher than that of the base metal. This becomes more difficult as the strength levels of base materials keep increasing. With increasing strength levels and decreasing carbon equivalents in the base metal, the carbon equivalent of the weld metal may become much higher than that of the base plate, making cracking of the weld metal much more likely. One of the most difficult tasks in welding TMCP steels is to obtain a balance between the toughness and the strength levels. The best balance is obtained when the resulting fusion zone has an acicular ferrite microstructure. In order to obtain acicular ferrite with the required strength and toughness levels, the composition of the weld metal and the welding procedure must be tightly controlled. This can usually be attained if manufacturers recommendations are closely adhered to. If welding is carried out at high heat inputs, dilution of the weld metal may become substantial. A change in the hardenability of the weld metal will result, along with changes in the alloying levels. Changes in the microstructure will occur as the compositions of the base and filler metal will be different. [de Meester, 1997]

### 2.5.3 HAZ Properties

The metallurgical and mechanical properties of the HAZ are directly related to that of the base metal. Problems encountered in the HAZ are much more difficult

to control when compared with those encountered in the weld metal. While some degree of control can be maintained over the HAZ through the use of preheats and welding parameters, the characteristics and mechanical properties of the TMCP processes may be altered. [ Somers, 1998] [de Meester, 1997]

#### 2.5.4 HAZ of Single Pass Welds

The heat-affected zone of a single pass weld can be divided into a number of distinct zones depending upon the peak temperature. The zones are the unmixed zone, partially melted zone (PMZ), course grain HAZ (CGHAZ), fine grained HAZ (FGHAZ), intercritical zone, and the subcritical zone. Each zone has a different microstructure and different mechanical properties due to the variations in peak temperature and time spent at temperature during the thermal cycle. A schematic diagram of the HAZ in a single pass weld is shown in Figure 2-14.

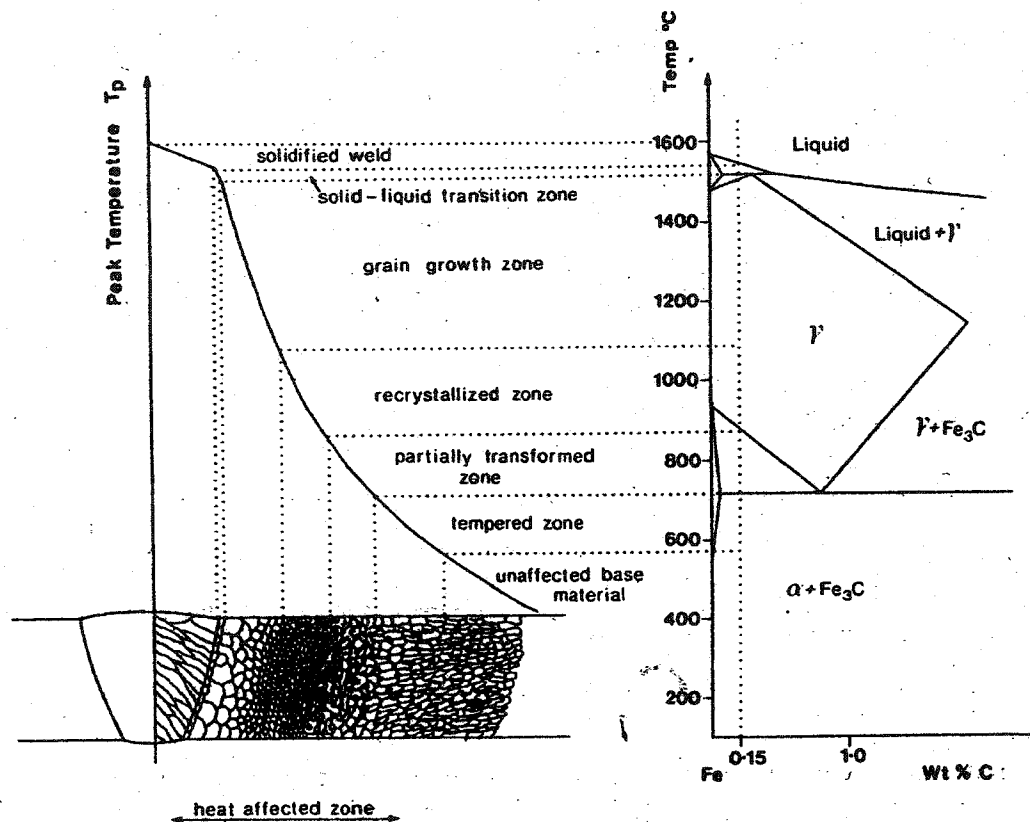


Figure 2-14 HAZ of a Single Pass Weld [Easterling, 1983].

The unmixed zone (UMZ) is the thin region between the weld metal and the HAZ. In this region, the molten material is not stirred into the bulk of the molten pool during welding. Next to the UMZ is the partially mixed zone. In this region the temperature is above the solid-liquid transition zone on the phase diagram. Here, some of the base material is melted into the weld metal.

The CGHAZ is the area next to the weld metal where significant grain growth occurs during welding. Temperatures in the region range between 1100 and 1450 $^{\circ}\text{C}$ , allowing for the formation and subsequent growth of austenite grains. The high temperatures experienced in the zone also lead to the dissolution of most precipitates. This results in an increase in the hardenability and the possible

formation of low temperature transformation products on cooling. The resulting microstructure in low carbon steels is typically bainitic or martensitic in structure due to the large austenite grains and limited nucleation sites. The transformation in microstructure is also accompanied by a decrease in toughness causing this area to be a major concern for joint integrity. [Losz, 1990]

In the FGHAZ, temperatures in the 850-950<sup>0</sup>C range are experienced by the base material. In this region the formation of austenite occurs but grain growth does not happen due to the large number of precipitates present and the short time spent in the temperature range. The precipitates that remain intact at these temperatures, restrict the grain growth of austenite by pinning grain boundaries. The resulting austenite grain size is therefore relatively small. The large grain boundary area present promotes the formation of ferrite due to the large number of nucleation sites that are present. [Losz, 1990]

The intercritical or partially transformed zone of the HAZ sees temperatures between the  $Ac_1$  and  $Ac_3$  region. As a result only areas rich in carbon will undergo a transformation to austenite. The resulting microstructure in the intercritical zone can vary from ferrite to martensite depending on carbon content and the thermal cycle. The remaining structure does not undergo any changes in microstructure thereby resulting in an area of mixed microstructures. Dislocation density reduction and precipitate coarsening are possible in this region. [Losz, 1990]



The subcritical zone of the HAZ is the region at which no visible effect of the welding process can be seen in the base material. Often referred to as unaffected base metal, the temperature in this region is not high enough to cause any changes in the base metal microstructure. [Losz, 1990]

The microstructures that form in various regions of the HAZ are essentially the same as those found in the weld metal. The classification system used to describe the structure of ferrite weld metal will also be applied to the HAZ.

#### 2.5.5 HAZ of Multi-Pass Welds

In the actual practice of welding, it is often necessary to use more than one pass to complete a weld. As additional passes are put onto the weld, the HAZ produced by the each pass will experience additional thermal cycles. The effects of multi-pass welding on the microstructure of the HAZ are shown in Figure 2-15. For point B, the CGHAZ is improved by the tempering and recrystallization effects of the second thermal cycle. For C and E, the structure is deteriorated by the second thermal cycle. At point C, the formation of martensite austenite (MA) constituents can occur on the austenite grain boundary by reheating into the two-phase region. These MA constituents become local brittle zones (LBZ) in the weld zone, which reduce the toughness of the HAZ. [Shiga, 1990] To improve the toughness in multi-pass welds, it is therefore beneficial to reduce the volume of MA constituents present. This can be achieved through careful weld procedure control and by reducing the levels of elements that promote the formation of MA.

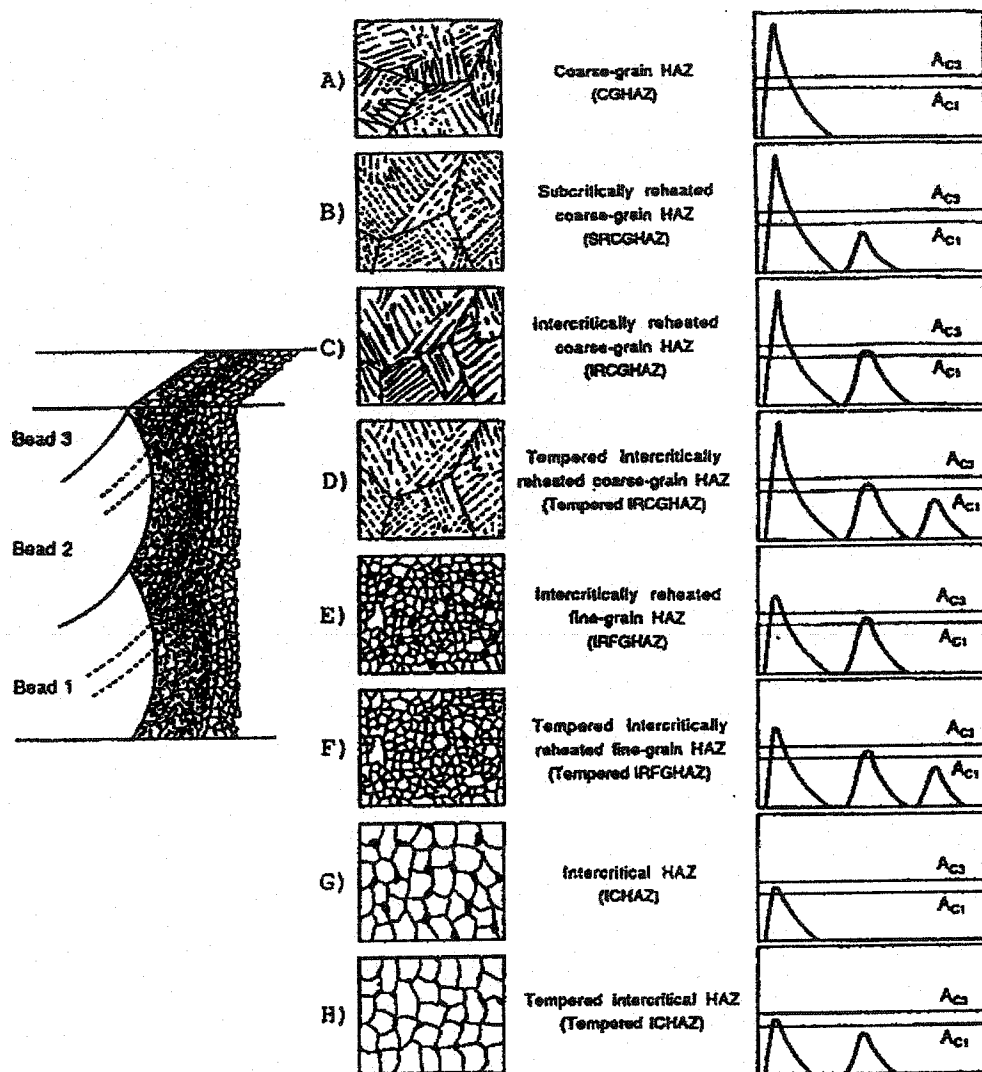


Figure 2-15 Schematic Illustration of the Effect of Multi-Pass Welding on the Microstructure of the HAZ.

### 2.5.6 HAZ Hardenability

Hardenability is the ability of a steel to form martensite on quenching. The ability to form martensite is dependent in turn on the ability to control the  $\gamma \rightarrow \alpha$  reaction

by suppressing the formation of other austenite decomposition products such as proeutectoid ferrite, cementite, pearlite and bainite. [Garcia, C, 1995]

Hardening of the HAZ is a serious problem in microalloyed steels as it is detrimental to the properties of the welded joint. The most critical region is the area closest to the fusion line where the austenite grain growth occurs. To control this problem, the hardness of the HAZ is limited to reduce the chance of cold cracking. A value of 300 – 350 HV is often set as a standard. While this is probably sufficient enough to avoid cold cracking in most steels, ultra high strength ( $YS > 690$  MPa) may still be susceptible at much lower values. [Somers, 1998] [de Meester, 1997]

#### 2.5.7 HAZ Toughness and Microstructure

The toughness of the HAZ is dependent upon its microstructure, which varies from the fusion line to the unaffected base metal. An optimum microstructure can be obtained through the use of the correct heat input. The optimum toughness will be attained when the resulting microstructure is lower bainite and it will gradually decrease as upper bainite is formed at slower cooling times. In the CGHAZ, grain boundary ferrite will form at prior austenite grain boundaries. Ferrite side plates and upper bainite will grow inwards rejecting carbon to the untransformed austenite. The austenite can then transform into mixture or non-transformed austenite and martensite known as martensite-austenite constituents resulting in a decrease in toughness. To improve the toughness in this region, the formation of MA constituents must be prevented or reduced. This can be

accomplished by reducing the area in which they can form or by altering the base metal chemistry to prevent their formation. [de Meester, 1997]

#### 2.5.8 HAZ Softening

Softening of the HAZ may occur in TMCP steels especially at high heat inputs as the microstructure is altered during the slow cooling. Slow cooling in the HAZ causes a deterioration in the toughness due to the coarsening of austenite and the subsequently transformed microstructure. [Jin, 1989] While softening does occur, it may not affect the overall strength of the weld zone due to the stronger weld metal and unaffected base metal on either side. This holds true as long as the width of the softened region is less than that of the materials thickness. [Somers, 1998] [de Meester, 1997][Jin, 1989] The toughness of the HAZ can also be maintained through the use of the particles such as TiN and Ca oxysulfide, which promote the formation of intragranular ferrite. The effect of heat input on the hardness in the HAZ of a TMCP steel is shown in Figure 2-16.

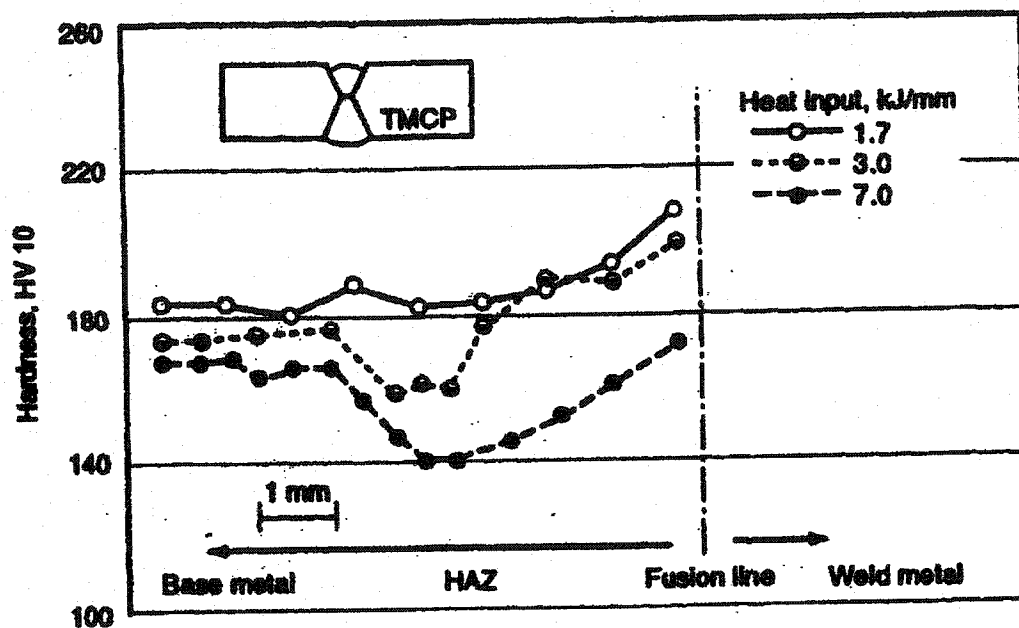


Figure 2-16 Variations in the Hardness in the HAZ of a TMCP Steel [ASM, 1998].

## 2.6 HAZ and Weld Metal Cracking

The severe thermal cycle and the high levels of restraint that occurred during the welding process often lead to the formation of cracks in either the base material or the weld metal. There are many forms of cracking that can occur as a result of the welding process. The common forms of cracking typically associated with structural steels are outlined below.

### 2.6.1 Hot Cracking

Hot cracking is a form of solidification cracking that result from the rejection of low melting constituents along the centerline of restrained welds. They occur at elevated temperatures after or during welding. The cracks are

generally a result of sulfur and phosphorus and are more common in high carbon steels. A steel's susceptibility to cracking can be evaluated based upon composition with empirical equations. The Weld Crack Susceptibility (WCS) equation;

$$WCS = 230C + 190S + 75P + 45Nb - 12.3Si - 5.4Mn - 1$$

where the elemental values are given in percent, indicates a high susceptibility to cracking with a resulting value greater than 30 and a low susceptibility with a value of 10 or less. Values between 10 and 30 indicate that welding procedures are the controlling factors. Hot cracking is more likely to occur with welding processes that have high amounts of dilution as the base material is usually the major source of sulfur and phosphorus. High welding speeds can also lead to the formation of cracks as a result of the teardrop shape produced, which promotes centerline segregation. Hot cracking can usually be avoided by keeping the combined sulfur and phosphorous level below 0.030%. Therefore, hot cracking is normally not a problem with microalloyed steel. [Lesnewich, 1998]

### 2.6.2 Lamellar Tearing

Lamellar tearing is a form of cracking that occurs in the base material when it is stressed through the thickness. The flaw normally occurs just below the HAZ and is most commonly found in steels that contain linearly aligned bands of inclusions. Propagation of the crack usually progresses from one inclusion to the next in a step-like fashion. There are many methods that can be employed to reduce the occurrence of lamellar tearing. Altering joint design to minimize strain in the through thickness direction, buttering the surface with weld metal, reducing

the amount of available hydrogen, and using preheat and interpass temperatures of 100°C are all effective methods. In modern steels, keeping sulfur levels below 0.008% along with the addition of sulphide shape controlling elements like Ca have helped to eliminate the problem even when joint restraint is very high. This type of cracking is typically not a problem any more, especially in steels less than 20 mm in thickness, and its occurrence in modern steel can be attributed to inadequate steel specification or incorrect structural design. [de Meester, 1997]

### 2.6.3 Reheat Cracking

Reheat cracking occurs at elevated temperatures during post weld heat treatments or after exposure to high in service temperatures. The cracks occur intergranularly in the CGHAZ or in the weld metal as a result of the precipitation of carbides within the grains. This causes an increase in the interior strength of the grain causing deformations to be confined to the grain boundaries. [Easterling, 1983] Impurity elements can enhance the tendency for cracking to occur by inter/intra-granular precipitation and/or segregation on prior austenite grain boundaries. While TMCP microalloyed steels are not particularly vulnerable to this form of cracking, due to low amounts of impurity elements, the problem becomes more of a possibility with increasing strength levels. [de Meester, 1997]

### 2.6.4 Cold Cracking

Also known as hydrogen assisted cracking (HAC), cold cracking occurs at temperatures below 200°C in weld zone usually within 72 hours of welding. In order for HAC to occur four requirements must be met,

1. Hydrogen
2. Tensile Residual Stresses
3. Susceptible Microstructure
4. Low Temperature

Hydrogen is a contaminant that is found in all arc welding processes due to its presence in water in fluxes, organic lubricants, and moisture in the air. The solubility of hydrogen in liquid iron at 1500 °C is about 30 ppm whereas it is 1ppm at 400 °C. With the rapid rates of solidification associated with welding, the hydrogen gas dissolves into the molten weld metal is retained as atomic hydrogen. While some of the hydrogen will escape from the weld, a significant amount is retained as atomic hydrogen dissolved in the lattice. [Somers, 1993]

While the weld pool is cooling, atomic hydrogen diffuses rapidly into the HAZ, some escapes into the air and the rest is trapped within the weld metal. Because hydrogen is so small compared to iron atoms, it is able to diffuse quickly into areas of discontinuity in the metal. In conjunction with the residual tensile stresses imposed by the shrinking of the weld metal, the hydrogen helps cracks grow at discontinuities. As atoms collect at these sites, stress will build up causing the crack to grow in order to relieve the stress. This will continue to occur until:

- The cross-sectional area is reduced enough to cause failure.
- Enough hydrogen escapes to lower its concentration below that required for cracking to proceed.



- Underbead cracks have reduced the residual stresses in the weld below the level needed for cracking to proceed.

The microstructure of the steel also plays an important role in cold cracking. The susceptibility of cracking decreases as the microstructure goes from martensite, to bainite, to ferrite. Inclusions in the steel also play a role in HAC, as they can act as a sink for hydrogen. With the extremely low levels of sulfur found in TMCP steels, these sinks are no longer sufficient. This renders the steel susceptible to HAC at a lower hydrogen concentration. The final requirement for HAC to occur is the need for a temperature below 200°C. At temperatures above 200°C, hydrogen will diffuse before it has time to build up at discontinuities in the weld. [Somer, 1993] [de Meester, 1997]

In order to prevent HAC from occurring in a weld, a number of approaches can be taken. Obvious steps would be to avoid susceptible microstructures, reduce the residual stresses, and reduce the amount of hydrogen present in the weld. While the option to be used is often influenced by cost along with the weld size and required properties, a combination of one or more of these steps can usually be employed. While the levels of residual stress and resulting microstructure will be fixed for a given welding set up, control over the cooling rates of the weld and hydrogen levels present is easily obtained. The rate at which the weld cools is determined by a combination of the ambient temperature, the joint thickness and the heat input of the weld. Slower cooling rates result from higher starting temperatures via preheating and from high heat inputs. Thickness of the joint also plays an important role as the body of the joint is a large heat

sink. Control over the level of hydrogen in a weld can be accomplished by varying the welding process and the consumables as shown in Table 2-1. [AWS, 1998]

**Table 2-1 Hydrogen Level in Various Electrodes [ASM, 1998 ].**

Type of Electrode	Diffusible H <sub>2</sub> , mL/100 g
GMAW solid wire	0 – 10
Basic SMAW electrode	3 – 20
Rutile SMAW electrode	20 – 40
SAW solid wire and flux	4 – 20
GMAW cored wire	3 - 30

The problem of predicting the susceptibility of a particular steel to hydrogen cracking has been examined over the last 60 years. Most efforts have centered on developing compositional type equations such as carbon equivalents as a means to measure the sensitivity to cold cracking. While carbon equivalents have been successful at determining process variables required to prevent HAC, they do not conclusively determine whether or not a weld will experience cold cracking. With conventional C-Mn steels, the presence of hydrogen has been a critical factor in preventing cold cracking as the high carbon content of these steels promotes the formation of martensite in the HAZ and diluted weld metal. The reduced carbon content of TMCP steels has made the HAZ zone less susceptible to HAC while shifting the probability of HAC to the weld metal.

## ***2.7 Post-Weld Heat Treatment***

Post weld heat treatment (PWHT) is a thermal cycle applied to a welded structure after the completion of welding. The goal of a PWHT is to reduce the level of residual stress in material after welding and to obtain a uniform microstructure in fabricated structure. [Somers, 1993] In general, PWHT steel should not be carried out on TMCP steels. Heat treating can alter the properties of the material attained during processing, resulting in a decrease in strength and toughness in the base material. With the reduction of carbon content, the need for post weld heat treatments should be negligible. [de Meester, 1997] While the base material should not require PWHT, the filler metals may require some heat treatment to prevent hydrogen build up and subsequent cracking. [AWS, 1998]

## ***2.8 Weldability Testing***

Weldability testing involves the testing of welded components for the purpose of procedural qualification and for evaluation of the effects of welding on base and weld metal properties. Tests involved in the procedural qualification include metallographic tests, destructive tests such as the tensile and the Charpy test, and nondestructive tests like magnetic particle and liquid penetrant inspection. These tests are usually carried out to meet the specifications of welding codes and standards to produce weld procedures. Weldability tests for the purpose of evaluating base and weld metal properties are carried out to examine characteristics such as cracking, ductility and bead formation.

Weldability tests are usually designed to be used as laboratory tests rather than production tests in the field. While actual service tests are the best means for evaluating the performance of a weld, the high cost to carry out service testing makes it impractical. As a result, welding tests are designed to evaluate specific problems associated with various welding conditions. Tests typically involve simple geometries and configurations with simple and uniform loading. Results obtained during testing are used to compare the effects of different variables on welding or to compare the response of varying materials to the same welding conditions. The tests used in this study and the variables associated with these are outlined below.

#### 2.8.1 Mechanical Testing

The only form of mechanical testing used in this study was the tensile test. Transverse tensile tests were carried out according to ASTM standards on composite coupons containing a weld in the center with base metal on both sides. The variables examined in the study include the affect of heat input and under and over matched weld metal strength on the yield and tensile strength of the material.

The effect of heat input on the strength of welds has been well documented. It is accepted that increasing the heat input will result in a decrease in tensile strength. This is a result of the changes in microstructures that result from varying heating and cooling rates. The change in yield strength of an AX-140 (GMAW) and an E11018 (SMAW) electrode as a function of cooling rate is shown in Figure 2-17.

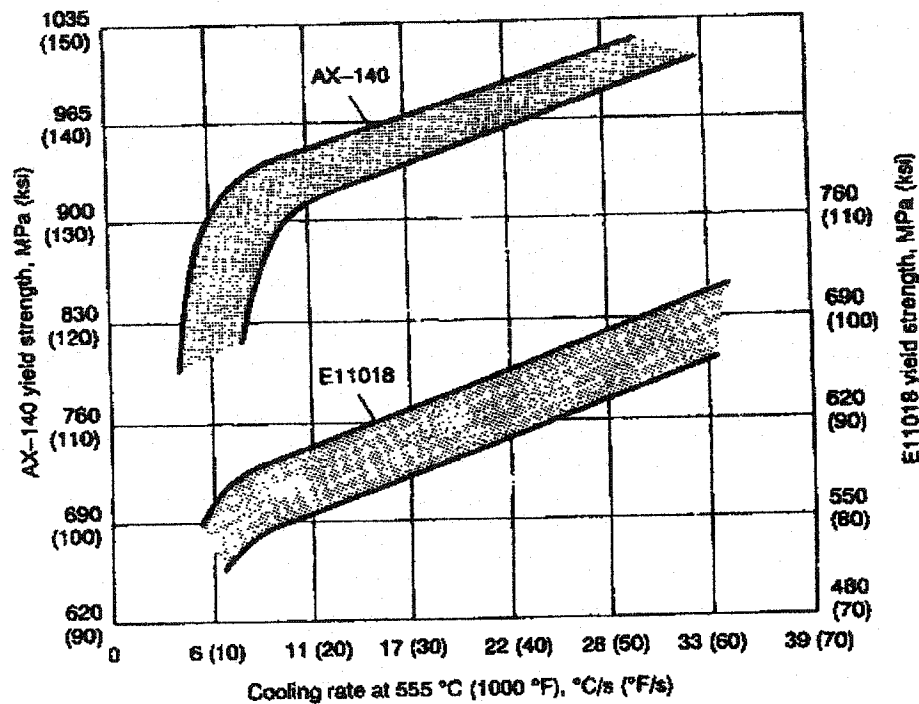


Figure 2-17 Effect of Cooling Rates on the Yield Strength of AX-140 and E11018 Filler Metals. [ASM, 1993]

The effect of under and overmatched weld metal strength on the properties of welded samples is far less thoroughly documented. Welding consumables are generally chosen on the basis of meeting the strength and toughness requirements of the specific application. With plain carbon steels, the choice of welding consumables is not an issue in terms of strength requirements, as there are numerous consumables available to meet the requirements. As higher and higher strengths of steel find their way into the market, there are fewer options available to meet either the yield or tensile strengths and toughness requirements of codes. Codes, however, do not recognize that the yield strength derived from electrode classification testing may not be obtained in an actual welded joint and that the

actual mechanical properties of a base material may be above that of the specified minimum values. [Denys, 1990]

In order to avoid failures in the weld metal of a structure, the weld metal yield and tensile strengths are often higher than that of the base metal. If the strength of the weld metal is greater than that of the base material, it will deform proportionally less if loaded in a transversely loaded sample. [Denys, 1989] As a result, the overmatched weld metal can protect itself from severe plastic strains that could develop around discontinuities. Should the weld metal strength be undermatched the reverse argument would be true. The strain distribution in the weld zone of a undermatched and overmatched sample can be see in Figure 2-18.

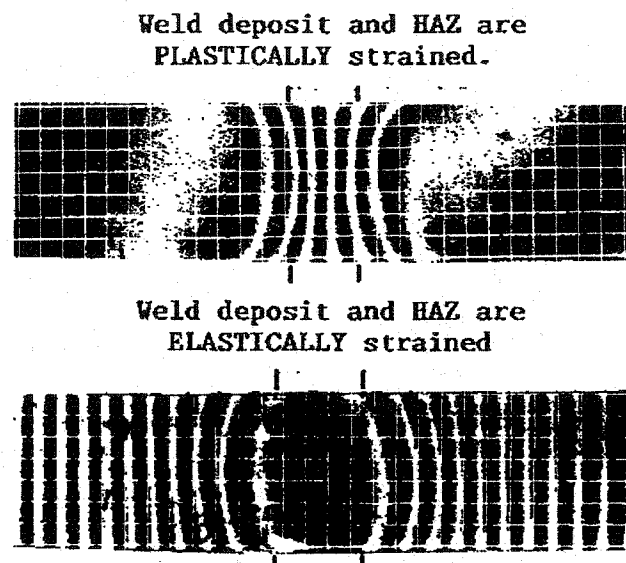


Figure 2-18 Moire Picture of the strain distribution in a Undermatched (top) and Overmatched (bottom) welded sample. [Denys, 1990]

If the weld metal yield stress is above that of the base material, the base material must undergo significant deformation and strain hardening before the weld metal

will yield. If the strength of the weld metal does exceed that of the base metal, the base material will govern the stress/strain distribution. [Denys, 1989] The deformation behavior exhibited by a weld with its length transverse to the applied stress can be seen in Figure 2-19.

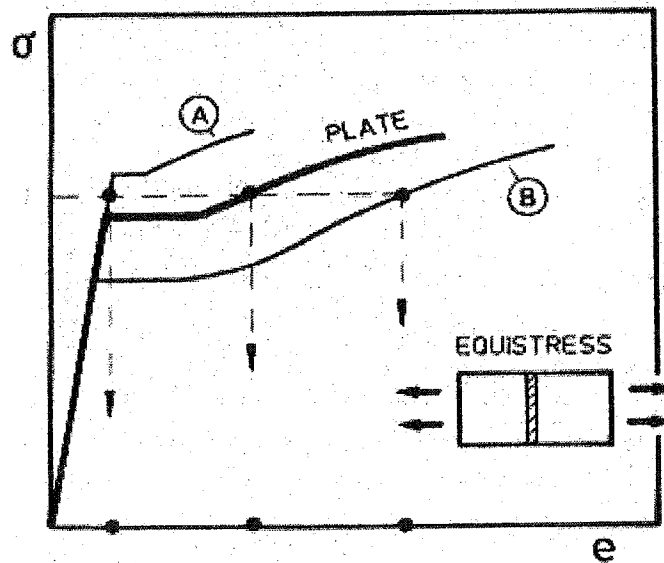


Figure 2-19 The Effect of Weld Metal Overmatching (A) and Undermatching (B) on the stress strain distribution of a transversely loaded tensile sample. [Denys, 1989]

### 2.8.2 Implant Testing

The implant test is a weldability test to assess the susceptibility of a base material to hydrogen assisted cold cracking. A summary of the test is taken from Watkinson, "The implant cracking test uses a cylindrical sample called the implant made from the steel under investigation, which is notched at some distance from one of its ends. This sample is inserted into a hole drilled in a base plate of the same grade of steel, or a comparable grade, so that the notched end is

flush with the plate surface. A weld bead is deposited on the plate in one pass under carefully controlled conditions, in line with the axis of the implant, using the welding process and consumables to be tested. The welding conditions are noted and the penetration must be such that the notch is located in the heat affected zone (HAZ). After welding and before complete cooling, the implant is put under a tensile static load and the stress this applies is measured in relation to the cross section at the notch. After a specified load holding time, if rupture has not occurred, the implant is extracted from the base plate and examined for cracks which may have occurred at the level of the notch in the HAZ."

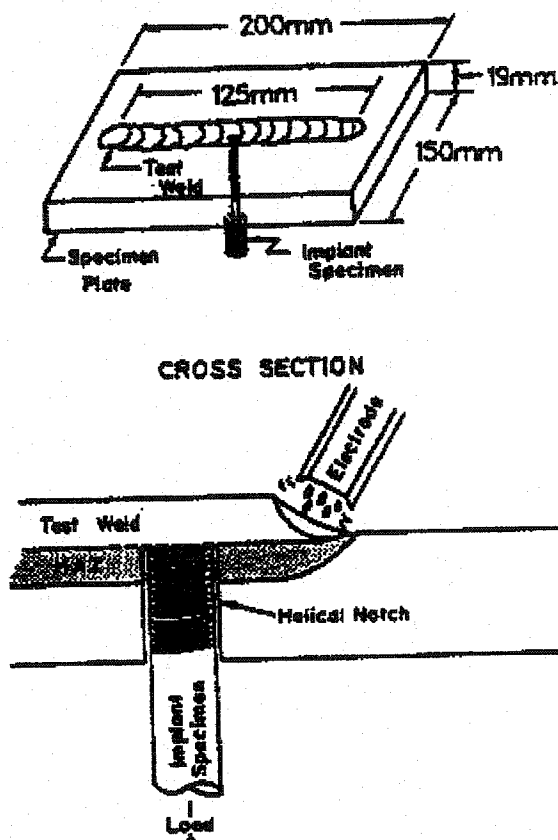


Figure 2-20 Typical Implant Test Setup



Since its inception, a number of researchers have made changes to the variables associated with the test. A list of the different variables and test methods used is given in Table 2-2.

**Table 2-2 Experimental Procedures for Implant Tests [Bryhan, 1981]**

<b>Implant Test Setup</b>		<b>Climax Method</b>	<b>IIW Method</b>	<b>Japanese Method</b>
Implant specimen geometry	Diameter	5.6 mm	6, preferably 8 mm	8 mm
	Notch configuration	Helical notch, angle 60 deg	Circular notch, maximum angle 45 deg, if possible 40 deg	Circular notch, angle 40 deg
Removal of implant blank	Notch Depth	0.46 mm	0.5 mm	0.5 mm
	Notch root radius	0.008-0.040 mm	0.1 mm	0.1 mm
	Specimen axis orientation	Transverse	Rolling direction	Rolling direction
	Position in thickness	Mid-Thickness	Mid-Thickness, t/4 if greater than 25 mm	Mid-Thickness
Supporting plate		C-Mn Steel	C-Mn Steel or similar composition	Same Steel
Load Application	Temperature when loading begins	Room Temperature	Between 150-100°C	150°C
	Load holding time	Minimum 16 h	Minimum 16 h	Minimum 48 h
Welding heat input		1.0 kJ/mm	1.7 kJ/mm	1.7 kJ/mm

Variables that can be altered in the test include the stress level, hydrogen level, cooling time, heat input, welding process and consumables. In examining the effects of test variables on the implant test results, Bryhan has shown that while the actual critical stress (the stress level below which a failure will not occur) value may change with changing variables, the rating of different steels is

independent of the test method used. Figure 2-21 shows the effect of test variables on critical stress of five HSLA steels.

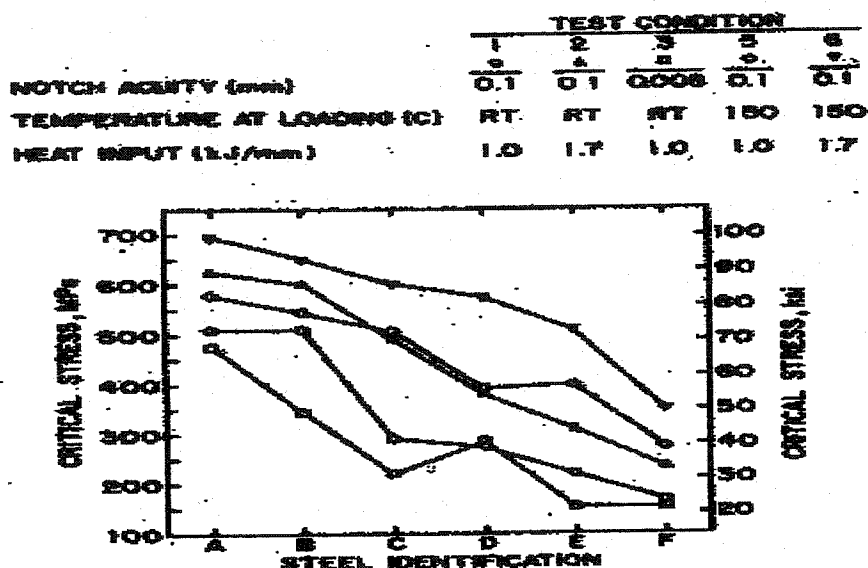


Figure 2-21 Effect of Test Variables on Implant Test Results [Bryhan, 1981]

When samples are loaded with high stress levels yielding may occur in the sample. Welding at high heat input levels in combination with high levels of stress can result in yielding outside of the HAZ of the sample. Determination of the critical stress level for this situation results in an increase in the standardization of the result. This situation indicates that yielding of the sample affects the fracture mode of the sample, making the test invalid for stress levels above the yield point. [Karppe, 1983]

In analyzing the results of implant test, attempts have been made to correlate the results with other tests and material properties. While no correlations between the implant test results and the carbon equivalent (composition) or maximum HAZ

hardness have been found, correlations between the implant test results and microhardness have been found. [Bryhan, 1981] Test results can be reported in a number of ways. Results can be reported as cracking vs. non cracking, rupture vs. non-rupture or critical stress (stress at rupture/UTS) vs. time. In this study, the main variables being examined are the effect of hydrogen level and heat input on the stress required to cause failure.

### 2.8.3 WIC Restraint Cracking Test

The Rigid Restraint Cracking test developed by the Welding Institute of Canada is another test used to assess cracking susceptibility by representing a butt weld subjected to high reaction stresses. In the test, two pieces of test material with edges machined to give the desired joint geometry are welded onto a backing plate. A restraint length between the two pieces is left unwelded. [Rothwell, 1990] A typical WIC test set up is shown in Figure 2-22.

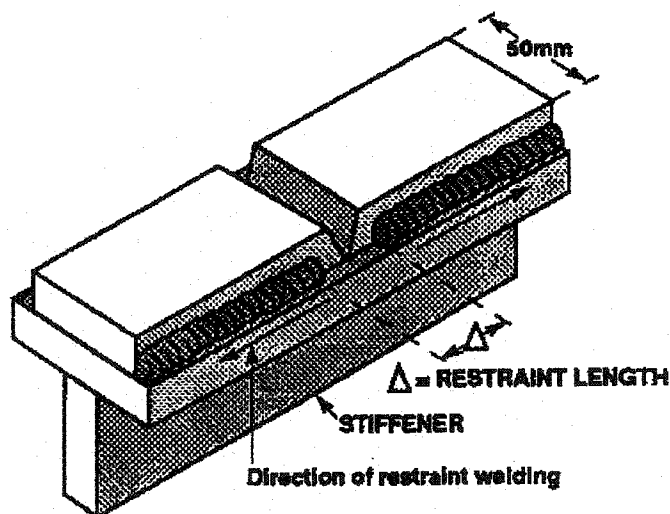


Figure 2-22 WIC High Restrain Cracking Test

A modified version of the test is used at the University of Alberta with the main difference being the addition of another horizontal stiffening plate to the bottom of the assembly. The addition of the bottom plate increases the overall stiffness of the test assembly and makes the test free standing for easier handling. Welding is carried out on the test assembly with run on and run off tabs at each end of the weld to ensure uniform weld distribution. Tests are conducted at increasing levels of preheat temperature until cracking is eliminated. Welds that do not crack through to the surface are removed after 24 hours are sectioned at four equal spaced lengths along the weld for examination.

The legitimacy of the WIC test comes from its ability to reproduce the right amount of restraint, in the correct amount of time, in the correct region of the weld. The restraint levels of various locations in a few structures in given in Table 2-3.

Table 2-3 Restraint Intensities for Different Structural Applications [Datta, 1997]

Applications	Location	Thickness(mm)	Restraint Intensity (K) kg/mm.mm
Ship	Transverse bulk head	16	1640
	Longitudinal bulk head	14	1260
	Bottom shell	28	780
	Upper deck	32	1280
Bridge	Diaphragm and web plate	19-38	200
	Diaphragm and flange plate	40-60	1800
Building frame	Building column construction	28	1090

The restraint level of the WIC test used in the study when calculated using the method proposed by Sato gives a restraint intensity of 2035 kg/mm-mm.[Sato,

1973] Within minutes of the completion of welding, the desired restraint level in the sample is achieved. Varying the joint geometry from a Y groove to a single V causes the stresses to be concentrated at the top of the weld, which is seen in service during the lifting of pipes. [Rothwell, 1990] WIC tests have been successfully used to determine the critical preheat on HSLA steels with values typically 25-30°C greater than those required in full scale weldability tests. [North, 1982] As with the implant test, attempts have been made to correlate WIC test results with material variables and other tests. While most correlation attempts have been unsuccessful, a linear correlation between the critical temperature and the base metal carbon equivalent does exist. [Signes, 1988]

## ***2.9 Literature Review Summary***

From the information presented in this literature study, it is known that welding adversely affects the properties of TMCP steels. The strength of TMCP steels is dependent upon grain refinement, rolled texture, and dispersion strengthening by fine microalloyed carbonitrides. With increasing strength levels, the steel's sensitivity to the effect of the welding thermal cycle and the susceptibility to hydrogen assisted cracking are both increased. Little is known at the present time of the effect that welding has on TMCP steels with yield strengths above 500 MPa.

The aim of this study is to determine the effects of welding on the metallurgical and mechanical properties of both Grade 80 and Grade 100 structural steel in terms of assessing the weldability of both materials.

## Chapter 3 Experimental Procedure

### 3.1 Material

The two materials used in this investigation were IPSCO Grade 80 and IPSCO Grade 100 structural plate supplied in the 5/16" (8 mm) gauge thickness. Both are TMCP microalloyed steels that contain copper, nickel, chromium, molybdenum and titanium along with other elements all grouped as other in Table 3-1. The mechanical properties for each grade are given in Table 3-2.

**Table 3-1 Chemical Composition of Grade 80 and Grade 100**

Grade 80		Grade 100	
C %	0.0640	C %	0.0780
Mn %	1.561	Mn %	1.800
S %	0.0073	S %	0.0014
P %	0.0147	P %	0.0130
Other %	1.7196	Other %	1.5956

**Table 3-2 Mechanical Properties of Grade 80 and Grade 100**

Grade 80		Grade 100	
YS (MPa) LRD	594	YS (MPa) LRD	764
YS (MPa) TRD	649	YS (MPa) TRD	828
UTS (MPa) LRD	784	UTS (MPa) LRD	909
UTS (MPa) TRD	800	UTS (MPa) TRD	943
El %	26	El%	22

- LRD: Longitudinal to Rolling Direction
- TRD: Transverse to Rolling Direction

From Table 3-2, the degree to which the materials exceed their SMYS values is clearly evident. As such the Grade 80 is close to a Grade 90 and the Grade 100 meets the requirements of a Grade 110.

### 3.2 Welding Procedures

The two welding processes used in the study were SMAW and GMAW. The SMAW tests were carried out using a Hobart R-600-S constant current power source and the GMAW welds were done using a Linde SVI 400 variable characteristic power source in the constant voltage mode set at minimum slope and maximum inductance. Autogenous GTAW used to examine the effects of welding on base metal microstructure were carried out using a Miller Dynasty. Variations in heat input levels were obtained by fixing the values of the current and voltage while manipulating the welding speed. The procedure for the SMAW process was set by the investigators based primarily upon past experience, while the procedure for the GMAW process was provided by Doepker Industries Ltd. as suggested by IPSCO. The settings used for both processes are outlined in Table 3-3.

**Table 3-3 Welding Procedures for SMAW for GMAW Process**

SMAW		GMAW	
Current	25 V	Current	26 V
Voltage	130 Amps	Voltage	235 Amps
Welding Speed	Variable	Welding Speed	Variable
Shielding Gas	N/A	Shielding Gas	92% Ar – 8% CO <sub>2</sub>
Electrical Characteristics	DCEP	Electrical Characteristics	DCEP in Spray Transfer Mode

GTAW	
Current	12 V
Voltage	150 Amps
Welding Speed	Variable
Shielding Gas	Ar
Electrical Characteristics	DCEN

The specific welding procedures used in each experiment are given in Appendix B.

### **3.3 *Welding Consumables***

Welding consumables for both processes investigated were chosen on the basis of matching YS values. Because SMAW electrodes are classified according to their UTS values, electrodes are chosen with a strength level of 10000 psi (70 MPa) greater than the base material to provide the required YS levels.

#### **3.3.1 SMAW Consumables**

Various grades of SMAW electrodes were examined in the investigation to assess the effect of under and over matched weld metal yield strength on the weldability of each material. Specifications on these consumables can be found in Appendix A. The two main low hydrogen electrodes used in the investigation were E9018 for the Grade 80 and E11018 for the Grade 100. Specifications for each of the consumables is given in Table 3-4 and Table 3-5.



**Table 3-4 Specifications for Canadian Liquid Air 9018**

Tensile Strength	640 - 685 MPa (90000-98000 psi)
Yield Strength	550 - 610 MPa (80000-85000 psi)
C %	0.05
Cr %	0.06
Ni %	1.64
Mo %	0.24
P %	0.016
S %	0.010
Mn %	1.13
Si %	0.27
Nb %	-
Ta %	-
V %	-
Cu %	-
Ti %	-

**Table 3-5 Specifications for Canadian Liquid Air 11018**

Tensile Strength	770 - 810 MPa (90000-98000 psi)
Yield Strength	690 - 730 MPa (80000-85000 psi)
C %	0.07
Cr %	0.23
Ni %	1.74
Mo %	0.36
P %	0.02
S %	0.011
Mn %	1.71
Si %	0.40
Nb %	-
Ta %	-
V %	-
Cu %	-
Ti %	-

### 3.3.2 GMAW Consumables

All GMAW welds were carried out using L-TEC HI-84 (AWS 80S-D2) solid MIG wire in the 0.045 in (1.143 mm) diameter. The as-welded composition and mechanical properties of HI-84 are given in Table 3-6.

**Table 3-6 As-Welded Properties of L-TEC HI-84**

	<b>Ar-Based As-Welded</b>
UTS MPa (ksi)	758-827 (110-120)
YS MPa (ksi)	689-758 (100-110)
C %	0.09-0.12
Mn %	1.60-1.80
Si %	0.50-0.65
Mo %	0.40-0.50
Ni %	0.03-0.06
Cr %	0.02-0.04
Ti %	0.005-0.015

Note that all the electrodes used for the SMAW and GMAW procedures have substantially different chemistry from the Gr. 80 and Gr. 100 steels. This is common with high strength materials in order to achieve the required strength and toughness levels in the as-cast microstructure.

### 3.4 Tensile Test Welds

Tensile test welds were fabricated using both the SMAW and GMAW processes with 75 mm X 150 mm (3" X 6") pieces of each grade of steel. Blanks were cut with the 150 mm length transverse to the rolling direction. For both processes, welds were made between the two 150 mm lengths of steel. Tensile samples were cut out with the weld in the middle so that testing was in the rolling direction and transverse to the weld zone. Figure 3-1 and Figure 3-2 show the set up for the

SMAW and GMAW process respectively. An interpass of temperature of  $100^{\circ}\text{C}$  was used for all welds.

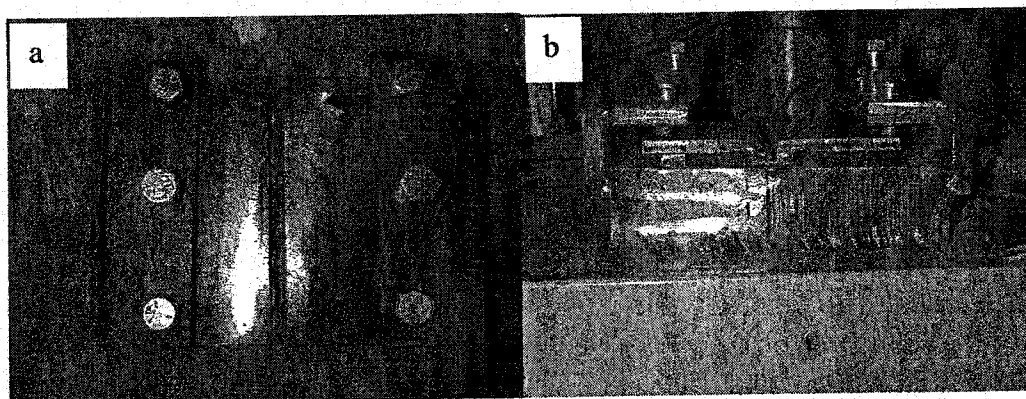


Figure 3-1 Picture of SMAW Tensile Test Set Up (a) Plan View (b) Side View

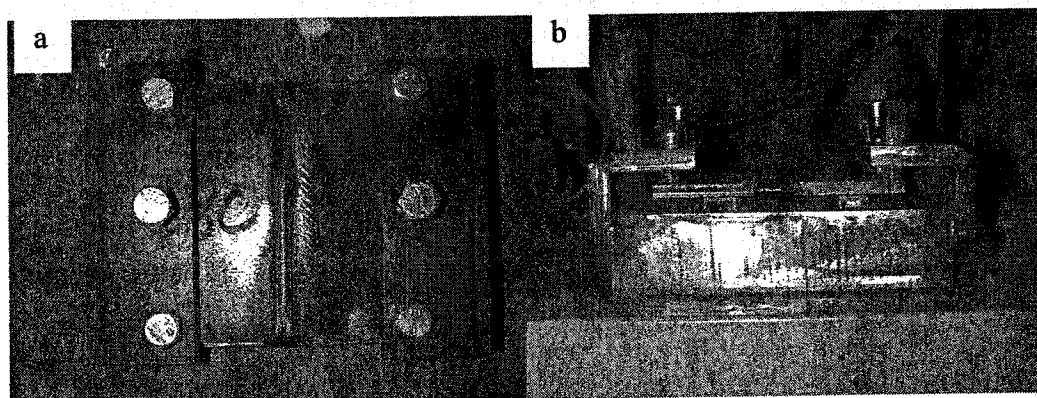
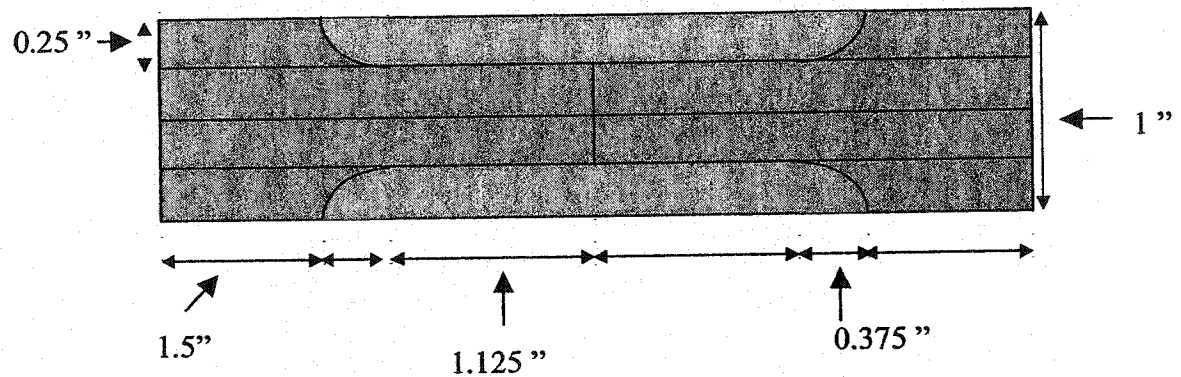


Figure 3-2 Picture of GMAW Tensile Test Set Up (a) Plan View (b) Side View

### 3.5 Tensile Tests

Tensile coupons were machined from the test welds according to ASTM standards with the dimensions indicated in Figure 3-3.



**Figure 3-3 Dimensions of Tensile Coupon**

Coupons were tested at a crosshead rate of 0.1418 in/min using a MTS Machine controlled by Instron Series IX software. All the recorded values are an average to two tensile tests.

### 3.6 Cruciform Tests

Two sets of cruciform test were fabricated using the geometries shown in

Figure 3-4. The tests were set up with base material in the center of two vertical members attached with fillet welds. One set of tests used a square edge on the vertical members, while the other used a 45° V joint preparation on the vertical members.

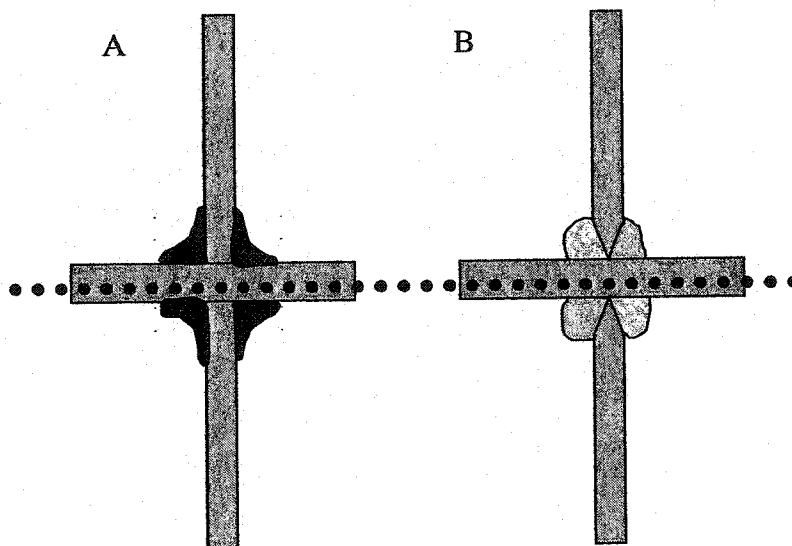


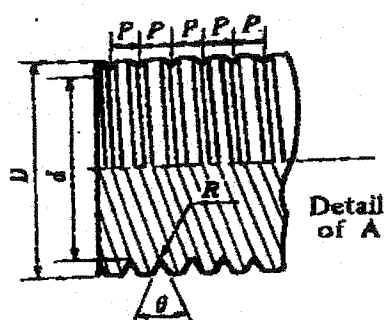
Figure 3-4 Schematic Diagram of Cruciform Joint Configurations.

The joint configuration shown in A was sectioned into two rectangular pieces with the excess center material outside of the fillet welds removed. The second joint configuration was machined into tensile samples as shown in section 3.5.

### 3.7 *Implant Tests*

Implant tests were carried out on both materials in the transverse and longitudinal directions using the SMAW and GMAW processes. Samples were machined to either a 7 mm or 6 mm diameter shaft with a 60° 0.5 mm deep helical notch as shown in Figure 3-6. The use of 7 and 6 mm samples as opposed to 8 mm samples used by other researchers was done for a number of reasons. The first

was the initial thickness of the steel plate. Material used in the study was supplied in the 5/16" (7.5mm) gauge. The use of 6 mm samples allows for the use of low heat input welding. At low heat inputs the width of the bead deposited is too small to cover the sample. The use of the 6 mm sample also dictates that the rupture method of recording the results is more appropriate as cracks in a 6 mm sample may be difficult to find. [Granjon, 1979]



Sample Type	D mm	d mm	$\theta^\circ$	R	P
Transverse	7	$6 \pm 0.02$	$60 \pm 2$	$0.1 \pm 0.02$	$1 \pm 0.02$
Longitudinal	6	$5 \pm 0.02$	$60 \pm 2$	$0.1 \pm 0.02$	$0.5 \pm 0.1$

Figure 3-6 Detail of Helical Implant Sample.

Consumables for the SMAW process were stored at 200°C for 48 hours or more after conditioning unless otherwise noted. Consumables for the GMAW process were stored at room temperature. Upon welding, samples were placed in the static load frame with the load being applied when the weld metal surface temperature reached 100°C. Tests were run for a minimum of 24 hours or until failure occurred. Experiments were done used various combinations of load and hydrogen levels to determine the materials susceptibility to cold cracking. Reported test values represent one test sample for each of the conditions tested.

### 3.8 *Diffusible Hydrogen Tests*

Measurement of Diffusible Hydrogen content of weld metal was carried out with the IIW Mercury method in accordance with ISO 3690. Test samples of AISI 1020 steels were vacuum degassed at 650<sup>0</sup>C prior to welding. A weld bead was placed on a set of four samples held in a jig as shown in Figure 3-7. After welding, the test piece was placed immediately in iced water followed by an alcohol and solid carbon dioxide mixture. This minimizes the loss of diffusible atomic hydrogen. Test samples were then separated, dried under a shield of dry nitrogen to avoid condensation from humidity, washed in alcohol, and dried before being placed into the tube of mercury. The sample was then transferred around the bend in the tube via a magnet. A vacuum was then reestablished on the collection apparatus. Collection of hydrogen was done in a precision bore glass tube for a 72 hour time period. The height of the gas collected in the tube column was then measured and the volume of gas collected was calculated. The volume of gas per 100 g of fused metal was recorded and corrected to STP for ambient temperature and pressure.

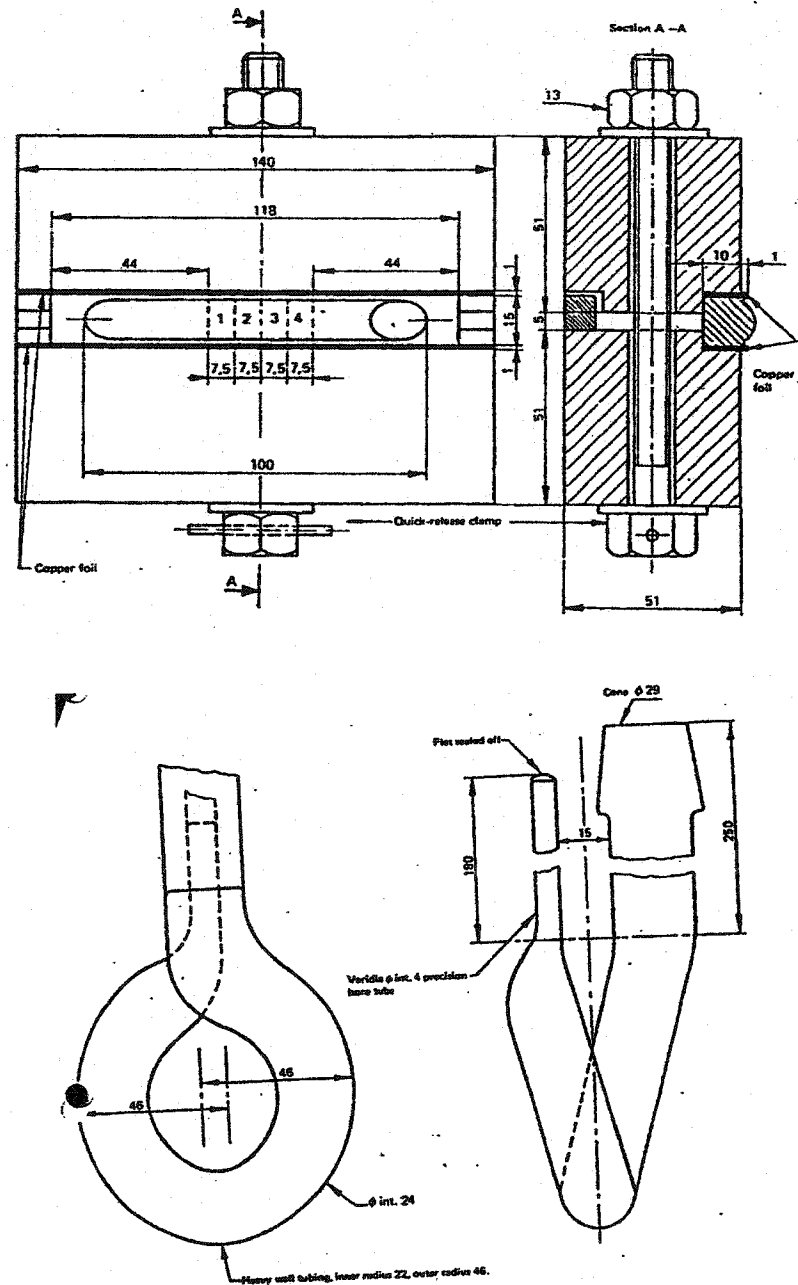


Figure 3-7 Diffusible Hydrogen Apparatus (a) Sample Jig & (b) Collection Apparatus [ISO 3690].



### 3.9 WIC Rigid Restraint Cracking Tests

Modified WIC Rigid Restraint Cracking Tests were performed on both materials using both the SMAW and GMAW process. The set up for the modified test is shown in Figure 3-8.

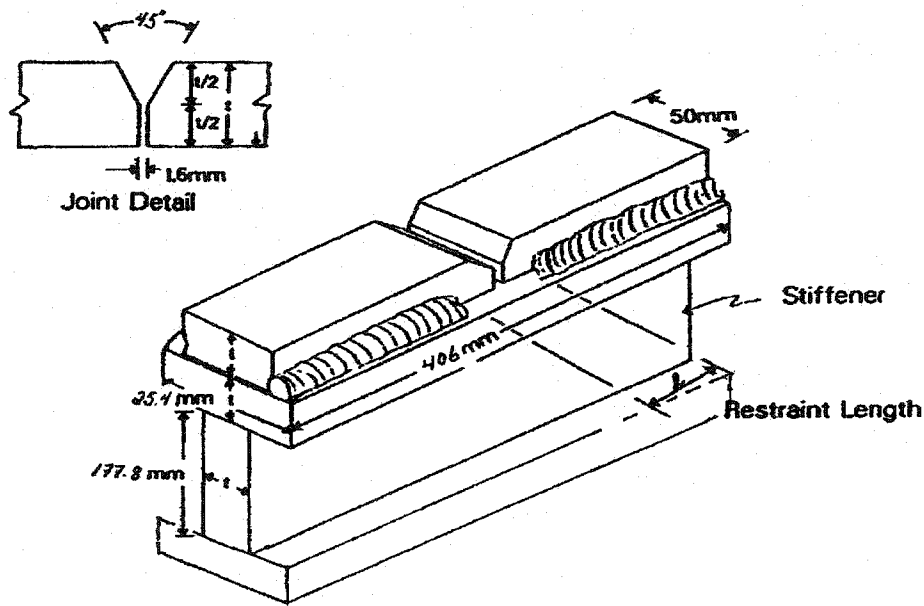


Figure 3-8 Modified WIC High Restraint Cracking Test

Restraint welds were done with a 7018 (480 MPa) electrode for a length of 5.5" on each piece leaving a restraint length of 1" (25mm). Welds were fabricated transverse to the rolling direction at a heat input of 1.0 kJ/mm for both processes. Tests were carried out using either a 45° vs. 45° joint or a 45° vs. a straight edge to vary the level of notch acuity present in the joint. Preheat temperatures of the test assembly were increased in an oven until cracking was eliminated.

### 3.10 Metallurgical Samples

All of the samples were mounted in 1.25" Bakelite molds using a manual hot press. They were mounted at a pressure of 20.7 MPa (3000 psi) until the temperature reached 60<sup>0</sup>C followed by a pressure of 41.4 MPa (6000 psi) until the temperature reached 140<sup>0</sup>C. The samples were then ground and polished according to the following procedure:

- I. Grinding
 

Medium:	200-600 grit SiC Sandpaper
Time:	30 sec
Wheel speed:	240 rpm
Force:	5 lbs/sample
Wheel Direction:	Counter Clockwise
Sample Direction:	Clockwise
  
- II. Rough Polish
 

Medium:	6 $\mu$ m diamond paste on nylon cloth
Time:	3 min
Wheel speed:	170 rpm
Force:	5 lbs/sample
Wheel Direction:	Counter Clockwise
Sample Direction:	Clockwise
  
- III. Fine Polish
 

Medium:	1 $\mu$ m diamond paste on a nylon cloth
Time:	3 min
Wheel speed:	150 rpm
Force:	3 lbs/sample
Wheel Direction:	Counter Clockwise
Sample Direction:	Clockwise
  
- IV. Final Polish
 

Medium:	0.05 $\mu$ m Alumina on a micro-polishing cloth
Time:	2.5 min
Wheel speed:	120 rpm
Force:	3 lbs/sample
Wheel Direction:	Counter Clockwise
Sample Direction:	Counter Clockwise

All four steps were performed on a Buehler Automet 2 Polisher, using a 6 sample holder. Samples were cleaned between each step by immersion in water followed by a 10% ethanol rinse to prevent oxidation of the metal surface. All samples were etched with a 1% Nital solution.

### ***3.11 Microhardness Testing***

Vickers microhardness measurements were taken in accordance with ASTM E 384-89. Measurements were done a Buehler Digital Microhardness Tester with a self-leveling sample holder.

Measurements were taken in each region of the weld zone using a 200 g load for a duration of 15 seconds. Hardness values reported are an average of a minimum of three tests. Samples were polished and etched with Nital prior to testing to allow for identification of the various regions within the weld zone.

## Chapter 4 Microstructure

The effect of welding on the microstructure of both grades of steels is examined in this chapter. Both materials were first examined in the as-received condition to provide a reference point for the effects of the welding thermal cycle. To eliminate the effects of filler metal composition on the resulting microstructures, autogenous welds were used as the means of examining the effects of welding. This results in a complete weld zone that is only affected by the heat input of welding with no other variables to consider. In any industrial weld, the weld metal would be different. Resulting microstructures were characterized according to the IIW guide as outlined in Section 2.5.1.

Microhardness measurements were taken in each region of the weld zone to determine the degree of hardening or softening that occurred during welding. Hardening in the weld zone increases the material's susceptibility to hydrogen cracking, while softening can result in a local loss of strength in the weld zone.

### ***4.1 Grade 80 As Received***

The as-received microstructure of the Grade 80 material at two different magnifications is shown in Figure 4-1.

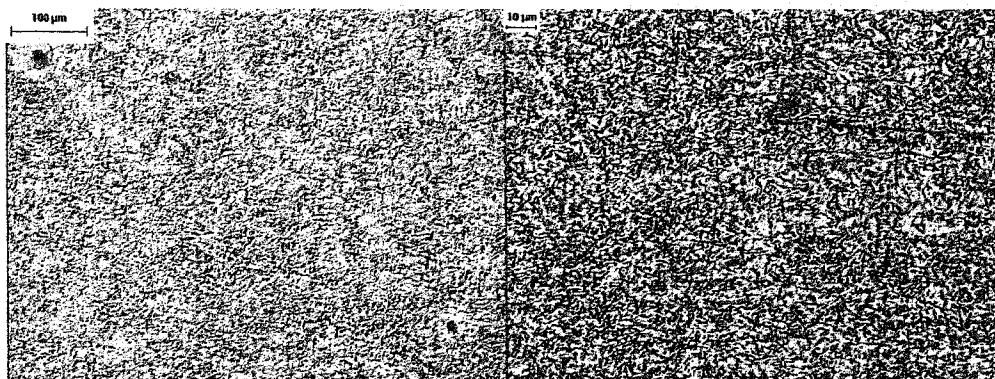


**Figure 4-1 Microstructure of As Received Grade 80**

The microstructure of the material consists of very small grains of intragranular polygonal ferrite. The presence of prior austenite grain boundaries is not evident. Examination at higher magnifications reveals the presence of subgrains within the ferrite grains, making the determination of grain size difficult. The average grain size is estimated to be below 5  $\mu\text{m}$ .

#### **4.2 *Grade 80 As Welded***

The as-welded microstructure of the Grade 80 was examined over a range of heat inputs. Characterization of the resulting microstructure was done by comparing the weld metal, coarse grain, and fine grain heat affected zone structures present at each of the heat input levels.

##### **4.2.1 Grade 80 Autogenous Microstructures**

Welds were produced at heat inputs ranging from 0.5 kJ/mm to 2.5 kJ/mm. The resulting weld metal microstructures are shown in Figure 4-2. The microstructures present in the weld metal are cast structures with varying solidification and cooling times.

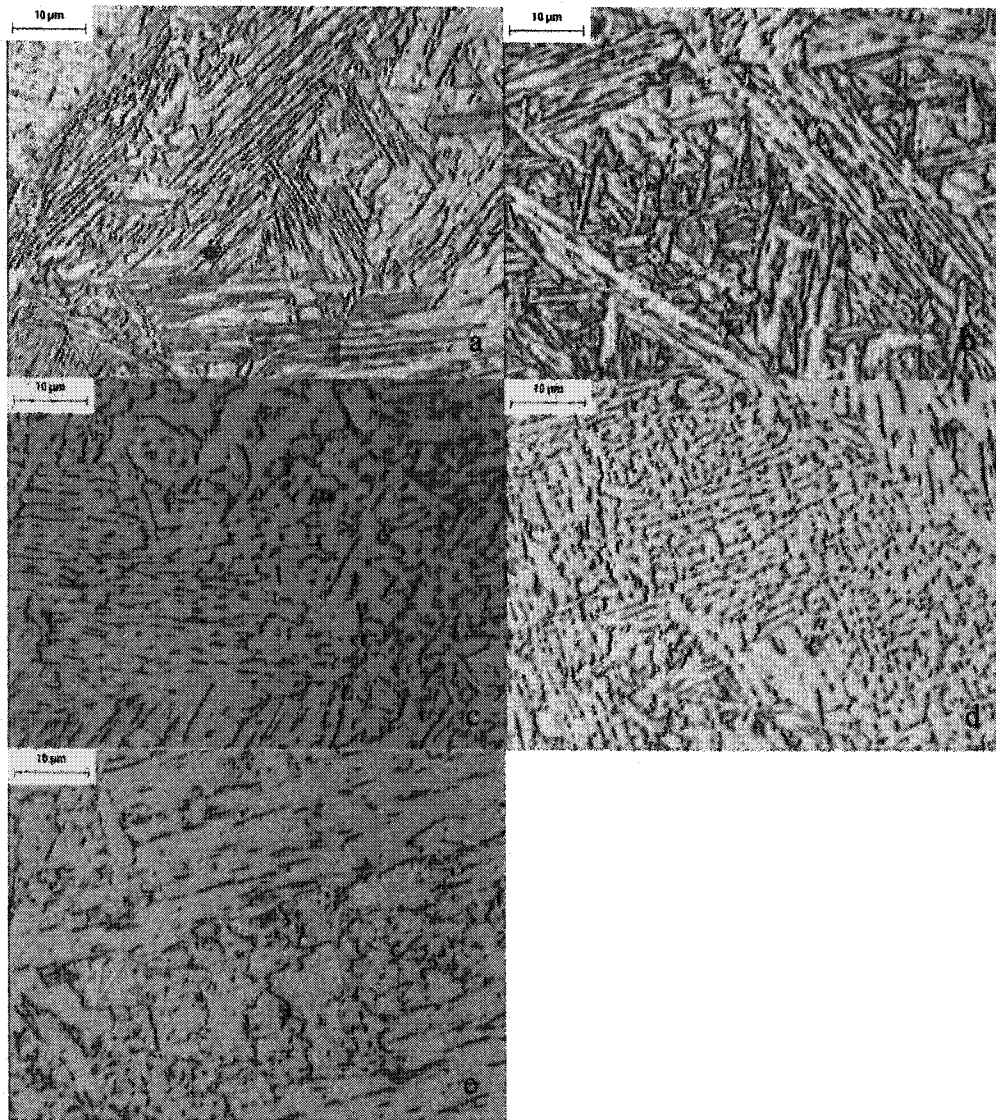


**Figure 4-2 Effect of Heat Input (kJ/mm) on Weld Metal Microstructure of Gr. 80  
Autogenous Welds: (a) 0.5 (b) 1.0 (c) 1.5 (d) 2.0 (e) 2.5.**

At a heat input of 0.5 kJ/mm the microstructure present in the weld metal consists of martensite, ferrite and aligned second phase. Increasing the heat input to 1.0 kJ/mm results in the formation of acicular ferrite along with areas of ferrite with aligned second phase. At a heat input of 1.5 kJ/mm and above the structure of weld metal changes to consist mainly of grain boundary and/or intragranular polygonal ferrite along with regions of ferrite with a non-aligned second phase.

The polygonal ferrite present increases in size along with the dispersion of the non-aligned second phase as the heat input is increased.

Coarse grain heat affected zone (CGHAZ) microstructures for the autogenous Grade 80 welds are shown in Figure 4-3.

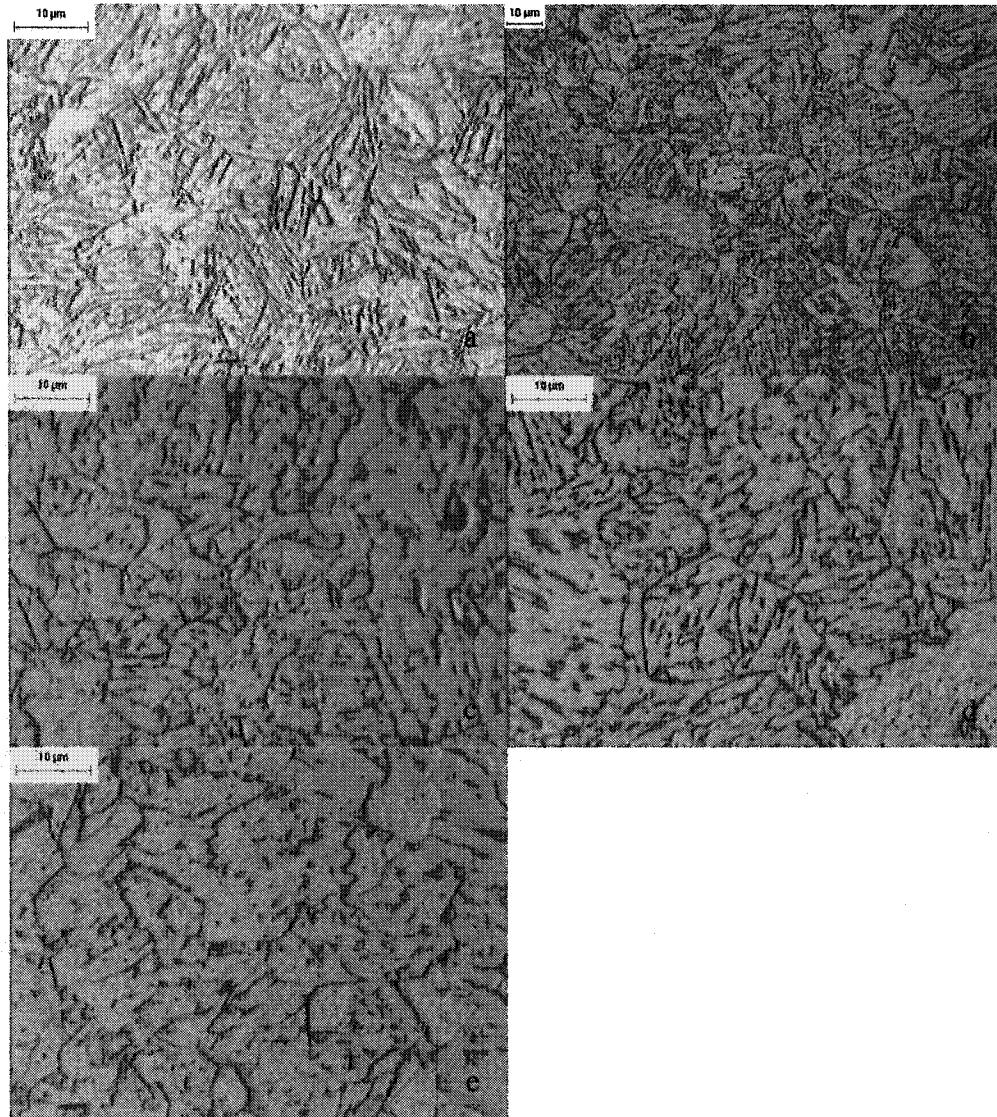


**Figure 4-3 Effect of Heat Input (kJ/mm) on CGHAZ Microstructure of Gr. 80 Autogenous Welds: (a) 0.5 (b) 1.0 (c) 1.5 (d) 2.0 (e) 2.5.**

The CGHAZ microstructure at a heat input of 0.5 kJ/mm consists of a fully martensitic structure as confirmed by hardness measurements in Section 4.2.2. Prior austenite grain boundaries are not clearly evident throughout most of the region. Increasing the heat input to 1.0 kJ/mm may result in prior austenite grain boundaries being evident. The internal structure of the grains consists of a mixture of ferrite with aligned and non aligned second phases. Increasing the heat input to 1.5 kJ/mm results in the formation of larger grains. The grains consist of ferrite with a non aligned second phase. Further increases to the heat input result in coarsening of the grains present in the CGHAZ and more random distribution of the second phase.

The fine grain heat affected zone (FGHAZ) microstructures are shown in Figure 4-4. The microstructure consists of polygonal ferrite for all of the heat inputs examined. There is an increase in grain size as the heat input is increased from 0.5 to 2.5 kJ/mm, but no significant change in microstructure is evident.



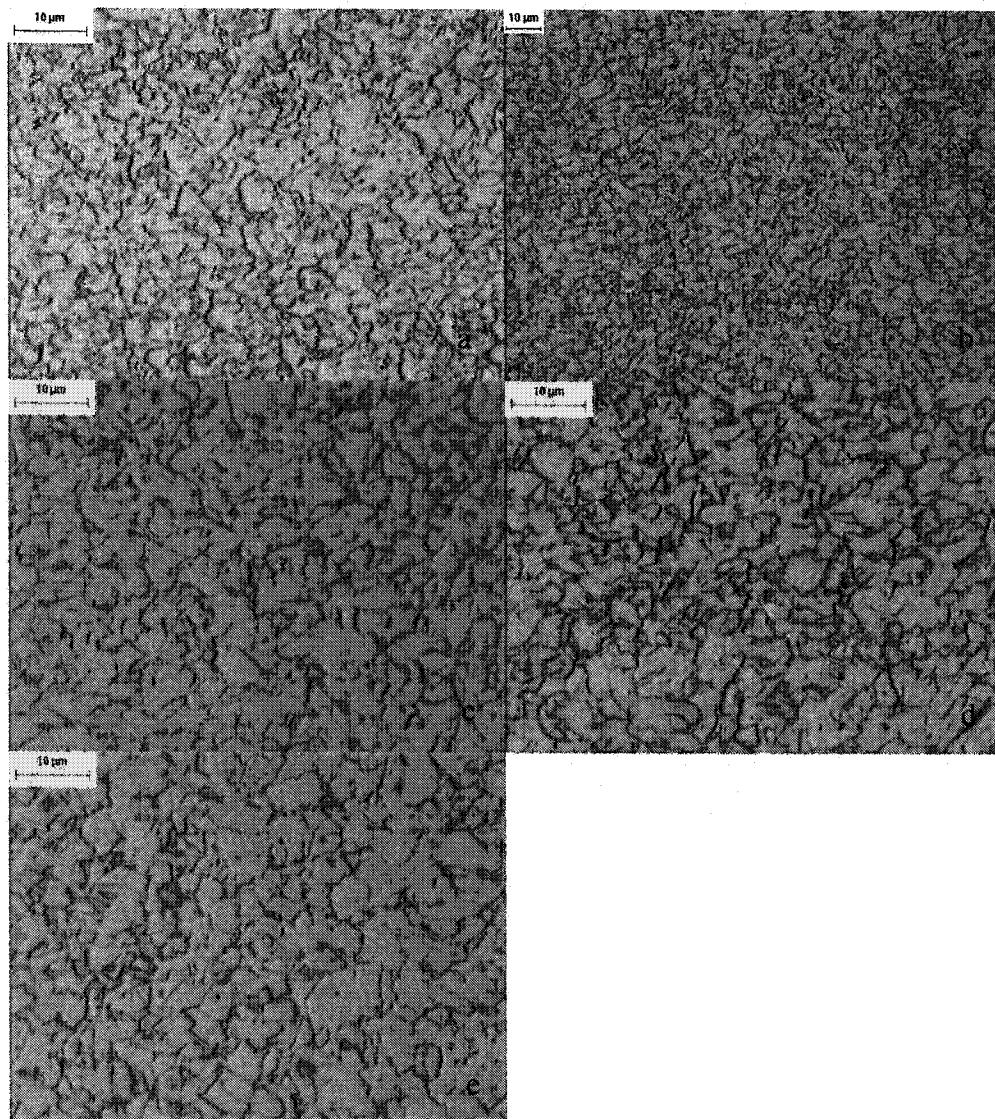


**Figure 4-4 Effect of Heat Input (kJ/mm) on FGHAZ Microstructure of Gr. 80 Autogenous Welds: (a) 0.5 (b) 1.0 (c) 1.5 (d) 2.0 (e) 2.5.**

#### 4.2.2 Grade 80 Microhardness Measurements

Microhardness measurements for each region of the HAZ were taken for all of the heat inputs examined. The results of the hardness test results are given in Table 4-1.

# NOTE TO USERS

Page(s) not included in the original manuscript and are unavailable from the author or university. The manuscript was scanned as received.

This reproduction is the best copy available.

along the CGHAZ of the various passes show no significant change in hardness level. This suggests that subsequent passes placed upon existing deposits have little effect on the properties of the HAZ. Hardness measurements for the varying passes are given in Table 4-2.

**Table 4-2 CGHAZ Hardness Measurements of Varying Passes in Grade 80 Steel**

<b>Location</b>	<b>Hardness (Hv)</b>
Pass 1	274
Pass 2	275
Pass 3	273
Pass 4	294
Pass 5	292

#### **4.3 Grade 100 As Received**

The as received microstructure of the Grade 100 material is shown in Figure 4-5.



**Figure 4-5 Microstructure of As Received Grade 100**

Like the Grade 80, the microstructure of the Grade 100 consists of very small grains of intragranular polygonal ferrite. There is no discernable presence of prior austenite grain boundaries or any secondary structures. Examination at higher magnifications reveals the presence of subgrains with the ferrite grains at

magnifications of 1000X. The average grain size of the Grade 100 is noticeably finer than the Grade 80 with an average estimated grain size of 3  $\mu\text{m}$ .

#### ***4.4 Grade 100 As Welded***

The as welded microstructure of the Grade 100 was examined over the same heat inputs as the Grade 80. Characterization of the resulting microstructures was carried out on all of the regions of the weld zone.

##### **4.4.1 Grade 100 Autogenous**

Welds were produced at heat inputs ranging from 0.5 kJ/mm to 2.5 kJ/mm. The resulting weld metal microstructures are shown in Figure 4-6.

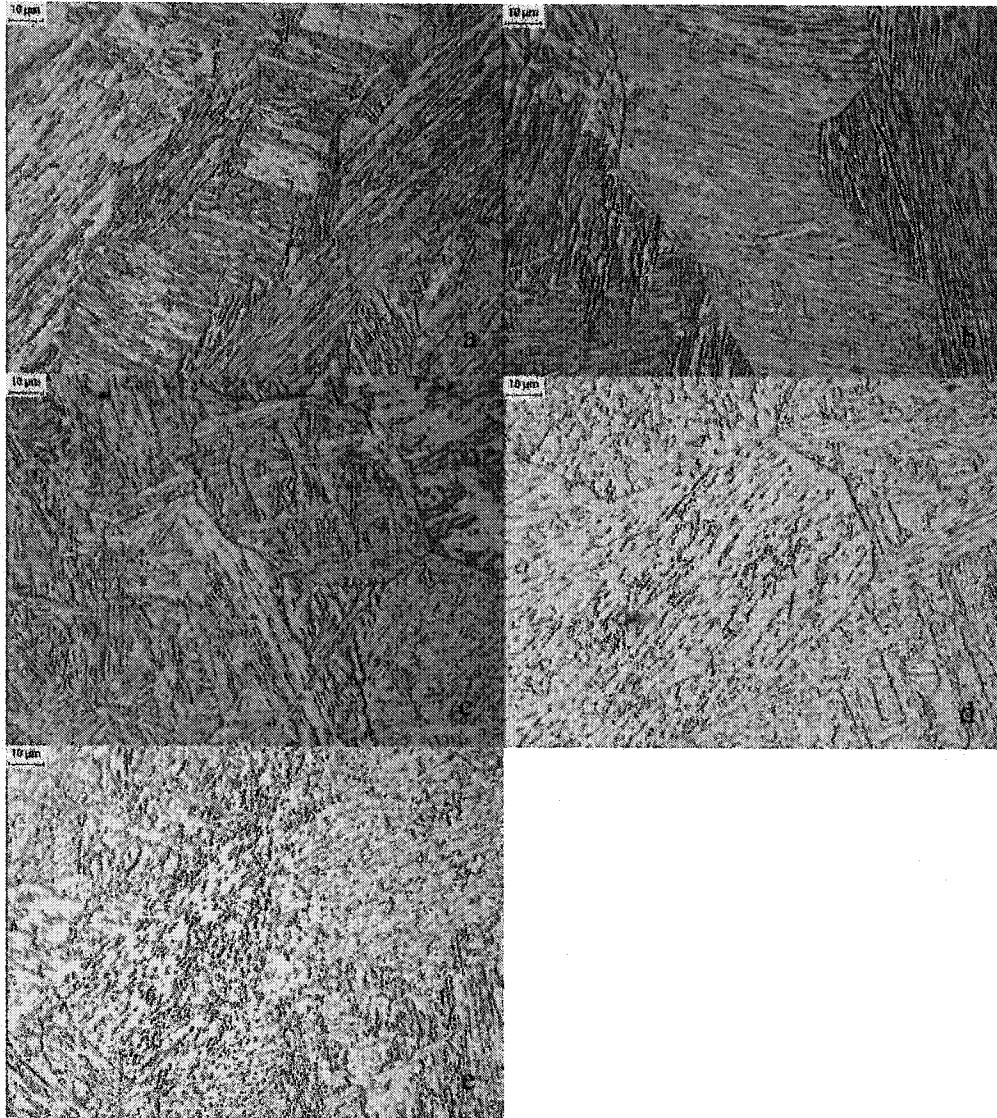


**Figure 4-6 Effect of Heat Input (kJ/mm) on Weld Metal Microstructure of Gr. 100  
Autogenous Welds: (a) 0.5 (b) 1.0 (c) 1.5 (d) 2.0 (e) 2.5**

At a heat input of 0.5 and 1.0 kJ/mm the microstructure of the weld metal consists of martensite and ferrite with an aligned second phase. The presence of columnar grains formed during solidification is clearly present in both figures a and b. Increasing the heat input to 1.5 kJ/mm results in the formation of some acicular ferrite and intragranular polygonal ferrite. The presence of side laths growing from austenite grain boundaries is also present in some of the grains. Further

increases to heat input results in the formation of ferrite with a non-aligned second phase.

The effect of heat input on the CGHAZ is shown in Figure 4-7.

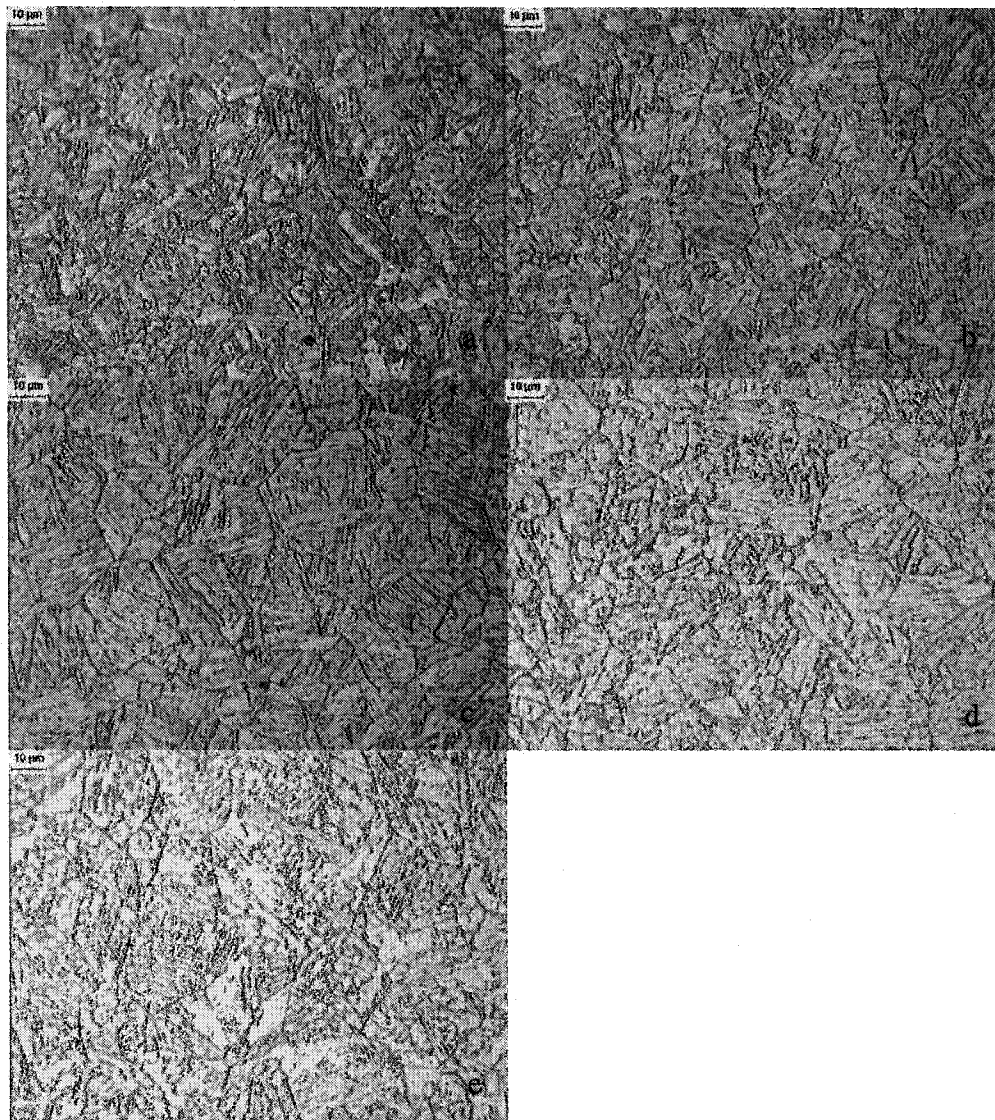


**Figure 4-7 Effect of Heat Input (kJ/mm) on CGHAZ Microstructure of Gr. 100 Autogenous Welds: (a) 0.5 (b) 1.0 (c) 1.5 (d) 2.0 (e) 2.5.**

As with the Grade 80 material, the CGHAZ microstructure at a heat input of 0.5 kJ/mm consists of a fully martensitic structure. Prior austenite grain boundaries are not clearly evident throughout most of the region. At a heat input of 1.0 and 1.5 kJ/mm the presence of the prior austenite grain boundaries may be evident.

The grain structure present consists of regions of martensite along with ferrite with an aligned second phase. Small regions of intragranular ferrite are also present. The size of the grains increases with increasing heat input. Increasing the heat input to 2.0 and 2.5 kJ/mm results in the internal structure of the grains being transformed to ferrite with a non-aligned second phase.

The FGHAZ microstructures for the varying heat inputs are shown in Figure 4-8.

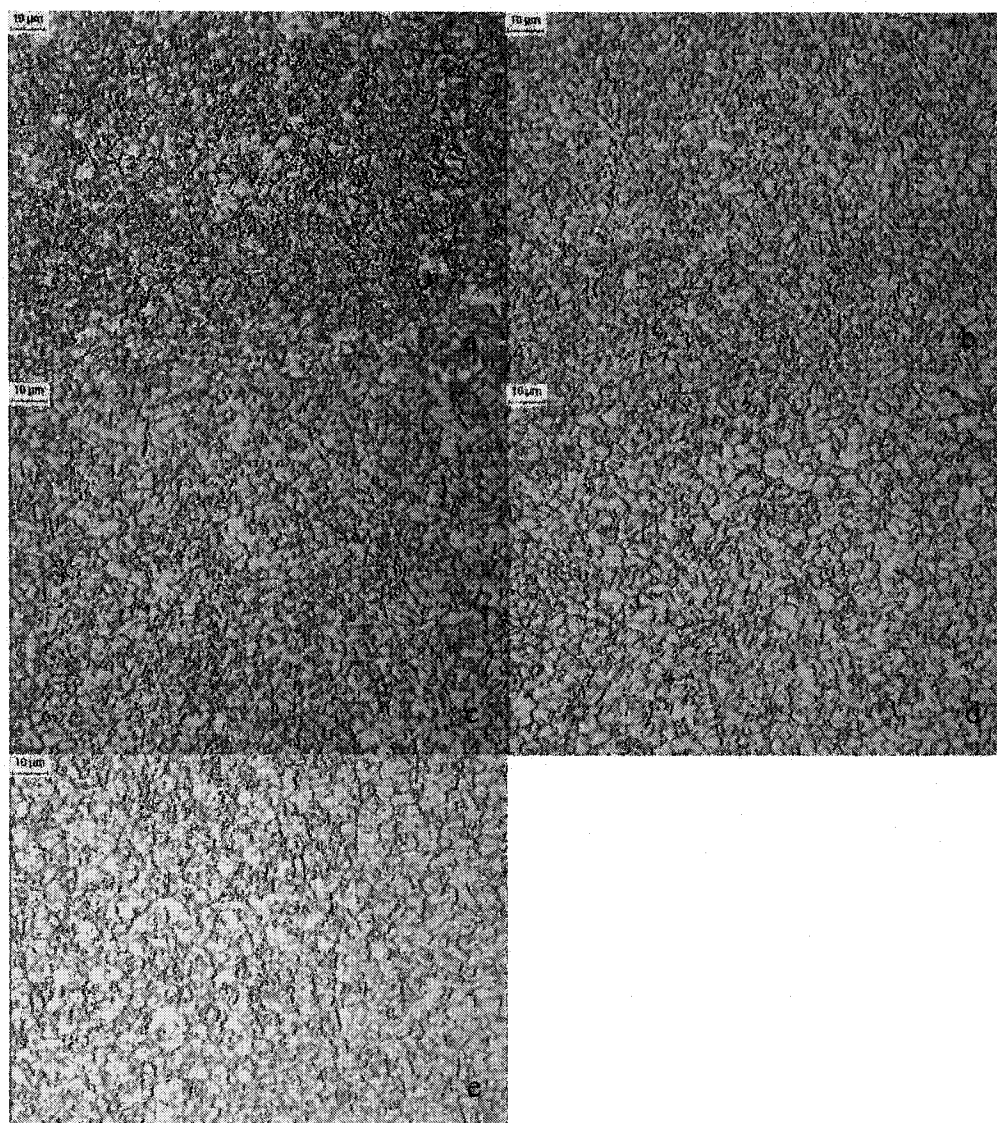


**Figure 4-8 Effect of Heat Input (kJ/mm) on FGHAZ Microstructure of Gr. 100 Autogenous Welds: (a) 0.5 (b) 1.0 (c) 1.5 (d) 2.0 (e) 2.0**



The microstructure present consists of polygonal ferrite for all of the heat inputs examined. There is an increase in grain size as the heat input is increased from 0.5 to 2.5 kJ/mm but no significant change in microstructure is evident.

#### 4.4.2 Grade 100 Microhardness Measurements

Vickers microhardness measurements for each region of the HAZ were taken for all of the heat inputs examined. Hardness results are given in Table 4-3.

**Table 4-3 Grade 100 Microhardness Measurements of the Weld Zone**

<b>Heat Input (kJ/mm)</b>	<b>Weld Metal (Hv)</b>	<b>CGHAZ (Hv)</b>	<b>FGHAZ (Hv)</b>	<b>Base Metal (Hv)</b>
0.5	392	363	338	317
1.0	371	363	302	317
1.5	354	349	263	326
2.0	328	292	253	317
2.5	288	264	262	299

For the Grade 100 material the base material hardness measurements gave an average reading of 317 Hv. For the 0.5 kJ/mm test weld, significant hardening occurred in all regions of the HAZ. Increasing the heat input to 1.0 kJ/mm also resulted in hardening of the weld metal and CGHAZ but at this heat input softening of the FGHAZ occurred. At 1.5 kJ/mm, hardening of the weld metal and CGHAZ are still present with the hardness values lower than that of the lower heat inputs. The FGHAZ shows a significant decrease in hardness level at this heat input indicating a large degree of softening. Further increases to the heat input level results in softening of the CGHAZ for both the 2.0 and 2.5 kJ/mm while only the 2.5 kJ/mm sample showed softening of the weld metal. The FGHAZ does not undergo any further decrease in hardness at these increased



levels of heat input. The recorded hardness values of the base metal Grade 100 are higher than typical for ferrite with a very low carbon level. The high values are likely a result of TMCP processing (texture, dislocation density and precipitation hardening) and the effect of welding.

#### 4.4.3 Effect of Multipass Welding

As with the Grade 80, the effect of multipass welding was not explicitly examined. Hardness measurements in the CGHAZ of multipass SMAW welds show no significant changes. Hardness results for the multipass HAZ readings are given in Table 4-4.

**Table 4-4 CGHAZ Hardness Measurements of Varying Passes in Grade 100 Steel**

<b>Location</b>	<b>Hardness (Hv)</b>
Pass 1	341
Pass 2	330
Pass 3	319
Pass 4	323

## Chapter 5 Mechanical Properties

The purpose of this chapter is to examine the effect of welding on the tensile properties of both the materials. It examines the effect of under and over matched weld metal strength, heat input and welding processes on the resulting tensile properties of as welded samples. The tensile properties of both of the materials were assessed using transverse tensile tests. Test parameters used for the testing were previously described in sections 3.2 and 3.5.

Transverse tensile tests are used to evaluate the performance of a weld in the composite formed between the weld and base material. Test results are normally expressed in terms of the overall tensile strength of the composite material and therefore reveal limited information about material. [Denys, 1990] In obtaining a value for the Yield Stress (YS) of a welded sample with the transverse tensile test, a problem arises in that the yield points of the weld metal, HAZ, and base metal can differ by a significant amount. Instead of yielding occurring at a single point, it occurs over a number of points as each section of the sample reaches its respective yield stress. As each section yields, it will undergo some degree of strain hardening until the yield strength of another portion of the weld is now lower than that of the strain hardened region. The situation is further complicated if the HAZ yield stress is lower than that of the base material as there is a HAZ on each side of the weld which can result in double necking. The overall result is a hard to define yield point on the stress strain curve. The software used to report

the YS often underestimates the value of the YS for a test as it reports the point where the stress-strain curve first deviates from a linear path. After taking the 0.2% offset the reported yield is still below the actual yield. An example of this is shown in Figure 5-1 where the software reported a YS of 74000 psi (507 MPa) and the YS is actually around 90000 psi (620 MPa). The underestimated YS value is also confirmed by the reported Young's Modulus, which for many tests was reported as greater than 500 GPa.

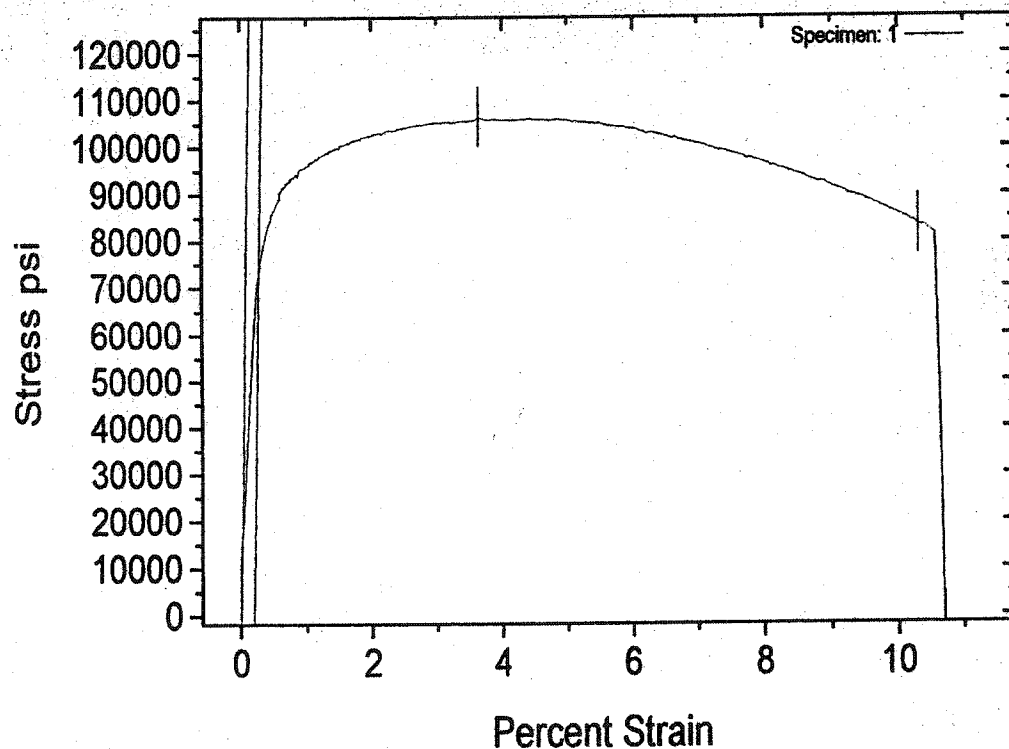


**Figure 5-1 Sample Stress-Strain Curve showing the Variations in yield Stress.**

As a result, reported values of YS were manually checked against the stress-strain curves and adjusted accordingly. This was done by manually by placing a best fit

line through the linear portion of the stress strains curve and then taking the 0.2 % offset. All reported values are calculated as an average from two transverse tensile test welds.

### 5.1 Grade 80

The tensile properties of the Grade 80 material were assessed on a pass/fail basis using a yield strength of 80000 psi (550 MPa) based on designing with the Specified Minimum Yield Stress (SMYS) as the criterion to determine whether or not a weld passed.

#### 5.1.1 Effect of Under and Over Strength Weld Metal

The effect of undermatched and overmatched weld metal strength was examined using a series of SMAW electrodes with increasing ultimate tensile stress values. All welds were fabricated using three passes and an interpass temperature of  $\leq 100^{\circ}\text{C}$ . Tensile test results for the effect of varying strengths of weld metal are given in Table 5-1.

**Table 5-1: Grade 80 SMAW with Variable Consumables**

Consumable	Heat Input (kJ/mm)	YS ksi/ (MPa)	UTS (ksi)/ (MPa)	El %	Failure Location
6018	1.5	62 (428)	81 (558)	11.33	WM
7018	1.5	69 (479)	91 (629)	12.53	WM
8018	1.5	73 (503)	93 (644)	11.83	WM
9018	1.5	83 (572)	104 (715)	13.29	WM
10018	1.5	90 (618)	113 (780)	13.94	BM/HAZ
11018	1.5	90 (620)	113 (780)	13.19	BM/HAZ
12018*	1.5	N/A	N/A	N/A	N/A
12018-B**	1.5	98 (672)	113 (776)	13.73	BM

\* Test sample cracked prior to testing

\*\* Electrode was used in the baked out condition (375°C)

Deliberate weld metal undermatching and overmatching was done to examine the effect of welding on the HAZ of the base material. In the case of weld metal undermatching, plastic strains developed during tensile testing will be concentrated in the WM and HAZ of the test sample. [Denys, 1990] This situation will result in a base metal failure only if the YS of the base metal drops below that of the weld metal. For the welds fabricated with 6018, 7018, and 8018 electrodes the base metal and HAZ yield strength remained above that of the weld metal as all of the plastic deformation was concentrated in the weld metal with no damage found in the HAZ, resulting in weld metal failures for all tests. This indicates that the tensile properties of the material are not significantly affected by the welding process under these test conditions. The degree of softening occurring in the HAZ is therefore minimal. Welding of Grade 80 material with a 9018 electrode should produce a weld with very similar properties to that of the base material with the as deposited weld having a higher strength level. The tensile test with the 9018 electrode resulted in a weld metal failure with the plastic deformation occurring in the weld. The YS of the test was 565 MPa (82000 psi), which is above the required SMYS producing a satisfactory weld. However, welds are normally designed to be stronger than the base material to ensure that weld metal failures do not occur. While 9018 electrodes should provide adequate strength levels for Grade 80 material, the true YS for the material is considerably higher than the SMYS. This difference between the true yield and the SMYS explains the weld metal failure in this case.

Weld metal overmatching results in plastic strain being concentrated outside of the WM in the HAZ or the base material. In this situation, a tensile test should reproduce the yield stress value of a pure base metal test, since the as deposited weld metal tensile properties will be higher than those for the base material. The test welds made with both the 10018 and 11018 electrodes resulted in base metal/HAZ failures. The location of the failures suggests that some degree of mechanical degradation is occurring in the HAZ, as the overmatched weld metal should provide some reinforcement for the HAZ causing failures to occur in unaffected base metal. [Denys, 1990] Both welds did meet the SMYS requirements resulting in acceptable welds.

The first weld made with the 12018 resulted in a through thickness weld metal crack down the center of the weld that was not detected until machining of the tensile samples. Due to the high strength level of the weld metal, the susceptibility to hydrogen cracking is high. When the weld was repeated with an electrode that was used directly from being baked out at 375<sup>0</sup>C, no cracking occurred. The effect of hydrogen levels on weld quality will further discussed in Chapter 6. Failure of the 12018 test sample occurred in just outside of the HAZ. This suggests that the extra reinforcement occurring as a result of the increased weld metal strength compensates for any degradation in mechanical properties that is occurring in the HAZ. During the testing of the 12018B weld, the sample cracked in the vertical axis of the tensile specimen prior to rupture in the

unaffected base material. A schematic drawing of the failure is shown in Figure 5-2.

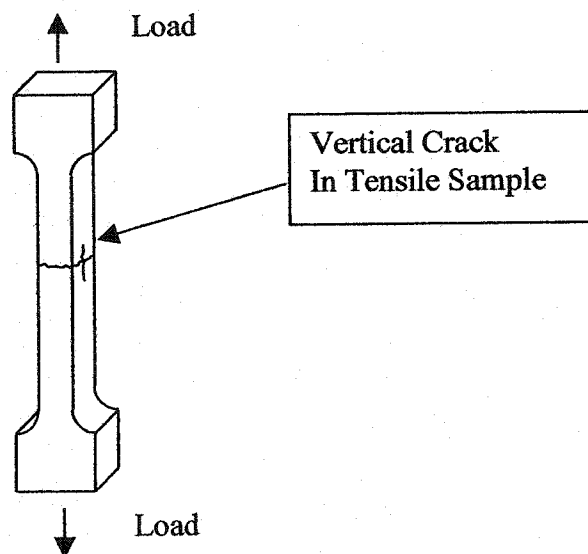


**Figure 5-2 Schematic Drawing of Failure in 12018B Weld Sample.**

The vertical crack that formed during testing suggests that the base material may have variations in through thickness properties due to centerline segregation as a result of the rolling process. Therefore, cruciform tests were carried out on base material to determine if the variations in the steel could be a potential problem. The results of the cruciform tests are given in section 5.3.

#### 5.1.2 Effect of Heat Input on SMAW Process

The effect of heat input on the tensile properties of Grade 80 SMAW welds was examined using a fixed SMAW consumable and varying the heat input levels

through manipulation of the welding speed. The effect of heat input on the tensile properties is given in Table 5-2.

**Table 5-2: Grade 80 SMAW with Variable Heat Inputs**

<b>Consumable</b>	<b>Heat Input (kJ/mm)</b>	<b>YS ksi / (MPa)</b>	<b>UTS ksi / (MPa)</b>	<b>El %</b>	<b>Failure Location</b>
9018	0.5	97 (665)	111 (761)	12.39	WM
9018	1.0	88 (606)	105 (722)	10.96	WM
9018	1.5	83 (571)	104 (715)	13.29	WM
9018	2.0	80 (554)	101 (693)	12.73	WM
9018	2.5	76 (525)	97 (672)	12.58	WM

With increasing levels of heat input, the microstructure of both the HAZ and the weld metal changes from a low temperature transformation product like martensite at a 0.5 kJ/mm heat input to higher temperature transformation products like ferrite plus carbide at a 2.5 kJ/mm heat input. As the heat input is increased, the values of both the YS and UTS decrease continuously as expected. The degree of softening in the HAZ should also be increasing with increased heat input. However, the strength levels of the HAZ remained above that of the weld metal for all of the heat inputs used as all of the tests failed in the weld metal. Welds fabricated at 0.5 and 1.0 kJ/mm both resulted in YS values in excess of the reported YS value for the base material. The test values of yield strength in particular can vary due to differences in specimen dimensions, strain rate and microstructure. All three parameters are involved in comparison of base material and welded specimens. The most likely effect is the effect of microstructure, since



the transverse weld specimen involves straining base metal, varying grain sizes and precipitate sizes and distributions in the HAZ and a weld metal that is significantly stronger than the base material (overmatched).

### 5.1.3 Effect of Heat Input on GMAW Process

As with the SMAW process, the effect of heat input on the GMAW process was done using one consumable with heat inputs varied by welding speed. The Grade 80 GMAW weld results are given in Table 5-3.

**Table 5-3: Grade 80 GMAW with Variable Heat Inputs**

<b>Consumable</b>	<b>Heat Input (kJ/mm)</b>	<b>YS ksi/ (MPa)</b>	<b>UTS ksi / (MPa)</b>	<b>El %</b>	<b>Failure Location</b>
HI 84	0.9	95 (655)	112 (772)	15.64	BM
HI 84	1.5	85 (586)	107 (743)	14.68	BM/HAZ
HI 84	2.0	80 (551)	105 (724)	13.46	BM/HAZ

With increasing levels of heat input both the YS and UTS decreased, will all welds still meeting the required YS level of 80000 psi (550 MPa). With the GMAW process the effective heat input of the process is higher due to the increased process efficiency. This increase in efficiency resulted in BM/HAZ failures as the degree of softening in the HAZ was more substantial than with the SMAW process. The welds fabricated with the 1.5 and 2.0 kJ/mm heat inputs both had YS values below that of the base material. While all of the welds meet

the SMYS requirements, the softening occurring with the GMAW process restricts the use of high heat input welding.

## 5.2 *Grade 100*

As with the Grade 80, the tensile properties of the Grade 100 material were assessed on a pass fail basis using a yield strength of 100000 psi (690 MPa); based on designing with Specifies Minimum Yield Stress (SMYS), as the criterion to determine whether or not a weld passed.

### 5.2.1 Effect of Under and Over Strength Weld Metal

The effect of undermatched and overmatched weld metal strength on the Grade 100 material was also examined using a series of SMAW electrodes with increasing ultimate tensile stress values. All welds were fabricated using three passes and an interpass temperature of  $\leq 100^{\circ}\text{C}$ . Tensile test results for the effect of varying strengths of weld metal are given in Table 5-4.

**Table 5-4: Grade 100 SMAW with Variable Consumables**

<b>Consumable</b>	<b>Heat Input (kJ/mm)</b>	<b>YS ksi / (MPa)</b>	<b>UTS ksi / (MPa)</b>	<b>El %</b>	<b>Failure Location</b>
8018	1.5	78 (534)	98 (672)	11.45	WM
9018	1.5	90 (620)	106 (730)	10.96	WM
10018	1.5	98 (673)	126 (872)	10.84	BM/HAZ
11018	1.5	100 (689)	124 (858)	11.68	BM/HAZ
12018	1.5	110 (758)	128 (880)	11.36	BM/HAZ
12018-B	1.5	110 (758)	127 (880)	11.28	BM/HAZ

Weld metal undermatching for the Grade 100 should have occurred with all of the electrodes below 11018. Both the 8018 and 9018 indicated weld metal undermatching, with both tests resulting in weld metal failures and yield strength levels below that of the base material. The use of a 10018 electrode should have also resulted in weld metal undermatching as the specified YS and UTS of the electrode are lower than that of the base metal. Failure of the HAZ in the base metal when welded with a 10018 electrode indicates a possible susceptibility to softening at this heat input as the HAZ yield stress is below the minimum specified value. The use of 11018 and 12018 electrodes also resulted in HAZ failures in the base metal with YS values meeting the 100000 psi (690 MPa) requirement. The increased YS levels obtained with the 11018 and the 12018 electrodes demonstrated the advantages of weld metal overmatching, as any softening effects are negated by the reinforcement of the stronger weld metal. As with the Grade 80 welded with the 12018 electrode, a central weld metal crack developed in the sample. The crack did not, however, propagate the entire length of the sample, enabling one tensile sample to be machined. Redoing the test with a baked out the electrode at 375<sup>0</sup>C again prevented the formation of a crack. During the testing of the 12018 sample, a centerline crack in the vertical section developed prior to rupture as for the Grade 80.

### 5.2.2 Effect of Heat Input on SMAW Process

The effect of heat input on the tensile properties of Grade 100 SMAW welds was examined using a fixed SMAW consumable and varying the heat input levels

through manipulation of the welding speed. The effect of heat input on the tensile properties is given in Table 5-5.

**Table 5-5: Grade 100 SMAW with Variable Heat Inputs**

<b>Consumable</b>	<b>Heat Input (kJ/mm)</b>	<b>YS ksi / (MPa)</b>	<b>UTS ksi / (MPa)</b>	<b>El %</b>	<b>Failure Location</b>
11018	0.5	N/A	N/A	N/A	N/A
11018	1.0	103 (708)	126 (870)	12.14	BM/HAZ
11018	1.5	100 (689)	124 (858)	11.68	BM/HAZ
11018	2.0	100 (689)	120 (827)	13.26	BM/HAZ
11018	2.5	100 (689)	120 (827)	12.82	WM

During the welding of the Grade 100 material, a significant magnetic field was developed, creating some arc instability (arc blow). At heat inputs of 1.0 and above, the speed of welding allows time for self-correction during the making of the weld bead. When the heat input was set to 0.5 kJ/mm, the time for self-correction became too small to allow for an acceptable weld bead to be deposited, resulting in no test at that heat input. Increasing the heat input of the weld resulted in decreased values for the YS and UTS of the weld joint. The problem of defining the true YS values for the Grade 100 was more pronounced than with the Grade 80. Due to the increase in the relative amount of softening occurring in the HAZ of the base metal, yielding occurs over a larger strain interval, making identification of the YS much more difficult. All of the heat inputs examined produced YS values above that of the SMYS indicating that the effect of heat input on the mechanical properties of the base material is minimal.

### 5.2.3 Effect of Heat Input on GMAW

The effect of heat input on the GMAW process was assessed using one consumable with heat inputs varied by welding speed. The Grade 100 GMAW weld results are given in Table 5-6.

**Table 5-6: Grade 100 GMAW with Variable Heat Inputs**

Consumable	Heat Input (kJ/mm)	YS ksi / (MPa)	UTS ksi / (MPa)	El %	Failure Location
HI 84	0.9	110 (758)	126 (868)	12.76	BM/HAZ
HI 84	1.5	95 (655)	119 (818)	13.13	WM
HI 84	2.0	90 (620)	115 (790)	14.31	WM

Increasing the level of heat input resulted in a substantial decrease in the YS and UTS of the welds. With increasing heat input, the resulting microstructure becomes weaker and the amount of base metal dilution increases. As a result, only the 0.9 kJ/mm weld was able to meet the 100000 psi (690 MPa) YS criterion. Failure of the weld metal at the 1.5 and 2.0 kJ/mm heat input levels suggests that weld metal microstructure and mechanical properties are more of a concern than HAZ softening.

### 5.3 Cruciform Tests

Cruciform tests were carried out on both materials to determine if any detrimental through thickness variations existed in the steel that could be a potential problem. By placing the centerline of the material in the middle of tensile sample any weak or brittle zones that exist in the material will be exposed upon testing. Two test

configurations were chosen to perform the test, as the first joint configuration does not allow for tensile samples to be machined (because the welds do not have full penetration). With full penetration welds as used in the second configuration, the as rolled structure of the material in the center plate will be completely lost during welding due to the HAZ on both sides of the plate.

#### 5.3.1 Grade 80

The first cruciform joint tested as shown in Figure 3-4 A, was tested as a regular tensile test without a reduced cross section. Both test samples resulted in shearing of the fillet welds. The excess weld metal present due to the combined throat thickness of both welds suggests that there is no weak zone at the centreline. Testing of the tensile samples cut from the second joint configuration resulted in weld metal failures with an average YS value of 586 MPa (85000 psi) indicating again that there is no weak zone at the steel centreline.

#### 5.3.2 Grade 100

As with the Grade 80, the first set of cruciform tests resulted in weld metal shear of fillet welds. Tensile samples tested from the second joint configuration resulted in an average YS level of 634 MPa (92000 psi) with one failure occurring at the centerline of the plate and two occurring the welds. The low YS values obtained indicate that the original as-rolled properties were diminished due to welding. The failures suggest that there is a slightly higher risk of a centerline weakness in the Grade 100 compared to the Grade 80. This may be due to greater

segregation of alloying and residual elements and/or a different texture due to rolling practices.

## Chapter 6 Weld and Base Metal Cracking

This chapter examines susceptibility of each material to cold cracking. It looks at the effect of hydrogen level, heat input, stress level, and preheat on the resistance to cracking. The susceptibility to cold cracking for both materials was assessed through the use of the implant test and the WIC rigid restraint cracking test. Test parameters used in the testing were previously described in sections 3.7 and 3.9.

Results of the implant tests are given below in Tables 6-1-6.9. Time is reported as hh:mm:ss and the background shade indicates the failure type where:

No Failure
Base Metal
Weld Metal Shear

### 6.1 Grade 80 Implant Tests

The effect of hydrogen level on the Grade 80's susceptibility to cold cracking was evaluated using three different SMAW electrodes. These tests show the effect of hydrogen level on the steel's ability to resist cold cracking. The use of an EXX10 electrode will typically produce hydrogen levels in the 25-65 ppm range, EXX24 will give 20-40 ppm, and the EXX18 will give 5-10 ppm. Implant test results for the Grade 80 welded with different electrodes are given in Table 6-1.



**Table 6-1: Effect of Hydrogen Level on Grade 80 Implant Specimens at 78% of SMYS.**

<b>Electrode</b>	<b>Heat Input</b>		
	<b>1.0</b>	<b>1.5</b>	<b>2.0</b>
8010	00:07:26	00:14:28	24:00:00
7024	24:00:00	24:00:00	24:00:00
9018	24:00:00	24:00:00	24:00:00

At a stress level of only 78% of SMYS (62400 psi) the Grade 80 implant tests resulted in base metal failures when welded with the 8010 electrodes. When welded with both the 7024 and 9018 electrodes no failures occurred in the test. Failures of the base metal at stress levels significantly below the SMYS indicates the necessity for low hydrogen welding procedures to be used.

Using low hydrogen electrodes, the effect of heat input on cracking susceptibility at varying load combinations was examined. Test results for the varying load and heat input combinations are given in Table 6-2.

**Table 6-2: Effect of Heat Input on Grade 80 Implant Specimens Welded with a 9018 Electrode.**

<b>Load % SMYS</b>	<b>Heat Input</b>				
	<b>0.5</b>	<b>1.0</b>	<b>1.5</b>	<b>2.0</b>	<b>2.5</b>
80	-	-	-	24:00:00	-
100	-	24:00:00	24:00:00	24:00:00	-
120	24:00:00	24:00:00	-	-	-
130	-	-	-	24:00:00	24:00:00
140	24:00:00	24:00:00	24:00:00	00:00:04	

From the results shown in Table 6-2 it is evident that the grade 80 material has a very low susceptibility to cold cracking. At a load of 100% of the SMYS, no failures occurred in the samples. This gives an ideal critical stress ratio of 1.0. While the validity of the implant test at stress levels above the yield stress have been questioned due to possible yielding of the base material, tests above 100% of the SMYS were carried out to assess the material's response to loads near the UTS. The results in Table 6-2 show that even in the presence of a notch in the sample, the grade 80 specimens were able to withstand loads just below the UTS of the material.

## 6.2 Hydrogen Analysis for Grade 80 Consumables

In order to quantify the typical level of hydrogen seen in each of the implant tests, diffusible hydrogen tests were conducted on all of the consumables used to weld the grade 80. Diffusible hydrogen test results are listed in Table 6-3.

**Table 6-3: Hydrogen Analysis of 9018**

Consumable	Heat Input (kJ/mm)	Diffusible Hydrogen (ppm)
9018	0.5	4.5
9018	1.0	3.9
9018	1.5	3.5
9018	2.0	2.6
9018	2.5	2.9

With increasing heat input levels the level of hydrogen in the weld metal decreases, as there is more time for the hydrogen to diffuse out of the weld metal as the metal remains hot for a longer time. From these results, the grade 80

material is resistant to diffusible hydrogen levels as high as about 5 ppm. This level of hydrogen should be obtainable with most commercial electrodes that are properly conditioned.

### 6.3 Grade 100 Implant Test

The effect of hydrogen level on the Grade 100's susceptibility to cold cracking was evaluated using two different SMAW electrodes. At higher strength levels, the number of consumables available for welding is reduced thereby only allowing for two hydrogen levels to be examined. The implant test results for the Grade 100 welded with different electrodes are given in Table 6-4.

**Table 6-4: Effect of Hydrogen Level on Grade 100 Implant Specimens at 78% of SMYS.**

Electrode	Heat Input		
	1.0	1.5	2.0
9010	00:03:21	00:05:25	
11018	24:00:00	24:00:00	24:00:00

At a stress level of 78% of SMYS (78000 psi) the Grade 100 implant tests resulted in base metal failures when welded with the 9010 electrodes. When welded with the 11018 electrodes no failures occurred in the test. As with the Grade 80 material, failures of the base metal at stress levels significantly below the SMYS indicates the necessity for low hydrogen welding procedures to be used.

The effect of heat input on cracking susceptibility when welding with low hydrogen electrodes was examined at varying load combinations. Test results for the varying heat input and load combinations are given in Table 6-5.

**Table 6-5: Effect of Heat Input on Grade 100 Implant Specimens Welded with a 11018 Electrode.**

Load % SMYS	Heat Input			
	1.0	1.5	2.0	2.5
80	24:00:00	N/A	N/A	N/A
90	24:00:00	24:00:00	24:00:00	N/A
95	05:18:42	08:20:02	24:00:00	N/A
100	02:30:16	03:23:48	02:35:08	24:00:00
100				06:18:30

In examining the effect of heat input on the resistance to cold cracking, it is clear that increasing the heat input decreases the probability of cold cracking, as expected. With increased heat input the resulting microstructure will be softer and less susceptible to cracking and atomic hydrogen will disperse more thoroughly. Unlike the Grade 80 material, loads in excess of 100% of the SMYS were not obtained for all the heat inputs examined. At a load of 95% of the SMYS, the only tests that did not fail were those at 2.0 and 2.5 kJ/mm. When the load was increased to 100% of the SMYS the 2.0 kJ/mm samples also failed. Because the time to failure of the 2.0 kJ/mm at 100% of the SMYS was very low, the successful test at the 2.5kJ/mm was repeated to verify the result. Retesting under the same conditions resulted in a failure at the 6 minute mark. It was speculated that the difference between the two tests may have been due to the condition of the electrodes, as the successful test had been done with an electrode that had been baked out and stored for less than 24 hours. To confirm this

speculation, the effect of the electrode storage condition on the implant results was examined by repeating the implant tests with electrodes that had been exposed to varying times in the electrode storage ovens. Baking of electrodes was done at 370°C for 1 hour as per AWS 5.3.2.4 and storage was at 200°C in accordance with AWS 5.3.2.1. The results of the varying storage conditions examined are given in Table 6-6.

**Table 6-6: Effect of Electrode Condition on Grade 100 Implant Specimens Welded with 11018 Electrodes**

Load 100 % SMYS	Heat Input			
	1.0	1.5	2.0	2.5
Bake Out		02:06:56		24:00:00
Bake Out & Held 24 hr				24:00:00
Bake Out Held 48 hr				1:50:10
Bake Out Held > 1 Week		03:23:48		00:52:36

In examining the effect of electrode condition on the occurrence of cold cracking, it was observed that using electrodes in the as baked out condition prevented failure at high heat input levels. This result suggests that the hydrogen content of the electrodes is increasing as a function of the amount of time they are stored. The above result also suggests that a load of 100 % of the SMYS may be attainable if the hydrogen content is further reduced. Testing at lower hydrogen levels was accomplished by performing GMAW implant tests. The results of the test are given in Table 6-7.

**Table 6-7: Comparison of GMAW and SMAW Implant Tests for Varying Heat Inputs at a Constant Load for Gr. 100**

	<b>Heat Input</b>			
<b>Load 120 % SMYS</b>	<b>1.0</b>	<b>1.5</b>	<b>2.0</b>	<b>2.5</b>
<b>SMAW</b>				
<b>Bake Out (371°C)</b>	02:33:198			03:58:57
<b>Bake Out &amp; Held</b>	05:41:11	03:50:32	06:35:40	06:18:11
<b>GMAW</b>	24:00:00	24:00:00		24:00:00

In comparing samples welded with GMAW vs. SMAW, the reduced hydrogen levels associated with GMAW allowed for stress levels of 120% of SMYS for all of the heat inputs examined. From this result it is evident that the susceptibility to cold cracking is very low as long as very low levels of hydrogen are present. Hydrogen tests done on electrodes show that a freshly baked out electrode will have as deposited hydrogen levels of  $\approx 3.3$  ppm whereas an electrode baked and stored for more than 48 hr at 200°C can have a level of  $\approx 5.0$  ppm. While this difference is small, it could account for the difference between a failure occurring or not occurring, if applied or residual stress levels are high.

#### **6.4 Hydrogen Analysis for Grade 100 Consumables**

Diffusible hydrogen analysis was carried out on both the SMAW and GMAW consumables for all of the heat inputs examined to quantify the amount of hydrogen present in the implants. The hydrogen results are listed in Table 6-8.

**Table 6-8: Diffusible Hydrogen Analysis for 11018 and HI 84 Electrodes**

<b>Consumable</b>	<b>Heat Input (kJ/mm)</b>	<b>Diffusible Hydrogen (ppm)</b>
11018	0.5	6.6
11018	1.0	5.0
11018 Baked Out	1.0	3.3
11018	1.5	5.0
11018	2.0	5.7
11018	2.5	3.2
HI 84	1.0	3.0
HI 84	1.5	2.9
HI 84	2.0	2.6

In comparing the results for the hydrogen tests of the 11018 electrodes to the 9018 electrodes it is clear that the levels for the 11018 electrodes have a higher hydrogen content. These results, in conjunction with the implant tests, suggest that a hydrogen level of less than 4 ppm is necessary to prevent hydrogen assisted cracking in the Grade 100 material.

### ***6.5 Comparison of Implant Results with Other Steels***

Many of the studies found in literature that use implant testing involve the use of high hydrogen electrodes. High hydrogen electrodes find wide application in the welding of plain carbon steel material but their use on HSLA is not appropriate. The high susceptibility to hydrogen cracking associated with increased strength levels require that low hydrogen processes be used with controlled procedure conditions.

In studying the susceptibility of a 0.52 carbon equivalent (CE) and a 0.44 CE plain carbon steel, Watkinson and Hart showed that when hydrogen levels are below 10ppm, no rupture occurred in the 0.44CE steel for all of all heat inputs examined at a stress level equal to the yield stress. [Watkinson, 2001] For the 0.52 CE steel, rupture occurred at hydrogen levels below 5 ppm for all of the heat inputs examined. More recent work by Datta et al. al. on TMCP plate material with a YS of 65000 psi (450 MPa), welded with 8018 electrodes, demonstrated that it was necessary to rebake electrodes at 350°C for 2 hours in order to prevent failure of implant samples at loads of 100% of the SMYS. The fact that this same result was found for the Grade 100 demonstrates that it has excellent weldability when compared to similar steels of lower strength. However, the Grade 100 steel is more sensitive than Grade 80 and must be welded only with electrodes that can ensure a diffusible hydrogen level of <4 ppm, if high residual or applied stresses may be present. Since base metal yield strength stresses can be expected in most welded structures, strict adherence to low hydrogen procedures is a prudent step for all welding of Grade 100.

#### ***6.6 Grade 80 WIC Rigid Restraint Cracking Tests***

WIC tests were carried out to determine the critical preheat required to prevent cracking of the test sample using different joint configurations and welding processes. The results of the grade 80 WIC tests are given in Table 6-9.



Table 6-9: WIC Test Results for Grade 80.

Process and Grade	Joint Design and Temperature	Result
SMAW Gr. 80	45° Bevel vs. Straight Edge @ Rm. Temp.	Small Crack $\leq 250\mu\text{m}$ <b>Pass</b>
SMAW Gr. 80	45° Bevel vs. Straight Edge @ 100°C	No Cracking <b>Pass</b>
SMAW Gr. 80	45° Bevel vs. 45° Bevel @ Rm. Temp.	No Cracking <b>Pass</b>
GMAW Gr. 80	45° Bevel vs. Straight Edge @ Rm. Temp.	No Cracking <b>Pass</b>

For all of the WIC tests conducted, a crack length of 250  $\mu\text{m}$  or less was set as the criterion for a pass. Cracks less than 250  $\mu\text{m}$  in length are too small to be detected using ultrasonic testing. As the purpose of this study was to assess the weldability of the base material and not the welding consumables, the presence of very small cracks in the weld metal was not a concern.

The first WIC test conducted using a straight edge vs. a 45° bevel at room temperature resulted in a small crack at the point where the weld metal meets the base material as can be seen in Figure 6-1.

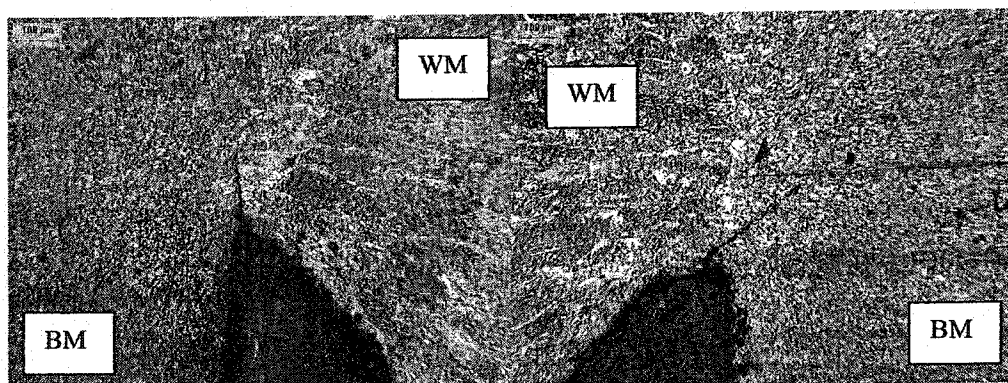
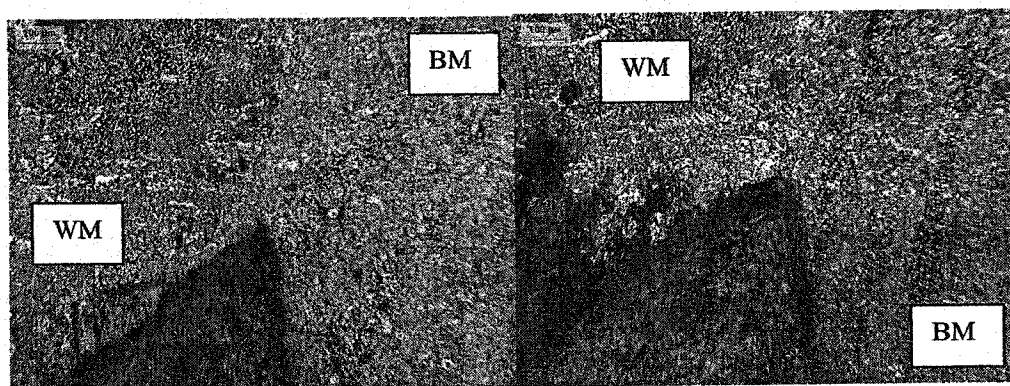


Figure 6-1 SMAW Grade 80 45 Bevel vs. Straight Edge.

In the first image the crack propagates through the weld metal, while in the second the cracks propagate into the adjacent base material. This result demonstrates the validity of the test in determining the crack susceptibility of the base material, as the crack will propagate along the path of least resistance. Repeating the test at a preheat temperature of 100°C resulted in the elimination of cracks at the weld root as shown in Figure 6-2.



**Figure 6-2 SMAW Grade 80 45° Bevel vs. Straight Edge at 100°C**

The effect of joint geometry on the preheat required to eliminate cracking was evaluated by decreasing the notch acuity present at the weld root. The joint design was changed to a 45° bevel vs. a 45° bevel in order to decrease the stress intensity at the root location. When welded at room temperature no cracks developed in the weld as shown in Figure 6-3.

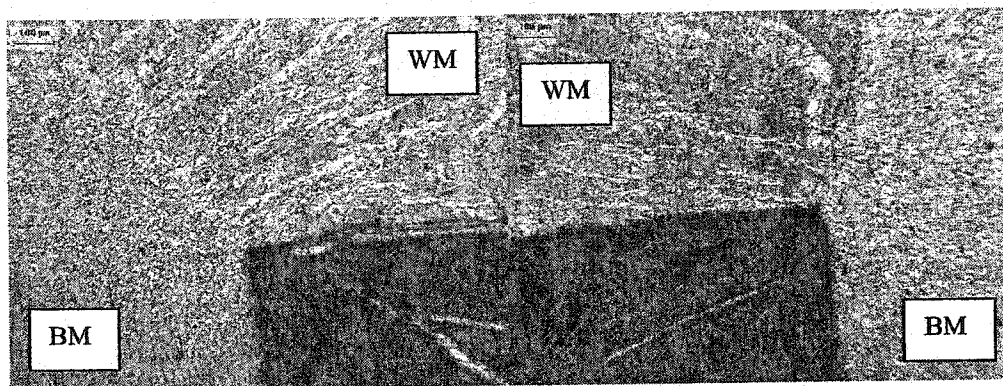


**Figure 6-3: SMAW Grade 80 45° Bevel vs. 45° Bevel**

The effect of GMAW on critical preheat temperature was evaluated using the initial straight edge vs. 45° bevel weld joint configuration. Micrographic examination of the weld joint revealed significant cracks greater than 250 $\mu$ m in length in the weld root. Figure 6-4 shows the cracks present on the both sides of the weld root.

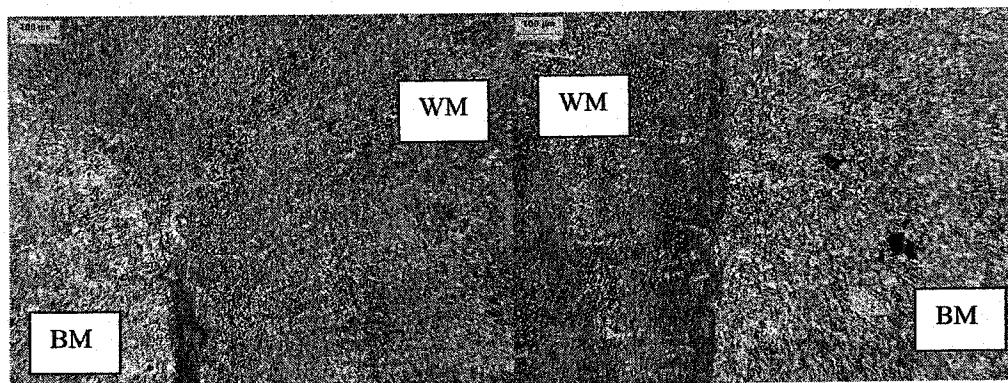


**Figure 6-4 : GMAW Grade 80 45° Bevel vs. Straight Edge**

While both cracks on either sides of the weld have lengths greater than 250 $\mu$ m in length, the cracks are due to a large amount of cold lap present in the weld. Figure 6-5 shows the large degree of cold lap present in the weld root.

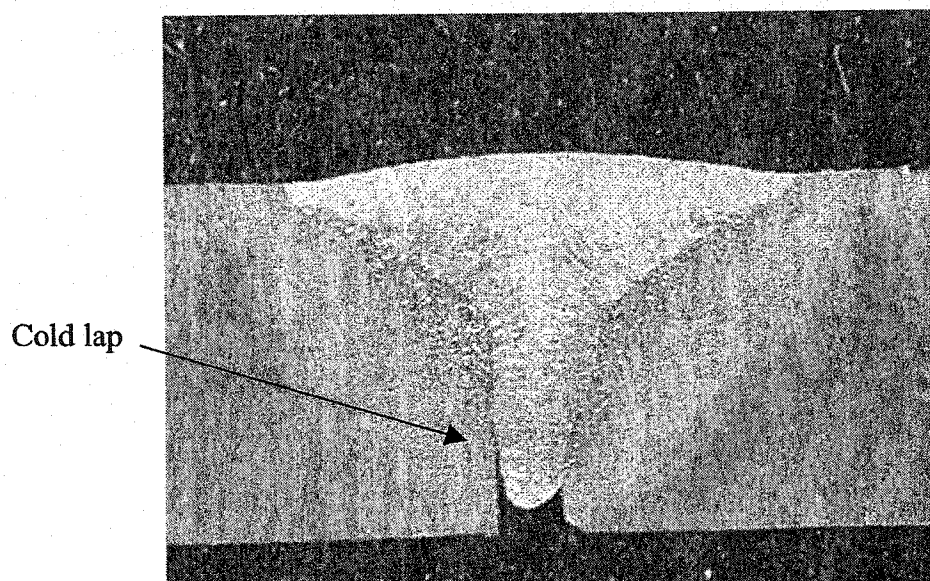


**Figure 6-5: Transverse Section of GMAW WIC Test**

The cold lap that results from a lack of fusion between the molten weld metal and un-melted base metal causes a large increase in the stress concentration at the crack tip due to the sharpness of the crack tip. [Anderson, 1995] Due to this increase in the stress concentration at the crack tip, this test was considered a pass even though the crack propagated further than 250 $\mu$ m.

#### ***6.7 Grade 100 WIC Rigid Restraint Cracking Tests***

WIC tests carried out on the grade 100 material were performed under the same conditions as the grade 80 tests. The results of the grade 100 WIC tests are given in Table 6-10.

Table 6-10: WIC Test Results for Grade 100

Process and Grade	Joint Design and Temperature	Result
SMAW Gr. 100	45° Bevel vs. Straight Edge @ Rm. Temp.	Small Crack $\geq 250\mu\text{m}$ <b>Fail</b>
SMAW Gr. 100	45° Bevel vs. Straight Edge @ 100°C	Small Crack $\leq 250\mu\text{m}$ <b>Pass</b>
SMAW Gr. 100	45° Bevel vs. 45° Bevel @ Rm. Temp.	Full Crack <b>Fail</b>
GMAW Gr. 100	45° Bevel vs. Straight Edge @ Rm. Temp.	Small Crack $\geq 250\mu\text{m}$ <b>Pass</b>

As with the grade 80 material, the WIC test conducted using a straight edge vs. a 45° bevel at room temperature resulted in the formation of cracks at the weld root where the weld metal meets the base material as shown in Figure 6-6.

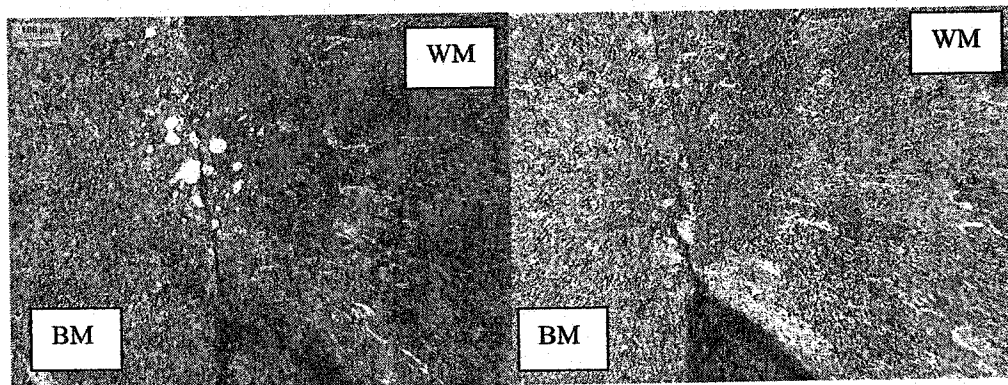
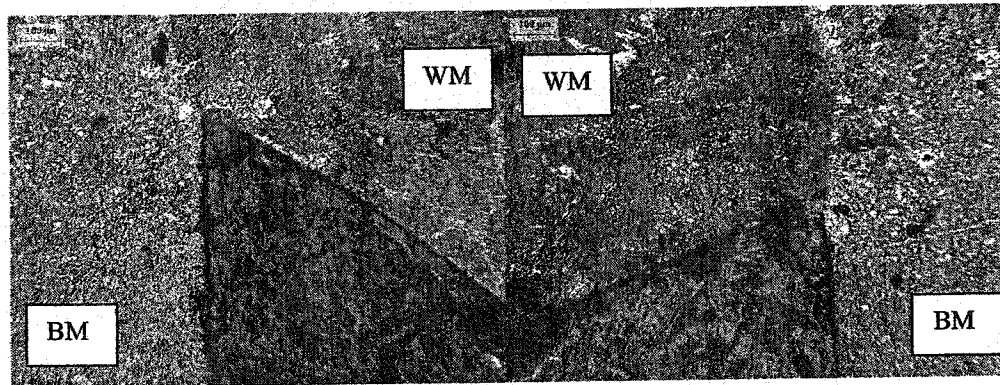


Figure 6-6 SMAW Grade 100 45° Bevel vs. Straight Edge

In the left image the crack propagates along the fusion line between weld and base metal while the image on the right shows the crack initially going into the base metal before turning back into the weld metal. The resulting crack length in the test was greater than the specified 250  $\mu\text{m}$  thereby resulting in a fail. Repeating

the test at a preheat temperature of 100°C resulted in the elimination of cracks at the weld root as can be seen in Figure 6-7.



**Figure 6-7 SMAW Grade 100 45° Bevel vs. Straight Edge at 100°C.**

Welding of the Grade 100 material using a 45° bevel vs. a 45° bevel joint geometry resulted in a full crack through the weld. Figure 6-8 shows the through thickness crack in the weld metal of the test sample.

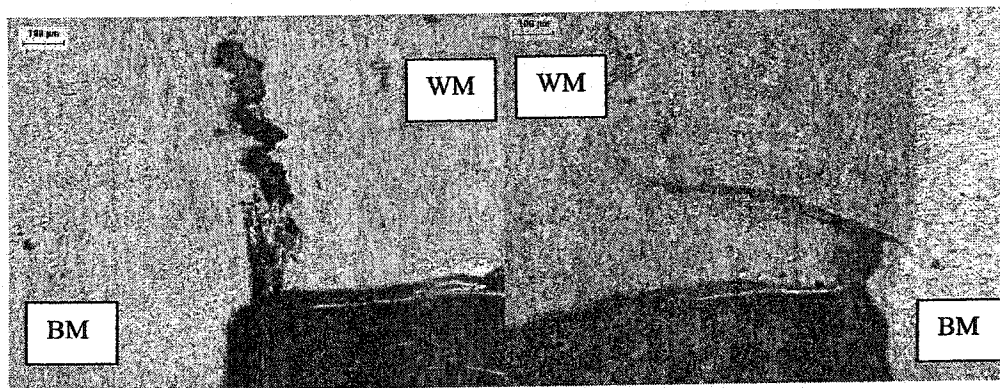


**Figure 6-8 SMAW Grade 100 45° Bevel vs. 45° Bevel.**

With a decrease in the notch acuity present in the weld joint, the degree of cracking should be less than that experienced in the 45° bevel vs. a straight edge. Macroscopic examination of the weld reveals that the throat thickness of the weld

deposit in this test is significantly smaller than that of the first test as there is a larger volume of space in the weld joint. This decrease in the effective weld size results in a higher stress in the weld metal. This fact in combination with the crack being limited to the weld metal and not the HAZ of the base material suggests a good result in terms of base metal weldability.

As with the Grade 80, GMAW WIC testing resulted in the formation of cracks greater than 250  $\mu\text{m}$  in length as a result of the cold lap present in weld joint.

Figure 6-9 shows the cracks present on the both sides of the weld root.

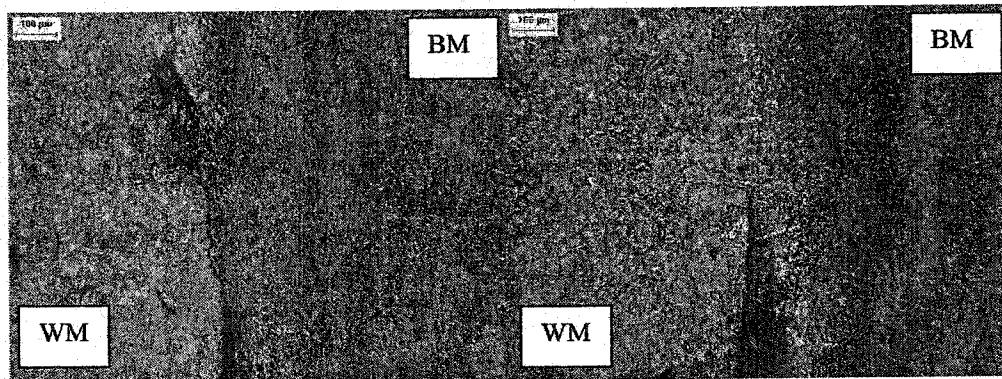


**Figure 6-9 GMAW Grade 100 45° Bevel vs. Straight Edge.**

Because the cracking in the GMAW test can be attributed to the cold lap present in weld, the test was considered a pass.

### **6.8 Comparison of WIC Results with Other Steels**

In order to quantify the minimum preheat temperature required to prevent cracking in the WIC test, the obtained results must be compared to other grades of

similar steels. Most studies that have employed WIC testing as a means to evaluate cracking susceptibility have been used on pipeline grade steels. These steels have a very similar composition to the steel used in this study, which are characterized by low carbon levels and low levels of sulphur and phosphorous.

In assessing HAC in high strength pipeline steels, Signes and Howe [Signes, 1988] demonstrated that the critical preheat temperature required to avoid cracking in a 70000 psi (480 MPa) YS material when welded with a low hydrogen electrode was  $-4^{\circ}\text{C}$ . Most other studies that employ WIC testing as a means of assessing cracking are carried out using cellulose electrodes, as this replicates the hot pass technique used in actual field welding. Studies by Sawhill [Sawhill, 1986] and North [North, 1982] have demonstrated that pipeline steels with a SMYS of 70000 psi (480 MPa) require a preheat of  $80^{\circ}\text{C}$  and  $120^{\circ}\text{C}$  respectively to prevent cracking when welded with a high hydrogen cellulose electrodes.



## Chapter 7 Conclusions and Recommendations

### 7.1 Conclusions

Based upon the work carried out in this study, the following conclusions about the weldability of Grade 80 and Grade 100 steels can be made:

1. Due to the low carbon equivalent of the both grades of steel, the microstructure present in the weld zone can vary from coarse ferrite plus carbide at high heat inputs to martensite at very low heat inputs. This allows for a large degree of control of the final microstructure present in the weld zone if procedural control is adequate.
2. Welding at very low heat inputs prevented any softening from occurring in the weld zone of both materials. The largest degree of softening for both materials occurred in the FGHAZ at heat inputs above 1.0 kJ/mm. Further increases to heat input had little effect on the FGHAZ hardness, but did cause significant softening to also occur in the CGHAZ. This suggests that precipitation hardening effects, as well as microstructural effects, are affected by the weld thermal cycle.
3. Both grades of steel exhibit excellent weldability with regard to their ability to retain their SMYS requirements under varying heat inputs. The Grade 80 was successfully welded with the SMAW process at heat inputs ranging from 0.5 – 2.0 kJ/mm and with the GMAW process at heat inputs from 0.9 – 2.0 kJ/mm. The Grade 100 material was also successfully

welded with the SMAW process at heat inputs from 1.0 – 2.5 kJ/mm and with the GMAW process at a heat input of 0.9 kJ/mm. GMAW at heat inputs of 1.5 and 2.0 kJ/mm were unsuccessful due to a decrease in filler metal mechanical properties at these levels.

4. Both materials showed a decrease in the HAZ strength with high heat input levels, with the Grade 100 showing a larger effect, as indicated by the hardness measurements.
5. Both materials exhibit sensitivity to hydrogen cracking when low hydrogen procedures are not used.
6. The Grade 80 material showed a very low susceptibility to hydrogen cracking when normal low hydrogen procedures were used, i.e., diffusible hydrogen levels about 5 ppm. Implant tests revealed no hydrogen cracking over a large range of heat inputs at stress levels above the yield stress of the material.
7. The Grade 100 material demonstrated a higher susceptibility to hydrogen cracking when compared with the Grade 80. Implant tests revealed that when welded with the SMAW process, stress levels at the SMYS were not obtainable unless the electrode was used in the baked out condition, i.e. diffusible hydrogen levels of less than 4 ppm. This demonstrates that the level of hydrogen tolerable in the Grade 100 material is measurably less than that of the Grade 80. The increased susceptibility to hydrogen cracking in Grade 100 is probably a result of the higher values of residual stress present in a welded structure.

8. GMAW can be used to avoid hydrogen cracking in both materials due to the lower diffusible hydrogen levels associated with the process (<3 ppm). This was shown with the Grade 100 implant samples that did not fail at loads above the SMYS.
9. Both materials were successfully welded under varying heat inputs with both the SMAW and GMAW process without the use of a preheat.
10. In situations of very high stress levels, a preheat of 100°C appears to be sufficient to prevent cracking.

## **7.2 Recommendations**

The following are recommendations for further study into the weldability of TMCP microalloyed steel:

1. Characterization of the HAZ microstructure to understand the effect of heat input on mechanical properties which determine strengthening mechanisms. This is required to determine why an increased heat input resulted in a much larger grain size without a substantial decrease in HAZ strength. Precipitation hardening effects should be assessed in conjunction with the observed microstructural effects of the weld thermal cycle at various heat inputs.
2. The effect of SMAW electrode storage condition on the level of diffusible hydrogen found in the weld zone needs to be determined to allow for adequate procedural control in the prevention of hydrogen cracking for the Grade 100 material in particular.

3. Maximization of the weld joint performance though the use of various consumable types and manufacturers should be examined to determine the full potential of the materials, as the weld metal strength was the limiting factor in a number of the tests conducted, primarily for the Grade 100 material.

## References

- Alam, N et al., 1997, "Weldment Cold Cracking-The Effects of Hydrogen and Other Factors," *Hydrogen Management in Steel Weldments*, DSTO, Melbourne, Australia, pp 49-60.
- Anderson, T.L., 1995, *Fracture Mechanics Fundamentals and Applications*, Second Edition, CRC Press, New York.
- AWS, 2000, *Structural Welding Code-Steel*, 17<sup>th</sup> Edition, AWS, Miami, Florida.
- AWS, 1991, *Welding Handbook Volume 2 Welding Processes*, Eighth Edition, American Welding Society, Miami, Florida.
- AWS, 1998, *Welding Handbook Volume 4 Materials and Applications- Part 2*, Eighth Edition, American Welding Society, Miami, Florida.
- Chen, S., Wang, S., Hsieh, R., 1991 "The Development of High Strength Low Alloy Steel Plates Suitable for High Heat Input Welding", *International Conference on Processing, Microstructure and Properties of Microalloyed and Other Modern High Strength Low Alloy Steels*, Pittsburgh, Pennsylvania, USA, pp. 435-441.
- Bryhan, A., 1981, "The Effect of Testing Procedures on Implant Test Results," *Welding Journal*, September, pp 169s-176s.
- Collins, L. Knight, R. Ruddle, Boyd, J.D., 1985, "Laboratory Development of Accelerated Cooling of Microalloyed Plate Steels," *Accelerated Cooling of Steel*, Pittsburgh, Pennsylvania, pp. 261-282.
- Collins, L. Godden, M. Boys, J., 1983, "Microstructures of Line Pipe Steels," *Canadian Metallurgy Quarterly*, Vol. 22, No. 2, pp 169-179.
- Datta, R., Mukerjee, D. Mishra, S., 1997, "Thermomechanical Processing of High Tensile Plates and Associated Weldability Properties", *Thermec 97 International Conference on the Thermomechanical Processing of Steels and Other Materials*, TMS, pp. 327-337.
- DeArdo, A.J., 1995, "Modern Thermomechanical Processing of Microalloyed Steel: A physical Metallurgy Perspective," *ISS Proceeding of the International Conference Microalloying 95*, Pittsburgh, Pennsylvania, pp. 15-33.
- De Meester, B., 1997, "The Weldability of Modern Structural TMCP Steels," *ISIJ International*, 37(6), pp.537-551.

- Denys, R.M., 1989, "Difference between Small and Large Scale Testing of Weldments," *Welding Journal*, Vol. 68, No 2., pp 33s-43s.
- Denys, R. M., 1990, "Research Directions in Welded High Strength Steel Structures," *Proc. Conf. On Advances Joining Technologies*, Chapman and Hill. Editor T. North
- Denys, R.M., 1990, "Implications of Overmatching/Undermatching of Weld Metal Yield Strength," *The Metallurgy, Welding, and Qualification of Microalloyed (HSLA) Steel Weldments*, AWS, Texas, pp 573-572.
- Easterling, K., 1983, *Introduction to the Physical Metallurgy of Welding*, Butterworths & Co., London.
- Garcia, C., 1995, "Transformation Strengthening of MA Steels," *ISS Proceeding of the International Conference Microalloying 95*, Pittsburgh, Pennsylvania, pp. 365-375.
- Gladman, T., 1997, *The Physical Metallurgy of Microalloyed Steels*, The Institute of Materials, London.
- Granjon, H., 1979, "Survey of Cracking Tests," *Welding in the World*, Vol. 17, No ¾, pp. 42-46.
- Graville, B.A., 1975, *The Principles of Cold Cracking in Welds*, Dominion Bridge Company Limited, Montreal.
- Honeycombe, R., Bhadeshia, H., 1995, *Steels Microstructure and Properties*, Edward Arnold, London.
- Hulka, K. Bauer, J., 1999, "Development Trends in HSLA Steels for Welded Construction," *International Symposium on Steel for Fabricated Structures*, Cincinnati Ohio, ASM International, pp. 11-20.
- Hulka, K., 1988, "Fundamental Aspects in Hot Rolling Microalloyed Plate Steel," *8<sup>th</sup> Process Technology Conference Proceedings*, IIS, Vol. 8, pp. 13-21.
- Jin, S., 1989, "Softening in HAZ of a Controlled Rolled Steel," *Conference JOM 4*, Helsingor, Denmark, Ingeniorhojskolen Helsingor Teknikum, pp. 53-57.
- Kinsey, A., 2000, "Welding of Structural Steels without Preheat," *Welding Journal*, Vol. 79, No. 4, pp 79-88.

- Karppi, R et al., 1983, "Note on Standardization of Implant Test," *IIW Doc. IX-1296-83*, Espoo, Technical Research Center of Finland, Research Reports 189, pp. 1-25.
- Kotecki, D., 1993, "Aging of Welds for Hydrogen Removal," *Welding Journal*, Vol. 73, No. 6, pp. 75-79.
- Langley, D.J, Smith D. Killmore. C., 1998, "Development of TMCR Higher Strength Structural Plate," *Proceeding of Materials 98*, CIM, pp. 159-165.
- Lesnewich, A., 1998, "Influence of Welding on Steel Weldment Soundness. Selection of Carbon and Low Alloy Steels," *ASM Handbook Volume 6: Welding, Brazing and Soldering*, ASM International.
- Lin, M. Bodnar, Y. Shen, Y, Brown , G, Feher, F., 1999, "Some Fundamentals for the Accelerated Cooling of Plate Products," *International Symposium on Steel for Fabricated Structures*, ASM International, Cincinnati, Ohio, pp. 95-103.
- Losz, J., Challenger, K., 1990, "HAZ Microstructure In HSLA Steel Weldments," AWS Conference, pp. 207-225.
- North, T. et al., 1982, "Weldability of High Strength Line Pipe Steels," *Welding Journal*, Vol. 61, No. 8, pp. 244s-257s.
- Patchett, B. Private Communication
- Patchett, B., 1998, *The Metals Blue Book: Welding Filler Metals*. Second Edition, Casti Publishing.
- IIW, 1985, "Cold Cracking test Methods using Implants," IIW Doc No 802-84, IX-1240-82.
- IIW, 1988, "Guide to the Light Microscope Examination of Ferritic Steel Weld Metals," IIW Doc.No.IX-1533-88, IXJ-123-87 Revision 2.
- Rothwell, A., 1990, "Assessment of Cracking Test for Pipeline Steels," *The Metallurgy, Welding, and Qualification of Microalloyed (HSLA) Steel Weldments*, Texas, pp. 151-180.
- Sage, A.M., 1983, "Physical Metallurgy of High Strength Low Alloy Line Pipe and Pipe Fitting Steels," *Metals Technology*, June, Vol. 10, pp. 224-234.
- Sawhill, J., Baker, J., Howe, P., 1986, "Hydrogen Assisted Cracking in High Strength Pipeline Steels," *Welding Journal*, Vol. 65, No. 7, pp. 175s-183s.

Sharma, U., 2000, "Microstructural Characterization of Microalloyed Linepipe Steel" Master's Thesis, Department of Chemical and Materials Engineering, University of Alberta.

Shiga, C., 1990, "Effects of Steelmaking, Alloying and Rolling Variables on the HAZ Structure and Properties in Microalloyed Plate and Linepipe," *The Metallurgy, Welding, and Qualification of Microalloyed (HSLA) Steel Weldments*, Texas, pp. 327-350.

Signes, E., Home, P., 1988, "Hydrogen Assisted Cracking in High Strength Pipeline Steels," *Welding Journal*, Vol. 67, No. 9, pp. 163s-170s.

Smith, W., 1993, *Structure and Properties of Engineering Alloys*, Second Edition, McGraw Hill.

Somers, B. 1993, "Selection of Carbon and Low Alloy Steels," *ASM Handbook Volume 6: Welding, Brazing and Soldering*, ASM International.

Tanaka, T., 1995, "Science and Technology of Hot Rolling Process of Steel," *ISS Proceeding of the International Conference Microalloying 95*, Pittsburgh, Pennsylvania, pp. 165-181.

Tanaka, T., 1993, "The Development of Thermo-Mechanical Controlled Processing of High Strength Low Alloy Steel," *Key Engineering Materials*. Vol. 84-85, pp. 331-355.

Wade, J., 1981, "Implant Testing of Steel," AWRA Contract 73, Australian Welding Research, December, pp 26-31.

Watkinson, F. Hart, P., "International Implant Cracking Test," Confidential, Vol. 14, No. 11.

Zajac, S., Langerborg, R., Siwecki, T., 1995, "The Role of Nitrogen in Microalloyed Steel," *IIS Proceeding of the International Conference Microalloying 9*, Pittsburgh, Pennsylvania, pp. 321-338.



## Appendix A

### *Consumable Information*

Electrode	6018
Tensile Strength	640 - 685 MPa (90000-98000 psi)
Yield Strength	550 - 610 MPa (80000-85000 psi)
C %	0.05
Cr %	0.06
Ni %	1.64
Mo %	0.24
P %	0.016
S %	0.010
Mn %	1.13
Si %	0.27
Nb %	-
Ta %	-
V %	-
Cu %	-
Ti %	-

Electrode	7018
Tensile Strength	574 MPa (83000 psi)
Yield Strength	483 MPa (70000 psi)
C %	0.05
Cr %	0.05
Ni %	0.04
Mo %	0.02
P %	0.012
S %	0.014
Mn %	1.06
Si %	0.52
Nb %	-
Ta %	-
V %	0.01
Cu %	-
Ti %	-

Electrode	8018
Tensile Strength	580 MPa (84000 psi)
Yield Strength	500 MPa (73000 psi)
C %	0.06
Cr %	0.63
Ni %	0.75
Mo %	0.02
P %	0.016
S %	0.009
Mn %	1.07
Si %	0.43
Nb %	-
Ta %	-
V %	0.02
Cu %	0.54
Ti %	0.02

Electrode	10018
Tensile Strength	710 MPa (103000 psi)
Yield Strength	665 MPa (97000 psi)
C %	0.06
Cr %	0.25
Ni %	1.60
Mo %	0.30
P %	0.018
S %	0.005
Mn %	1.58
Si %	0.46
Nb %	-
Ta %	-
V %	0.01
Cu %	-
Ti %	-

Electrode	12018
Tensile Strength	910 MPa (132000 psi)
Yield Strength	786 MPa (114000 psi)
C %	0.06
Cr %	0.90
Ni %	2.22
Mo %	0.31
P %	0.021
S %	0.011
Mn %	1.90
Si %	0.34
Nb %	-
Ta %	-
V %	-
Cu %	-
Ti %	-

Electrode	7010
Tensile Strength	539 MPa (78000 psi)
Yield Strength	450 MPa (65000 psi)
C %	0.08
Cr %	0.04
Ni %	0.04
Mo %	0.022
P %	0.017
S %	0.014
Mn %	0.55
Si %	0.30
Nb %	-
Ta %	-
V %	-
Cu %	-
Ti %	-

Electrode	7024
Tensile Strength	540 MPa (78000 psi)
Yield Strength	447 MPa (65000 psi)
C %	0.08
Cr %	0.06
Ni %	0.08
Mo %	0.024
P %	0.016
S %	0.016
Mn %	0.76
Si %	0.55
Nb %	-
Ta %	-
V %	-
Cu %	-
Ti %	-

**Appendix B**  
***Test Procedures***

## Heat Input Calculations for Test Welds

Weld	Material	Voltage V	Current A	Speed (mm/sec)	Heat Input (KJ/mm)	Process	Current	Electrode	Passes	Shielding Gas	Gas Rate	Joint Type
1	Grade 80	12	150	2.40	0.75	GTAW	DCEN	Tungsten	1	Ar	10 L/min	N/A
2	Grade 80	11.8	150	1.19	1.49	GTAW	DCEN	Tungsten	1	Ar	10 L/min	N/A
3	Grade 80	11.9	150	0.72	2.48	GTAW	DCEN	Tungsten	1	Ar	10 L/min	N/A
4	Grade 80	12.5	150	3.62	0.52	GTAW	DCEN	Tungsten	1	Ar	10 L/min	N/A
5	Grade 80	12.5	150	4.00	0.47	GTAW	DCEN	Tungsten	1	Ar	10 L/min	N/A
6	Grade 80	12.5	150	3.00	0.63	GTAW	DCEN	Tungsten	1	Ar	10 L/min	N/A
7	Grade 80	12.5	150	2.75	0.68	GTAW	DCEN	Tungsten	1	Ar	10 L/min	N/A
8	Grade 80	12.2	150	2.58	0.71	GTAW	DCEN	Tungsten	1	Ar	10 L/min	N/A
9	Grade 80	12.2	150	1.80	1.02	GTAW	DCEN	Tungsten	1	Ar	10 L/min	N/A
10	Grade 80	12.1	150	1.44	1.26	GTAW	DCEN	Tungsten	1	Ar	10 L/min	N/A
11	Grade 80	11.9	150	0.90	1.98	GTAW	DCEN	Tungsten	1	Ar	10 L/min	N/A
Weld	Material	Voltage V	Current A	Speed (mm/sec)	Heat Input (KJ/mm)	Process	Current	Electrode	Passes	Shielding Gas	Gas Rate	Joint Type
12	Grade 80	25	130	2.16	1.51	SMAW	DCEP	90-18 M	3	N/A	N/A	Double Bevel Groove
13	Grade 80	25	130	2.16	1.51	SMAW	DCEP	100-18 D2	3	N/A	N/A	Double Bevel Groove
14	Grade 80	25	130	2.16	1.51	SMAW	DCEP	110-18 M	3	N/A	N/A	Double Bevel Groove
15	Grade 80	25	130	2.16	1.51	SMAW	DCEP	120-18 M	3	N/A	N/A	Double Bevel Groove
16	Grade 80	25	130	2.16	1.51	SMAW	DCEP	80-18 C3	3	N/A	N/A	Double Bevel Groove
17	Grade 80	25	130	2.16	1.51	SMAW	DCEP	70-18 1	3	N/A	N/A	Double Bevel Groove
18	Grade 80	25	130	2.16	1.51	SMAW	DCEP	60-18 1	3	N/A	N/A	Double Bevel Groove
19	Grade 80	25	130	1.30	2.50	SMAW	DCEP	90-18 M	2	N/A	N/A	Double Bevel Groove
20	Grade 80	25	130	1.63	1.99	SMAW	DCEP	90-18 M	3	N/A	N/A	Double Bevel Groove
21	Grade 80	25	130	3.27	0.99	SMAW	DCEP	90-18 M	4	N/A	N/A	Double Bevel Groove
22	Grade 80	25	130	6.50	0.50	SMAW	DCEP	90-18 M	9	N/A	N/A	Double Bevel Groove

Weld	Material	Voltage V	Current A	Speed (mm/sec)	Heat Input (KJ/mm)	Process	Current	Electrode	Passes	Shielding Gas	Gas Rate	Joint Type
23	Grade 100	12.5	150	4.00	0.47	GTAW	DCEN	Tungsten	1	Ar	10 L/min	N/A
24	Grade 100	12.2	150	3.62	0.51	GTAW	DCEN	Tungsten	1	Ar	10 L/min	N/A
25	Grade 100	12.2	150	3.00	0.61	GTAW	DCEN	Tungsten	1	Ar	10 L/min	N/A
26	Grade 100	12.1	150	2.75	0.66	GTAW	DCEN	Tungsten	1	Ar	10 L/min	N/A
27	Grade 100	12.2	150	2.57	0.71	GTAW	DCEN	Tungsten	1	Ar	10 L/min	N/A
28	Grade 100	12.2	150	2.40	0.76	GTAW	DCEN	Tungsten	1	Ar	10 L/min	N/A
29	Grade 100	12.0	150	1.80	1.00	GTAW	DCEN	Tungsten	1	Ar	10 L/min	N/A
30	Grade 100	12.2	150	1.44	1.27	GTAW	DCEN	Tungsten	1	Ar	10 L/min	N/A
31	Grade 100	12.1	150	1.19	1.52	GTAW	DCEN	Tungsten	1	Ar	10 L/min	N/A
32	Grade 100	12.2	150	0.92	2.00	GTAW	DCEN	Tungsten	1	Ar	10 L/min	N/A
33	Grade 100	12.2	150	0.72	2.54	GTAW	DCEN	Tungsten	1	Ar	10 L/min	N/A
Weld	Material	Voltage V	Current A	Speed (mm/sec)	Heat Input (KJ/mm)	Process	Current	Electrode	Passes	Shielding Gas	Gas Rate	Joint Type
34	Grade 100	25	130	2.16	1.51	SMAW	DCEP	80-18 C3	3	N/A	N/A	Double Bevel Groove
35	Grade 100	25	130	2.16	1.51	SMAW	DCEP	90-18 M	3	N/A	N/A	Double Bevel Groove
36	Grade 100	25	130	2.16	1.51	SMAW	DCEP	100-18 D2	3	N/A	N/A	Double Bevel Groove
37	Grade 100	25	130	2.16	1.51	SMAW	DCEP	110-18 M	3	N/A	N/A	Double Bevel Groove
38	Grade 100	25	130	2.16	1.51	SMAW	DCEP	120-18 M	3	N/A	N/A	Double Bevel Groove
39	Grade 100	25	130	2.16	1.51	SMAW	DCEP	120-18 M (B)	3	N/A	N/A	Double Bevel Groove
40	Grade 80	25	130	2.16	1.51	SMAW	DCEP	120-18 M (B)	3	N/A	N/A	Double Bevel Groove
41	Grade 100	25	130	3.27	0.99	SMAW	DCEP	110-18 M	4 - 2 Cap	N/A	N/A	Double Bevel Groove
42	Grade 100	25	130	6.50	0.50	SMAW	DCEP	110-18 M	0	N/A	N/A	Double Bevel Groove
43	Grade 100	25	130	1.63	1.99	SMAW	DCEP	110-18 M	3-1 Stop	N/A	N/A	Double Bevel Groove
44	Grade 100	25	130	1.30	2.50	SMAW	DCEP	110-18 M	2 - 1 stop	N/A	N/A	Double Bevel Groove

Weld	Material	Voltage V	Current A	Speed (mm/sec)	Heat Input (KJ/mm)	Process	Current	Electrode	Passes	Shielding Gas	Gas Rate	Joint Type
45	Grade 80	25	130	1.63	1.99	SMAW	DC Elect. Pos	10018-D2	1	N/A	N/A	Fillet
46	Grade 100	25	130	1.63	1.99	SMAW	DC Elect. Pos	110-18 M	1	N/A	N/A	Fillet
Weld	Material	Voltage V	Current A	Speed u(mm/sec)	Heat Input H (KJ/mm)	Process	Current	Electrode	Passes	Shielding Gas	Gas Rate	Joint Type
47	Grade 80	26	235	6.77	0.90	GMAW	DCEP	HI 84	1	92% Ar, 8% CO2	27 CFH	Square 3/32 Gap
48	Grade 80	26	235	6.77	0.90	GMAW	DCEP	HI 84	2	92% Ar, 8% CO2	27 CFH	Square 1/16 Gap
49	Grade 80	26	235	4.07	1.50	GMAW	DCEP	HI 84	2	92% Ar, 8% CO2	27 CFH	Square 1/16 Gap
50	Grade 80	26	235	3.05	2.00	GMAW	DCEP	HI 84	2	92% Ar, 8% CO2	27 CFH	Square 0 Gap
51	Grade 80	26	235	3.05	2.00	GMAW	DCEP	HI 84	1	92% Ar, 8% CO2	27 CFH	Square 0 Gap
52	Grade 80	26	235	3.05	1.50 / 0.5	GMAW	DCEP	HI 84	1 and 1	92% Ar, 8% CO2	27 CFH	Square 1/16 Gap
53	Grade 100	26	235	6.77	0.90	GMAW	DCEP	HI 84	2	92% Ar, 8% CO2	27 CFH	Square 1/16 Gap
54	Grade 100	26	235	4.07	1.50	GMAW	DCEP	HI 84	2	92% Ar, 8% CO2	27 CFH	Square 1/16 Gap
55	Grade 100	26	235	3.05	2.00	GMAW	DCEP	HI 84	2	92% Ar, 8% CO2	27 CFH	Square 0 Gap
56	Grade 100	26	235	3.05	2.00	GMAW	DCEP	HI 84	1	92% Ar, 8% CO2	27 CFH	Square 0 Gap
Weld	Material	Voltage V	Current A	Speed u(mm/sec)	Heat Input H (KJ/mm)	Process	Current	Electrode	Passes	Shielding Gas	Gas Rate	Joint Type
57	Grade 80	25	130	1.63	1.99	SMAW	DCEP	10018-D3	1	N/A	N/A	Double Bevel
58	Grade 100	25	130	1.63	1.99	SMAW	DCEP	110-18 M	3 per side	N/A	N/A	Double Bevel

Grade 80 Implant Tests  
6 mm Samples

Experiment #	Notch Depth	Current (A)	Voltage (V)	Speed (mm/min)	Heat Input kJ/mm	Electrode	Electrode Size	Load % SMYS	Test Time hh:mm:ss	Failure Location
59	Full	130	25	129.5	1.51	9018	1/8	78	72:00:00	None
60	Full	130	25	129.5	1.51	7024	1/8	78	72:00:00	None
61	Full	130	25	129.5	1.51	8010	1/8	78	72:00:00	None
62	Full	130	25	260	0.75	8010	5/32	78	0:07:26	WM
63	Half	130	25	260	0.75	8010	5/32	78	0:04:20	WM Shear
64	Half	130	25	196	0.99	8010	5/32	78	0:05:07	WM / BM
65	Full	130	25	196	0.99	8010	5/32	78	0:14:28	WM / BM
66	Full	130	25	196	0.99	7024	1/8	78	1:42:31	BM
67	Half	130	25	196	0.99	7024	1/8	78	0:16:00	BM
68	Half	130	25	259	0.75	7024	1/8	78	0:11:42	BM
69	Half	130	25	259	0.75	9018	1/8	78	72:00:00	None
70	Full	130	25	259	0.75	7024	1/8	78	72:00:00	None
71	Full	130	25	259	0.75	7024	1/8	78	48:00:00	None
72	Full	130	25	196	0.99	7024	1/8	78	30:00:00	None
92	Full	130	25	98	1.99	9018	1/8	100	24:00:00	None
93	Full	130	25	129	1.51	9018	1/8	100	24:00:00	None
94	Full	130	25	196	0.99	9018	1/8	100	24:00:00	None
95	Full - redone	130	25	196	0.99	7024	1/8	78	24:00:00	None
96	Full - redone	130	25	196	0.99	7024	1/8	78	24:00:00	None

**Grade 80 Implant Tests**  
5mm Samples

Experiment #	Notch Depth	Current (A)	Voltage (V)	Speed (mm/min)	Heat Input kJ/mm	Electrode	Electrode Size	Load % SMYS	Test Time hh:mm:ss	Failure Location
115	Full	130	25	196	0.99	9018	1/8	120	72:00:00	None
116	Full	130	25	390	0.50	9018	1/8	120	24:00:00	None
117	Full	130	25	390	0.50	9018	1/8	140	0:00:41	WM Shear
118	Full	130	25	390	0.50	9018	1/8	140	72:00:00	None
119	Full	130	25	196	0.99	9018	1/8	140	24:00:00	None
120	Full	130	25	78	2.5	9018	1/8	140	0:02:18	BM Failure
121	Full	130	25	96	2.0	9018	1/8	140	0:00:04	BM Failure
122	Full	130	25	129.5	1.5	9018	1/8	140	48:00:00	None
123	Full	130	25	96	2.0	9018	1/8	130	24:00:00	None
124	Full	130	25	78	2.5	9018	1/8	130	25:00:00	None



Grade 100 Implant Tests  
6 mm Samples

Experiment #	Notch Depth	Current (A)	Voltage (V)	Speed (mm/min)	Heat Input kJ/mm	Electrode	Electrode Size	Load % SMYS	Test Time hh:mm:ss	Failure
73	Full	130	25	196	0.99	11018	1/8	78	72:00:00	None
74	Full	130	25	196	0.99	9010	5/32	78	0:03:21	BM
75	Full	130	25	129.5	1.51	9010	5/32	78	0:05:25	BM / WM
76	Full	130	25	129.5	1.51	11018	1/8	100	3:23:48	BM / WM
77	Full	130	25	196	0.99	11018	1/8	100	2:30:36	WM Shear
78	Full	130	25	98	1.99	11018	1/8	100	2:35:08	BM
79	Full	130	25	98	1.99	9010	5/32	100	0:02:36	BM
80	Full	130	25	78	2.50	11018	1/8	100	24:00:00	None
81	Full	130	25	78	2.50	11018	1/8	100	0:52:36	BM
82	Full	130	25	78	2.50	11018	1/8	100	1:50:10	BM
83	Full	130	25	78	2.50	11018	1/8	100	6:18:30	BM
84	Full	130	25	78	2.50	11018	1/8	100	72:00:00	None
85	Full	130	25	129	1.51	11018	1/8	100	9:06:56	WM Shear
86	Full	130	25	98	1.99	11018	1/8	90	24:00:00	None
87	Full	130	25	129	1.51	11018	1/8	90	24:00:00	None
88	Full	130	25	196	0.99	11018	1/8	90	24:00:00	None
89	Full	130	25	196	0.99	11018	1/8	95	5:18:42	WM Shear
90	Full	130	25	129	1.51	11018	1/8	95	8:20:02	BM / WM
91	Full	130	25	98	1.99	11018	1/8	100	72:00:00	None
103	Full	130	25	196	0.99	11018	1/8	120	2:33:19	WM Shear
104	Full	130	25	129	1.51	11018	1/8	120	1:41:18	BM
105	Full	130	25	129	1.51	11018	1/8	120	3:50:32	WM Shear
106	Full	130	25	196	0.99	11018	1/8	120	5:46:11	WM Shear
107	Full	130	25	98	1.99	11018	1/8	120	6:35:40	BM
108	Full	130	25	78	2.50	11018	1/8	120	6:18:11	BM
109	Full	130	25	78	2.50	11018	1/8	120	3:58:57	BM
110	Full	235	26	146	2.51	HI 84	1/8	120	24:00:00	None
111	Full	235	26	244.6	1.50	HI 84		120	24:00:00	None
112	Full	235	26	366	1.00	HI 84		120	24:00:00	None

GMAW

Grade 100 Implant Tests  
5mm Samples

Experiment #	Notch Depth	Current (A)	Voltage (V)	Speed (mm/min)	Heat Input kJ/mm	Electrode	Electrode Size	Load % SMYS	Test Time hh:mm:ss	Failure
125	Full	130	25	196	1.0	11018	1/8	130	0:32:58	BM
126	Full	130	25	390	0.5	11018	1/8	130	0:33:39	WM Shear
127	Full	130	25	294.0	0.66	11018	1/8	130	1:01:12	BM
128	Full	130	25	98.0	1.99	11018	1/8	100	6:04:21	BM
129	Full	130	25	196.0	0.99	11018	1/8	100	4:31:31	BM
130	Full	130	25	196.0	0.99	11018	1/8	100	24:00:00	None Baked Out
131	Full	130	25	196.0	0.99	11018	1/8	100	3:33:40	BM Bake Out Stored 24H
132	Full	130	25	196.0	0.99	11018	1/8	100	3:20:04	BM Bake Out Stored 48H
133	Full	130	25	98.0	1.99	11018	1/8	100	24:00:00	None Baked Out
134	Full	130	25	98.0	1.99	11018	1/8	100	24:00:00	None Bake Out Stored 24H
135	Full	130	25	98.0	1.99	11018	1/8	100	24:00:00	None Bake Out Stored 48H +
136	Full	130	25	196.0	0.99	11018	1/8	100		

## WIC Testing

Experiment	Material	Process	Temperature	Speed	Current	Voltage	Consumable	Joint Geometry	Cracking Surface
97	Gr. 80	SMAW	Rm. Temp	196	130	25	9018	1/2 Depth 45 vs Stringht Edge	No
98	Gr. 100	SMAW	Rm. Temp	196	130	25	9018	1/2 Depth 45 vs Stringht Edge	No
99	Gr. 80	SMAW	100 C	196	130	25	9018	1/2 Depth 45 vs Stringht Edge	No
100	Gr. 100	SMAW	100 C	196	130	25	9018	1/2 Depth 45 vs Stringht Edge	No
101	Gr. 80	SMAW	Rm. Temp	196	130	25	9018	1/2 Depth 45 vs 1/2 Depth 45	No
102	Gr. 100	SMAW	Rm. Temp	196	130	25	9018	1/2 Depth 45 vs 1/2 Depth 45	Yes
113	Gr. 80	GMAW	Rm. Temp	366	235	26	HI-84	1/2 Depth 45 vs Stringht Edge	No
114	Gr. 100	GMAW	Rm. Temp	366	235	26	HI-85	1/2 Depth 45 vs Stringht Edge	No